SHRP-A-409

Validation of Relationships Between Specification Properties and Performance

Rita B. Leahy
Edward T. Harrigan
Strategic Highway Research Program

Harold Von Quintus
Brent Rauhut Engineering

Strategic Highway Research Program
National Research Council
Washington, D.C. 1994

SHRP-A-409
ISBN 0-309-05813-9
Product no. 1012

Program Manager: *Edward T. Harrigan*
Project Managers: *Rita B. Leahy and Harold Von Quintus*
Program Area Secretary: *Juliet Narsiah*
Typesetters: *Laurie Dockendorf, Teresa Culver, and Peggy Blair*
Production Editor: *Katharyn L. Bine*

August 1994

keywords:
aging
asphalt binder
fatigue
permanent deformation
specifications
thermal cracking
validation

Strategic Highway Research Program
National Research Council
2101 Constitution Avenue N.W.
Washington, DC 20418

(202) 334-3774

1.5M/NAP/894

Acknowledgments

The work reported herein was supported by the Strategic Highway Research Program (SHRP). SHRP is a unit of the National Research Council that was authorized by section 128 of the Surface Transportation and Uniform Relocation Assistance Act of 1987.

The patience and expertise of Laurie Dockendorf, Teresa Culver, and Peggy Blair, Oregon State University, are gratefully acknowledged. It was largely through their tireless efforts at the keyboard that this report made it to press.

Contents

List of Figures

List of Tables

Abstract

This report summarizes the two-stage validation of the proposed binder and mix specifications and tests. Stage 1 addresses the validation of the specifications and tests with laboratory data; Stage 2, with field performance data. The report is divided into four chapters, the first of which outlines the validation process. Chapters 2 and 3 are devoted to Stage 1 and 2 validation, respectively, and include a comprehensive discussion of the laboratory testing undertaken to evaluate asphalt concrete performance in terms of permanent deformation, fatigue cracking and low-temperature cracking. Chapter 4 addresses the validation testing conducted using modified materials.

Executive Summary

A critical element of the Strategic Highway Research Program (SHRP) Asphalt Program was the validation of the proposed binder and mix tests and specifications using both laboratory and field data. SHRP planned the validation as a three-stage process. The first two stages were completed within the 5-year program life, and the final stage in the post-SHRP era. The initial two-stage process was a coordinated effort among researchers at Pennsylvania State University, Texas Transportation Institute, the University of California at Berkeley and Oregon State University. The post-SHRP validation will be accomplished primarily through the Federal Highway Administration's (FHWA) Special Pavement Studies (SPS-9). The SPS-9 effort is an extension of SHRP's Long Term Pavement Performance Program (LTPP), and involves state participation in the design and construction of controlled test sections based on SHRP binder and mix tests and specifications. Sections constructed as part of the SPS-9 program will be monitored for 15 years to allow a comparison between predicted and actual performance.

The purpose of the stage 1 validation was to confirm that variation in binder properties produce meaningful changes in mix performance as measured by laboratory tests. Researchers at the University of California at Berkeley and Oregon State University accomplished this by using simulative laboratory tests ("torture tests") such as wheel-tracking devices, thermal stress restrained specimen and flexural beam tests, specifically designed accelerated performance tests and accelerated load facilities.

The stage 2 validation established the degree of correlation between binder and mix properties and field performance. Additionally, the stage 2 validation provided experimental results needed to set specification limits for the binder and mix properties selected to control pavement performance. The stage 2 validation was conducted by researchers at Texas Transportation Institute and Pennsylvania State University and relied almost exclusively on sampling and testing of LTPP General Pavement Studies (GPS) sections.

All materials used in the stage 1 validation effort were obtained from the SHRP Materials Reference Library (MRL). From eight to 16 asphalt binders were employed for the various studies. The asphalts selected are representative of materials currently used in the United States and produced from crude-oil sources around the world. Two to four aggregates were used in the various studies.

Laboratory compacted specimens were evaluated to determine the binder's influence on permanent deformation, fatigue cracking and low-temperature cracking. The relationship between the binder specification property, $G^*\sin\delta$, and fatigue life is very strong. Overall, it was concluded that binder properties play a critical role in the fatigue response of asphalt-aggregate mixes; but air void content and aggregate characteristics can also significantly affect fatigue response. Results from both wheel track and shear tests indicate that the relationship between the binder specification property, $G^*/\sin\delta$, and mix performance is weak because of the dominant effect of the aggregate on the permanent deformation response. When aggregate characteristics and/or compaction conditions are expected to result in a mix that is susceptible to permanent deformation, selection of an asphalt that can overcome these deficiencies will be important. The value of $G^*/\sin\delta$ may be used screen binders that will provide inferior performance in such cases. Thermal stress restrained specimens tests (TSRST) indicate that the influence of the binder on low-temperature cracking mix performance is critical. Fracture temperature of the mix was highly correlated to specification properties of temperature at limiting stiffness, *m*-value and the ultimate strain at failure. In summary, the stage 1 validation findings indicate the binder's influence on asphalt concrete mixes varies with distress. In order of decreasing influence, the binder's effect on performance is as follows: low-temperature cracking, fatigue cracking and permanent deformation.

The key objective of the stage 2 validation was to validate the selected binder and mix properties with field performance data. Ideally, this would have required a widespread geographic distribution of sites to encompass a range of climatic zones and data from well-documented, in-service pavement sections. Although data from several field studies were available, the preponderance of the data was generated from the LTPP's GPS sites. The experimental design included one for the load-related distresses (rutting and fatigue cracking) and one for the non-load-related distress (low-temperature cracking). Each included pavement sections located in different climatic zones with different types and severity of distress. The total number of pavement sections in the overall experiment was 72, with 48 in the load-related portion and 24 in the non-load-related portion. The validation program included extensive sampling and testing of field cores and extracted binders, as well as nondestructive testing data.

Test results from the load-related sections show no clear relationships between binder properties and either rutting or fatigue cracking. This lack of clear trends may reflect the effect of mix design, construction, climate or any combinations of these factors. Furthermore, it underscores the fact that the binder specification cannot be used in isolation to increase the probability of enhanced pavement performance. Test results from the non-load-related sections indicate that the binder properties included in the specification (stiffness (*S*) and slope (*m*)) are reasonable parameters for controlling thermal cracking, and that the 6°C temperature range used to define different binder grades allows for a reasonably accurate evaluation of performance. It was also concluded, however, that thermal cracking of a particular binder is mix-dependent, i.e., mix performance is not controlled solely by the binder properties.

Although the binder and mix specifications and tests are appropriate for both unmodified and modified materials, the validation testing undertaken with modified materials was limited in scope. The materials used were drawn from the following general categories of modifiers: polymers such as styrene butadiene (SBS), styrene butadiene rubber (SBR), ethylene vinyl acetate (EVA); reclaimed rubber, extenders, oxidants, antioxidants, mineral fillers, and antistripping agents.

To determine the suitability of the binder tests and specifications, 11 modifiers and 5 asphalts were included in the experiment design. The modified materials were selected based on the collective knowledge and opinions of the expert task group (ETG), SHRP and A-001 staff. The performance data were drawn primarily from *laboratory* test data, not *field* performance data, such that any influences made with respect to field performance are preliminary at best.

It was observed that all the binder tests could accommodate the range of modified binders evaluated. There were no reported difficulties regarding specimen preparation or testing. However, there was no clear correspondence between the material properties of the modified binders and performance as measured by the dynamic shear and bending beam rheometers and the direct tension device.

Validation testing with modified mixes was limited to that associated with permanent deformation and fatigue cracking. For permanent deformation, three asphalts, two aggregates and four modifiers were considered. Specimens were compacted over a range of air void contents and tested in the simple shear device. As expected, the performance of the modifiers is dependent upon the base asphalt. It was observed, however, the performance ranking of the modifiers, despite the difference in void content, was nearly identical to that hypothesized by the ETG, whose members were instrumental in the selection of modifiers used in the validation testing. The fatigue experimental design included three asphalts, one aggregate and three modifiers. Beam specimens were tested in flexure (controlled-strain). Though limited in extent, the results suggest that both binder type and modifier type substantially affect flexural stiffness and fatigue life.

1

Validation Process

A critical element of the Strategic Highway Research Program (SHRP) Asphalt Program was the validation of the proposed binder and mix tests using both laboratory and field data. In terms of the performance-based specifications, validation is defined as the verification of relationships between binder and asphalt-aggregate mix properties and pavement performance through the correlation of those properties with measured characteristics of in-service pavements.

SHRP planned the validation as a three-stage process: The first two stages were to be completed within the 5-year program life, and the final stage in the post-SHRP era (TRB, 1986). The initial two-stage process was a coordinated effort between SHRP contracts A-003A and A-005, as illustrated in Figure 1.1. A brief description of the major contracts of the SHRP asphalt program is found in Table 1.1. The work done by the A-003A and A-005 contractors—and discussed in Chapters 2 and 3, respectively—was focused primarily on *unmodified materials* (TRB, 1986). Validation testing of *modified materials*, the focus of the A-004 contract, is addressed in Chapter 4. The post-SHRP validation will be accomplished under the auspices of the Federal Highway Administration (FHWA) via two mechanisms: the Accelerated Loading Facility (ALF) at the Turner-Fairbank Highway Research Center; and Special Pavement Studies, SPS-9. The SPS-9 effort, an extension of SHRP's Long Term Pavement Performance Program (LTPP), involves state participation in the design and construction of controlled test sections based on SHRP binder and mix tests and specifications. In accordance with a statistically designed sampling plan and testing schedule, SPS-9 considers the interaction of material properties, traffic, structural design, and environment to estimate the relative influence of key factors on pavement performance. The sections will be monitored for 15 years to allow a comparison between predicted and actual performance.

1.1 Stage 1 Validation

The purpose of the stage 1 validation was to confirm that variation in binder properties selected for specification yielded physically reasonable, meaningful changes in mix performance as measured by laboratory tests. SHRP contract A-003A accomplished this by

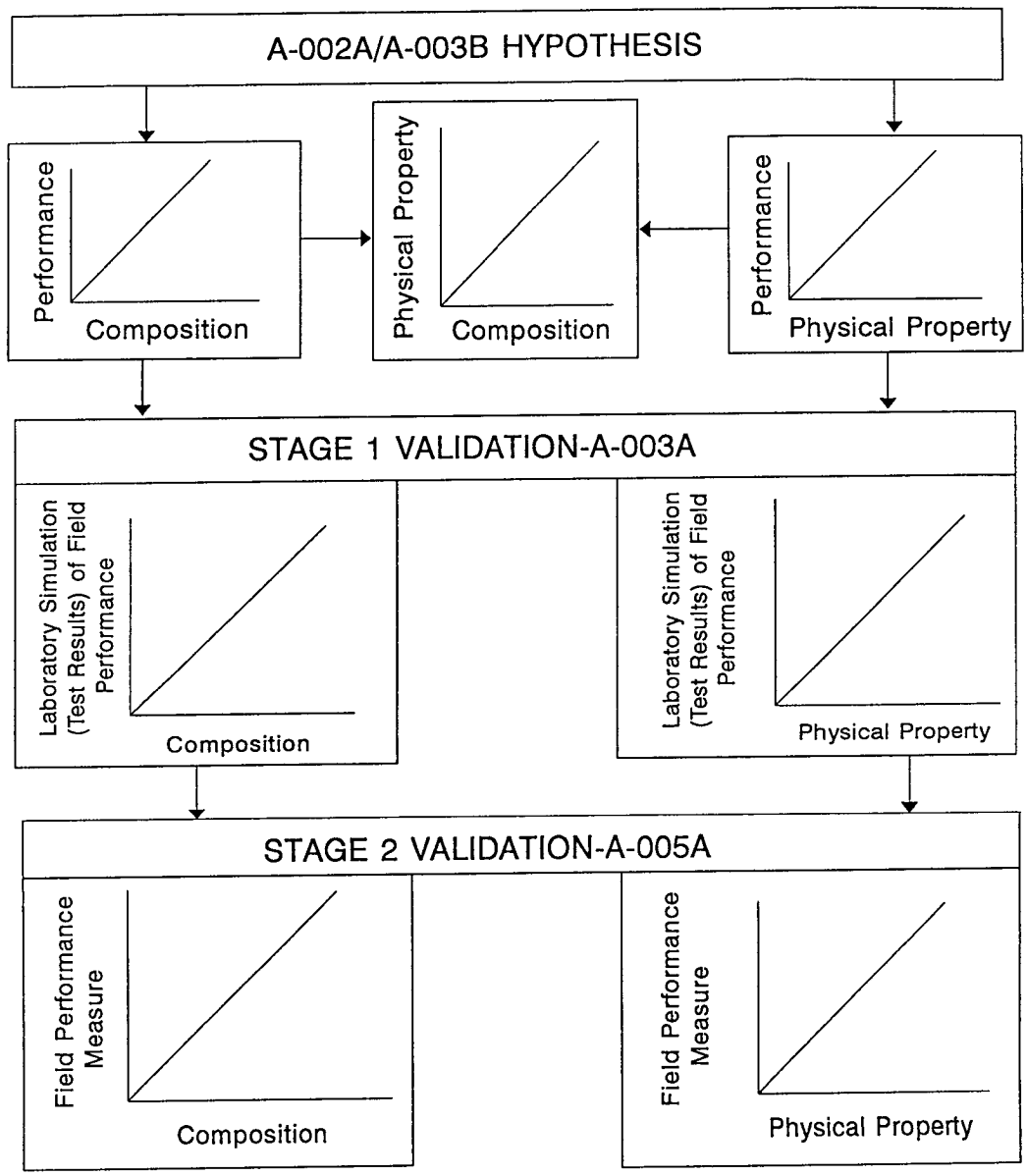

Figure 1.1. The two-step validation process using accelerated performance tests and field performance data

Table 1.1. SHRP asphalt contracts involved in the validation process

A-002A	Binder characteristics and evaluation
A-003A	Performance related testing and measuring of asphalt-aggregate mixes
A-003B	Fundamental properties of asphalt-aggregate interactions including adhesion and absorption
A-005	Validation and performance prediction models

the use of simulative laboratory tests ("torture tests") with wheel-tracking devices, thermal stress restrained specimen and flexural beam tests, specifically designed accelerated performance tests, and accelerated load facilities.

1.2 Stage 2 Validation

The stage 2 validation established the degree of correlation between binder and mix properties and field performance. Additionally, the stage 2 validation provided experimental results needed to set specification limits for the binder and mix properties selected to control pavement performance. The stage 2 validation was conducted by SHRP contract A-005 and relied almost exclusively on sampling and testing of LTPP General Pavement Studies (GPS) sections (Lytton et al, 1993). The GPS sections are in-service pavements that were constructed in the late 1970s and early 1980s. The two approaches used in the stage 2 validation are shown schematically in Figure 1.2.

Ideally, the field validation process would provide data from which specification properties and limits could be established directly. As shown in Figure 1.3, there were three key steps: 1) the identification of field sections with a broad range of compositional and physical properties as well as observed distress; 2) measurement of selected binder and mix properties and comparison to observed pavement distress; and 3) determination of correlation between binder and mix properties and observed pavement distress. The advantage of this *empirical* method was that it would demonstrate clearly that a particular binder or mix property directly affected field performance as measured by the selected laboratory test. Although eminently practical and dictated by time and budgetary constraints, this method presented a problem—i.e., the inevitable uncertainties associated with the uncontrolled nature of the field pavements used in the analysis. The analysis, as evidenced by typical results shown in Chapter 3, was imprecise due to lack of experimental control of key variables that affect pavement performance, e.g., traffic, climate, pavement geometry, subgrade, drainage, construction quality control, and maintenance. Since the laboratory-measured parameters were not highly correlated with the observed distress, one might attribute the lack of correlation to the fact that 1) the selected material property was not related to performance, or 2) that the material property was related to performance, but factors such as traffic, environment, pavement geometry, and subbase/subgrade support also affected the performance. Therefore, to provide incontrovertible proof that the selected material property

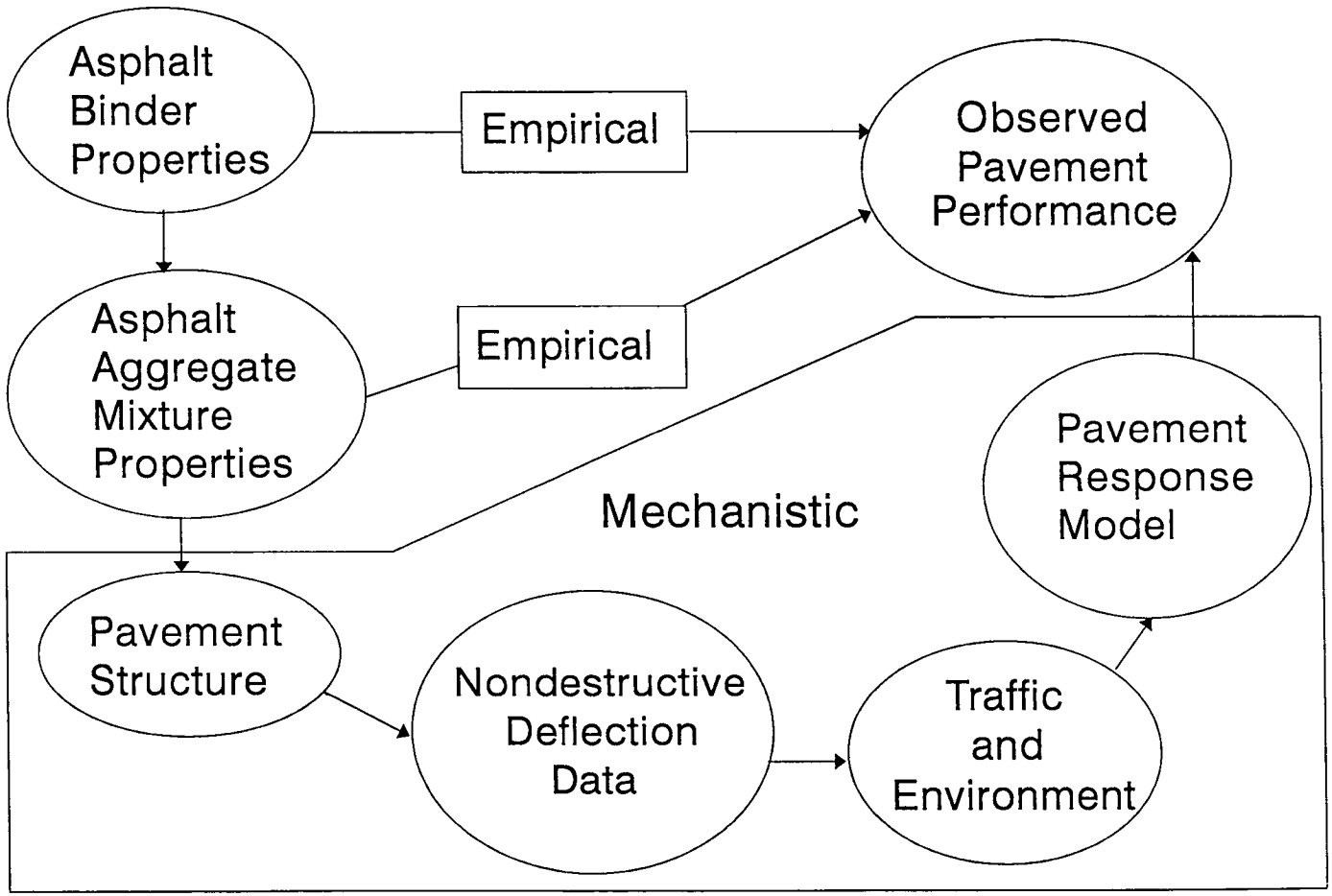

Figure 1.2. Flow chart illustrating the two-step validation process

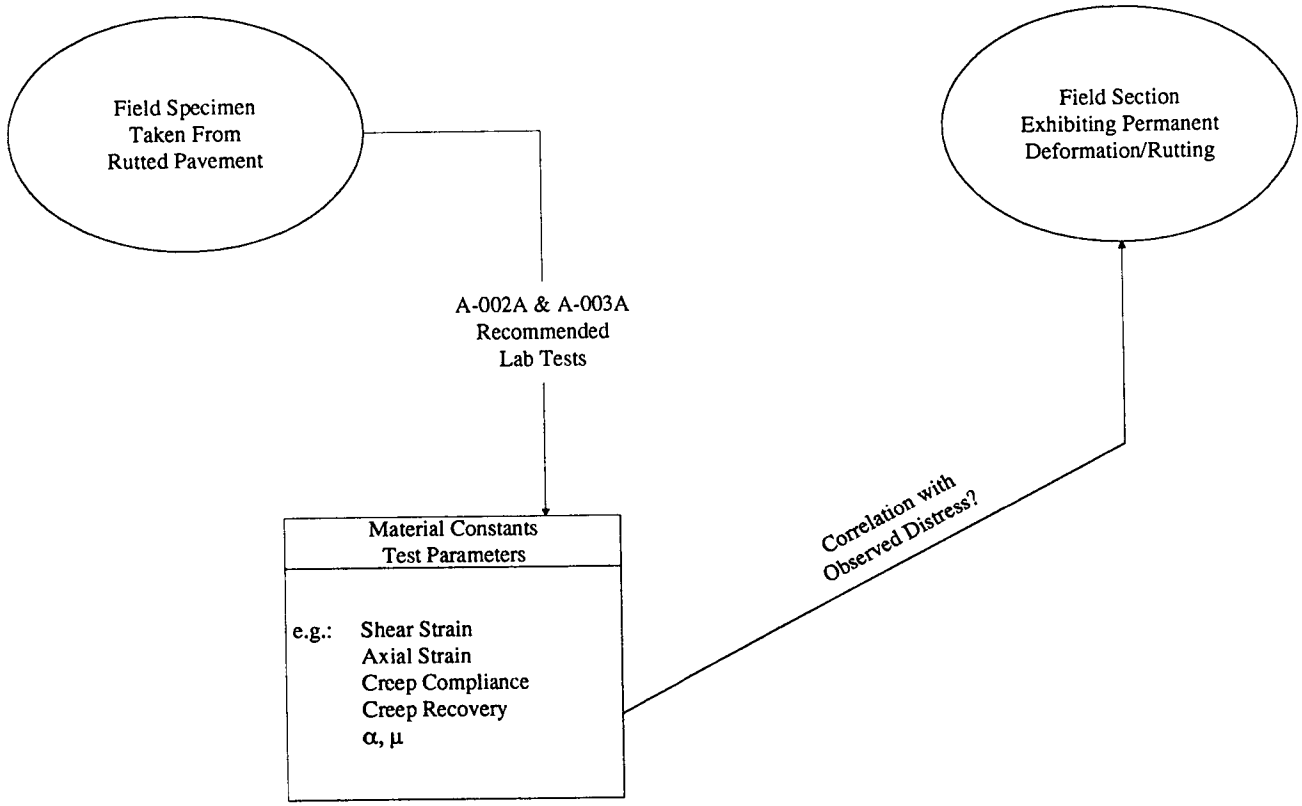

Figure 1.3. Example of direct/empirical validation for permanent deformation

was related to the observed distress or performance, the effect had to be isolated from all other variables that affect overall performance. Because of the limited size of the data set, normalizing the data to identify the relative contribution of the other variables limited the effectiveness of the empirical approach to validation.

To address the shortcomings of the empirical validation approach, the A-005 contractor proceeded in parallel with a more complex *mechanistic* method of field validation. In this approach, material relationships were used in mechanistic models to predict distress, whereas the empirical approach attempts a simple correlation between material properties and observed distress. As in the empirical method, field cores were taken from distressed pavements and subjected to a series of laboratory binder and mix tests to measure specific properties that were identified by the A-002A and A-003A contractors as related to a particular distress. With this approach, generation of material properties is the result of an iterative solution, thus requiring initial estimates of the parameters. In cases where the laboratory-determined parameters did not match those generated by the mechanistic models, the model coefficients were adjusted iteratively until the predicted properties matched the measured properties within acceptable limits.

The obvious advantage of this method is that it provides a mechanism to normalize and calibrate performance data from real-world, uncontrolled field sections to isolate the effect of material properties on performance from other factors. Moreover, this approach permits a reasonable extrapolation of the performance prediction capabilities of the mechanistic models beyond the limits of the experimental data upon which it was based.

2

Stage 1 Validation

The approach to the validation effort and individual contract responsibilities are shown in Figure 2.1. Binder properties and tests were validated in parallel using both laboratory tests and field performance data by the A-003A and A-005 contractors, respectively. A similar approach was used for validation of the mix properties/tests. Both laboratory and field validation efforts are reviewed in the following sections.

This discussion summarizes the validation of the binder tests and properties as they relate to the performance of asphalt-aggregate mixes. Specifically, it addresses the validation of the binder properties proposed by the A-002A contractor to predict asphalt-aggregate mix performance in terms of fatigue cracking, permanent deformation, and low-temperature cracking. A comprehensive discussion of the stage 1 validation may be found elsewhere (SHRP, 1994).

2.1 Binder Tests

The following tests have been selected to characterize the fundamental properties of the binder:

1) **Dynamic Shear Rheometer**. This test is used to measure the rheological properties of the binder in terms of dynamic shear modulus (stiffness), G^*, and phase angle, δ. In the SHRP binder specification, the parameter $G^* \sin \delta$ relates to fatigue cracking, and $G^*/\sin \delta$ relates to permanent deformation.

2) **Bending Beam Rheometer**. This test is used to measure the creep stiffness, S, of the asphalt at low temperatures and the slope of the creep stiffness, m, versus loading time curve. In the SHRP binder specification, both of these values relate to low-temperature cracking, and m also is related to fatigue cracking.

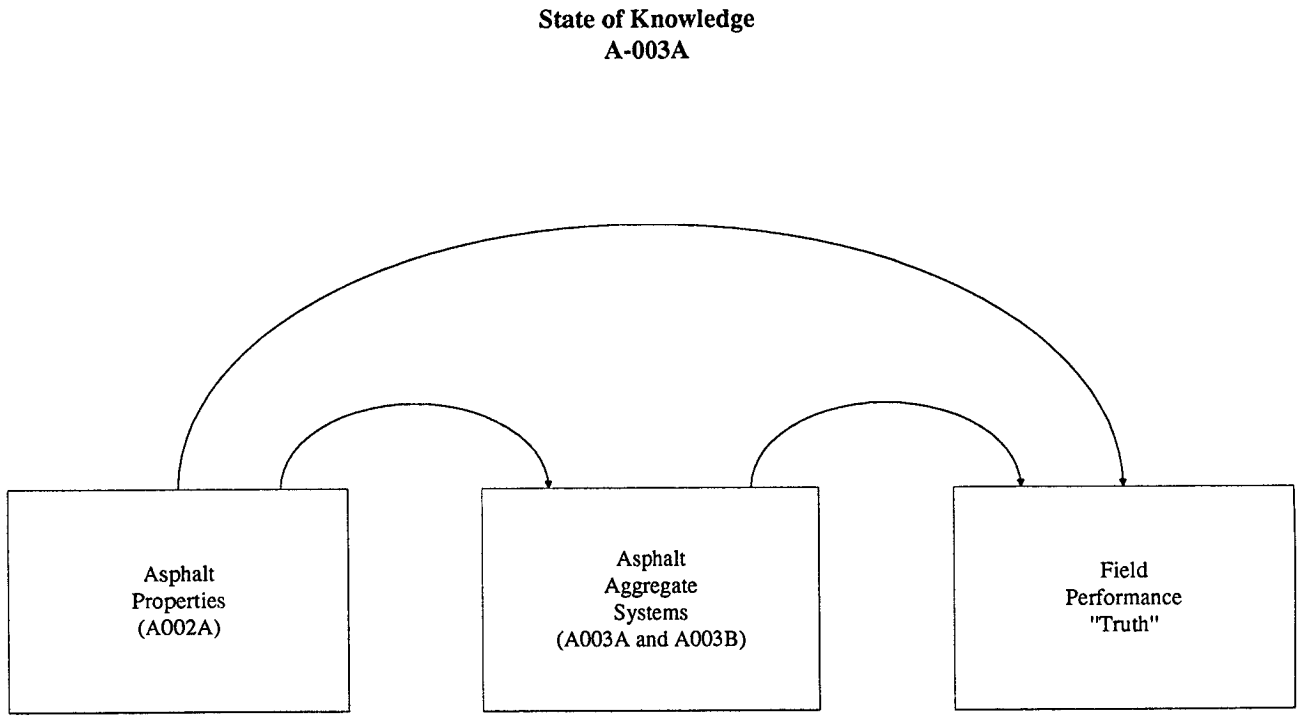

Figure 2.1. General approach used in validation effort

3) **Direct Tension Test.** This test is used to measure the low-temperature failure properties of the binder. The tensile strain at failure indicates the performance of mixes in cold environments.

2.2 Experimental Design

All materials used in the validation effort were obtained from the SHRP Materials Reference Library (MRL). From eight to 16 asphalt binders were employed for the various studies, the properties of which are reported elsewhere (Anderson et al, 1994). The asphalts selected are representative of materials currently used in the United States and produced from crude-oil sources around the world. Two to four aggregates were used in the various studies. Two aggregates were employed for fatigue, permanent deformation, and thermal cracking studies. For fatigue and thermal cracking, aggregate characteristics are less significant than the asphalt properties. For permanent deformation, time and material constraints precluded the testing of more than two aggregates despite of the universally recognized effect of aggregate on mix resistance to rutting. Four aggregates were used for the aging and water-sensitivity studies because of the aggregate's dominant effect. The MRL binders and aggregates used in the validation effort are shown in Table 2.1.

2.3 Fatigue

2.3.1 Flexural Fatigue

For fatigue, combinations of eight asphalts and two aggregates were tested using a flexural beam test device developed at the University of California at Berkeley (UCB) (Figure 2.2). All tests were conducted on prismatic specimens 5 cm × 6.25 cm × 37.5 cm (2 in. × 2.5 in. × 15 in.) in the controlled strain mode at 20°C (68°F) using a sinusoidal loading at a frequency of 10 Hz.

All asphalt-aggregate mixes were prepared at a fixed asphalt content near the optimum determined by the California Department of Transportation (Caltrans) mix design procedure (ASTM D1560, D1561). Mixes were prepared by rolling wheel compaction to produce specimens with target air void contents of 4 and 7 percent.

A full factorial experiment was designed to test all main effects and two-factor interactions. The factorial matrix consisted of 8 asphalts, 2 aggregates, 2 air void levels, and 2 strain levels, resulting in a total of 64 cells. Each cell had two replicates to allow for estimation of experimental error, resulting in a total of 128 flexural fatigue tests. The factorial experiment is summarized below:

Table 2.1. Asphalt binders and aggregates used in validation effort

Asphalts	
MRL Code	Grade
AAA-1	150/200
AAB-1	AC-10
AAC-1	AC-8
AAD-1	AR-4000
AAF-1	AC-20
AAG-1	AR-4000
AAK-1	AC-30
AAL-1	150/200
AAM-1	AC-20
AAV	AC-5
AAW	AC-20
AAX	AC-20
AAZ	AC-20
ABA	AC-20
ABC	AC-20
ABD	AR-4000
Aggregates	
MRL Code	Characteristics
RC	Limestone, high absorption
RD	Limestone, low absorption fully crushed quarry rock
RH	Greywacke, partially crushed river gravel
RJ	Conglomerate, gravel

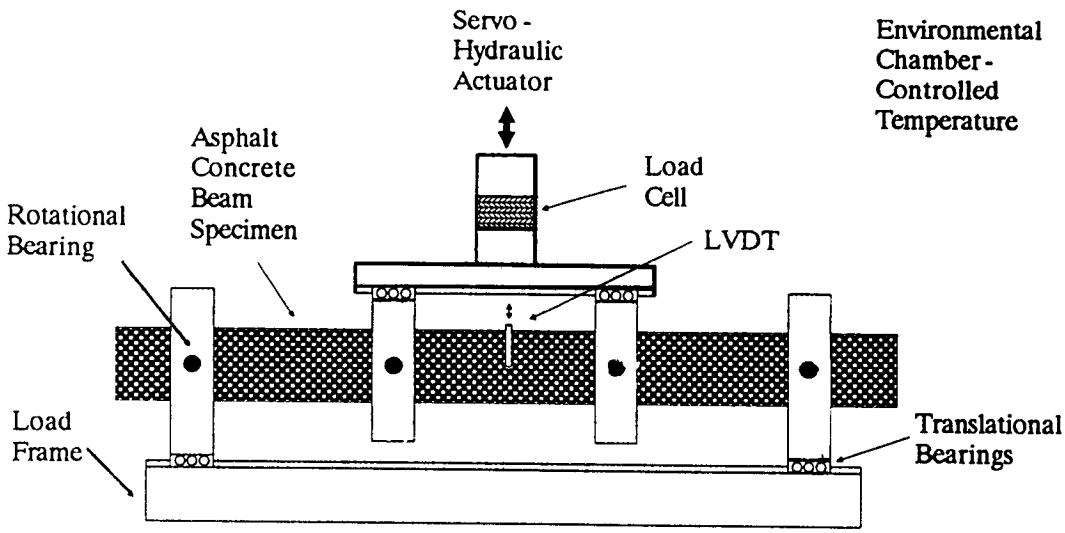

Figure 2.2. Schematic of flexural fatigue device

Factor	Levels
Asphalt Source	AAA, AAB, AAC, AAD, AAF, AAG, AAK, AAM
Aggregate Source	RD, RH
Air Voids	4 percent, 7 percent (target levels)
Strain Level	400, 700 μmm/mm
Replicates	2/cell
Total No. of Tests	128

Response variables included a) initial flexural stiffness measured at the 50th load cycle; b) fatigue life in terms of the number of load cycles corresponding to a 50 percent reduction in flexural stiffness; and, total dissipated energy, i.e., the summation of dissipated energy per cycle until a 50 percent reduction in flexural stiffness occurs.

Binder properties provided by A-002A included complex shear modulus (G^*), phase angle (δ), storage modulus (G', which is equal to $G^*\cos\delta$), loss modulus (G'', which is equal to $G^*\sin\delta$), and loss tangent (tan δ, which is equal to G''/G') (Anderson et al, 1994).

$G^*\sin\delta$ includes the viscous component of asphalt binder stiffness. The A-002A contractor hypothesized that $G^*\sin\delta$ relates to the accumulation of dissipated energy during repetitive loading. Therefore, it also should relate to the dissipated energy parameter measured in asphalt-aggregate mixes by the flexural fatigue test. Both parameters include terms for stiffness and phase angle.

Dissipated energy for a single load cycle in the flexural beam fatigue test is equal to $\pi\epsilon_i^2 S_i^*\sin\phi_i$. It should be noted that the phase angles δ and ϕ_i are equal; however, for notational purposes, δ is used for the phase angle of the binder and ϕ_i is used for the phase angle of the mix.

A-002A binder properties are based on thin film oven test (TFOT)-aged materials to simulate short-term aging during construction. The binders used in this study were aged and the properties calculated for conditions different from those required in the SHRP binder specification for fatigue cracking evaluation. This was done to represent more closely the properties of the binder in the asphalt-aggregate mixes tested in the fatigue validation effort. The specification calls for binders to be aged in the pressure aging vessel (PAV), before first testing to simulate long-term aging effects, and to test binder specimens at a loading frequency of 10 radians per second (rad/s). Asphalt-aggregate mixes were subjected to short-term aging (4 hours at 135°C [275°F]) but not long-term aging, and were tested at a loading frequency of 10 Hz.

Despite this minor modification from the binder aging and testing protocols, there is excellent correlation between $G^*\sin\delta$ after PAV aging and the value of $G^*\sin\delta$ after TFOT aging, as seen in Figure 2.3. Thus, it is expected that the conclusions drawn from this study would not change significantly if asphalt binder properties had been determined in accordance with the A-002A testing protocol. Furthermore, if asphalt binder properties resulting from long-term binder aging in the PAV accurately represent those in mixes subjected to long-term aging, then the conclusions reported herein regarding fatigue relationships will probably hold

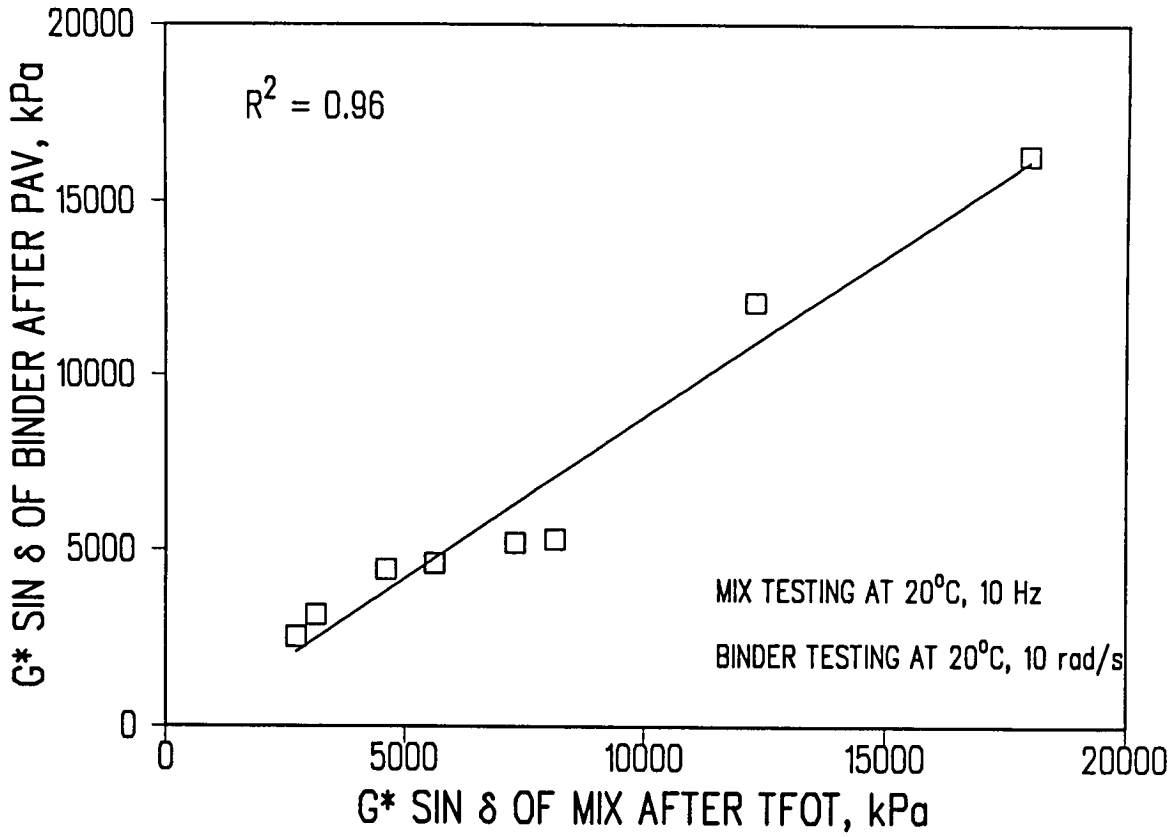

Figure 2.3. Relationship between G^*sin δ after TFOT and PAV

for mixes subjected to long-term aging (except for possible asphalt-aggregate interaction effects on aging).

Flexural stiffness, fatigue life, and total dissipated energy were the response variables measured in the flexural fatigue tests and used in the analysis herein. Flexural stiffness is an important parameter in that it affects the strain on an asphalt concrete layer when subjected to a load. Although flexural stiffness was measured throughout the test, only the "initial" flexural stiffness is reported. This initial stiffness was measured at the fiftieth load cycle to allow the specimen to become seated in the test equipment (SHRP, 1994).

For purposes of this study, fatigue life was defined as the number of load cycles corresponding to a reduction in flexural stiffness of 50 percent of the initial flexural stiffness.

Total dissipated energy also was measured, because research reported by European investigators has indicated it is related to the fatigue response of asphalt-aggregate mixes (SHRP, 1994). In addition, the research has suggested that dissipated energy is independent of the testing mode (i.e., controlled-strain versus controlled-stress) and frequency of loading (thus allowing fatigue testing to be completed more quickly). Total dissipated energy is the cumulative sum of the dissipated energy per load cycle upon reaching the fatigue life.

Since asphalt source significantly affected fatigue response, it was expected that additional analyses would find relationships between asphalt binder properties and asphalt-aggregate mix fatigue response. But since aggregate and air void characteristics also significantly influenced the fatigue response of asphalt-aggregate mixes, it was expected that the effect of

asphalt properties might be masked somewhat by these other factors. Because of the significance of the interactions between asphalt source, aggregate source, and air void level, the relationships between binder properties and mixture fatigue response were evaluated separately for each aggregate source and air void level. Flexural strain level did not interact with any of the other factors in its effect on mixture fatigue response. Therefore, flexural stiffness, fatigue life, and dissipated energy results were averaged across strain level to simplify subsequent analyses (SHRP, 1994). Typical results are shown in Figures 2.4, 2.5, and 2.6.

Figure 2.4 indicates that the *flexural stiffness* of mixtures is strongly related to the recommended binder property, $G^*\sin\delta$, as illustrated by the R^2 value of 0.88. As the binder stiffness increases, whether it is the result of an increase in the storage modulus (G'), the loss modulus ($G^*\sin\delta$, or G''), or a combination of both moduli (G^*), the mix flexural stiffness also increases. Figure 2.5 suggests an inverse relationship between binder stiffness and *mix fatigue life*: As binder stiffness increases, fatigue life decreases. Figure 2.6 shows the relationship between *total dissipated energy* and $G^*\sin\delta$. The trend of the relationship is the same as that observed for fatigue life, but the overall relationship is not as strong, suggesting that prediction of dissipated energy based on $G^*\sin\delta$ is not as reliable as that of stiffness and fatigue life. Though not shown here, the comprehensive statistical analysis revealed that comparisons of flexural stiffness, fatigue life, or dissipated energy to all binder (G) properties ($G^*\sin\delta$, G^*, G') were equally strong (SHRP, 1994).

2.3.2 Elastic Layer Theory

Asphalt binder properties were compared with fatigue life estimates for "hypothetical" pavements constructed with various asphalts. Fatigue life estimates were made for two hypothetical structural sections by calculating the maximum principal tensile strain (using an elastic layer analysis program) at the bottom of the asphalt concrete layer, and then calculating the corresponding fatigue life from the tensile strain using the relationship between fatigue life and strain for a given mix. The strain calculated by ELSYM5 for the hypothetical pavement was entered into the equation shown below, and the corresponding fatigue life was predicted.

$$N_f = K_1\,(1/\epsilon)^{K2}$$

where:

	N_f	=	fatigue life,
	ϵ	=	strain (in./in.), and
	K_1, K_2	=	regression coefficients.

In general, the relationship between $G^*\sin\delta$ and predicted pavement fatigue life was much weaker than that observed with the lab testing, as linear regression between $G^*\sin\delta$ and predicted pavement fatigue life produced coefficients of determination (R^2) ranging from 0.21 to 0.38. More important, the *direction* of the trend is opposite to that observed in the

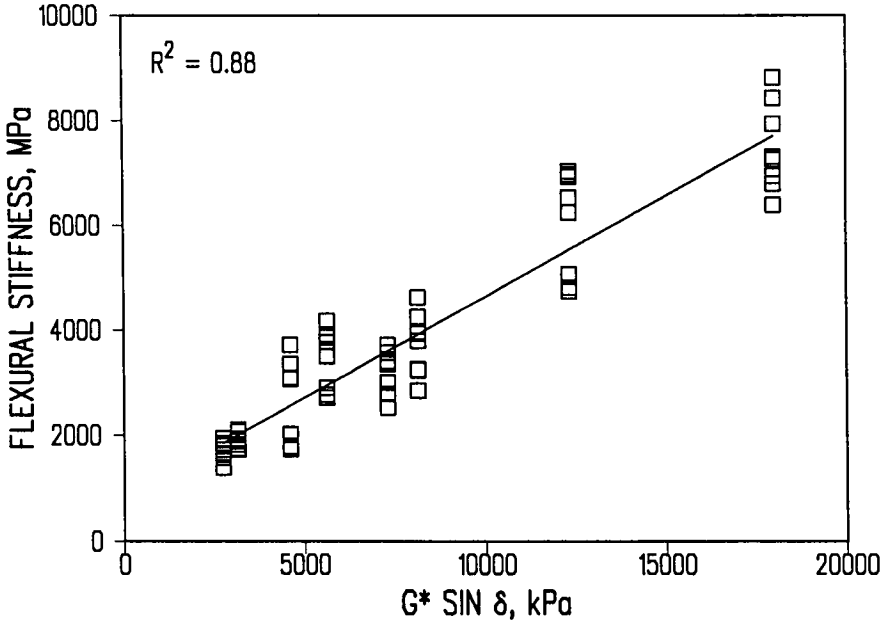

Figure 2.4. Relationship between $G^*\sin\delta$ and flexural stiffness

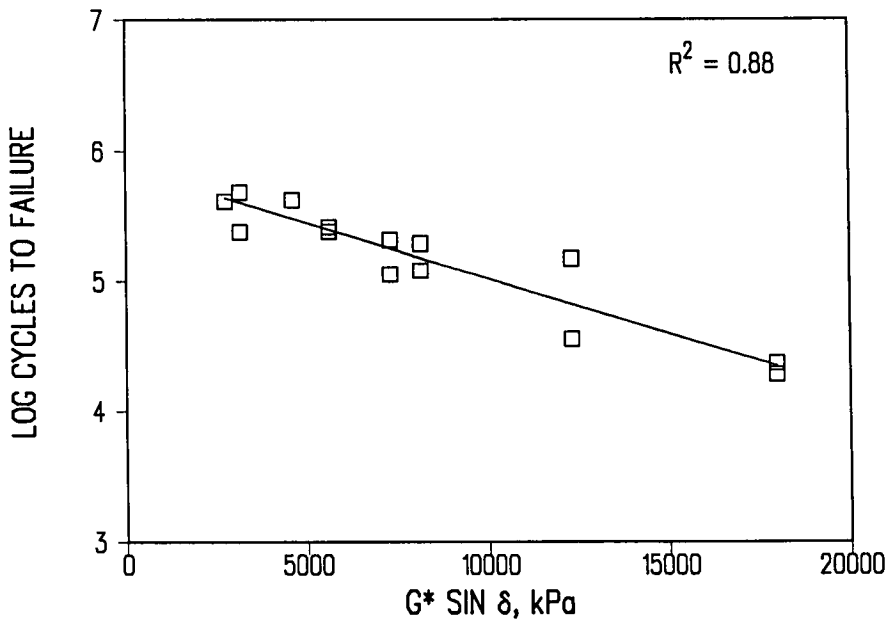

Figure 2.5. Relationship between $G^*\sin\delta$ and cycles to failure

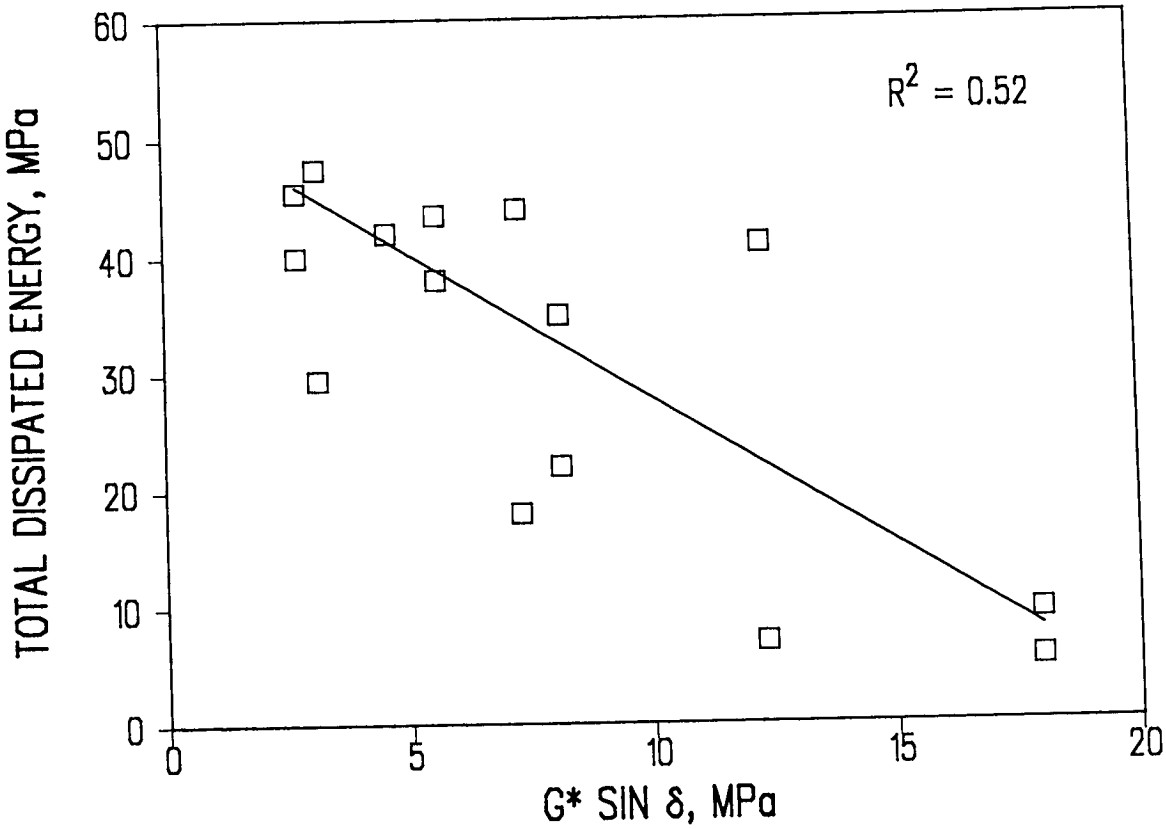

Figure 2.6. Relationship between $G^*\sin\delta$ and total dissipated energy

laboratory flexural fatigue analysis: In this analysis, *predicted fatigue life generally increased as binder stiffness increased.* It should be noted that this analysis was based on asphalt sections 15 to 25 cm (6 to 10 in.) thick and it indicates that with increasing section thickness and stiffness, both controlled-strain testing and controlled stress-testing yield the same results. Furthermore, controlled-strain testing and analysis of sections less than 3 in. thick would yield, as expected, a directly proportional relationship between $G^*\sin\delta$ and fatigue life.

A comparison between the SHRP binder specification for $G^*\sin\delta$ related to fatigue cracking and the pavement fatigue life predicted from elastic layer theory is difficult because of the reversed relationship between $G^*\sin\delta$ and predicted pavement fatigue life. If this relationship is confirmed in future studies, the binder specification limit will need to be modified. The results of this study still indicate that asphalt binder properties are important in evaluating fatigue cracking. But the importance of considering the influence of pavement structure effects also is demonstrated.

2.3.3 Conclusions

In summary, the conclusions with respect to the A-002A binder tests/properties for fatigue are:

1) $G^*\sin\delta$, G^*, and G' all result in relationships of equivalent strength with mix fatigue response. Hence, one may conclude that the effect of the sin δ term of

specification. The effect of sin δ, however, may still be important for modified asphalts.

2) The relationships between the binder specification property, $G^*\sin\delta$, and mix flexural stiffness and fatigue life were very strong. The relationship with dissipated energy was significantly weaker.

3) In the prediction of fatigue cracking in pavement structures, it appears that asphalt binder properties are again important, but pavement structure effects may be equally or more important. In fact, pavement structure effects may influence fatigue cracking to the extent that the relationship between $G^*\sin\delta$ and pavement fatigue life may be completely reversed as the thickness of the asphalt concrete layer changes. It is recognized that the study performed by A-003A to evaluate these effects has some limitations. Nevertheless, it identifies an issue that is worthy of further evaluation. If further study confirms that the direction of the relationship between $G^*\sin\delta$ and pavement fatigue life is dependent on the pavement structure, the binder specification will need to include provisions for pavement structure effects.

4) Overall, asphalt binder properties play a critical role in the fatigue response of asphalt-aggregate mixes. But other mix characteristics, such as air void levels and aggregate characteristics, can also significantly affect fatigue response. Therefore, asphalt binder properties alone may not provide sufficiently reliable estimates of fatigue cracking in pavements. In critical design situations (unusual traffic volume or loading conditions, modified materials), asphalt-aggregate mix fatigue testing should be conducted to increase the reliability of estimates of pavement fatigue cracking.

2.4 Permanent Deformation

This section summarizes research conducted to validate the relationships between asphalt binder properties and the permanent deformation response of asphalt-aggregate mixes. The relationship between binder properties and permanent deformation response of asphalt-aggregate mixes was evaluated using the wheel-tracking device at the University of Nottingham (England) and a shear device developed at UCB as part of the SHRP-sponsored research.

2.4.1 Wheel-Tracking Tests

In this study, a wheel-tracking device was used to simulate the stress conditions caused by a dynamic wheel load on the pavement surface. An experiment was designed to test all main factors and two-factor interactions. The factorial matrix consisted of 16 asphalts, 2 aggregates, and 2 air void levels, resulting in a total of 64 cells. All mixes were prepared

at a fixed asphalt content near the optimum determined by the Caltrans mix design procedure (ASTM D1560, D1561). Mixes were compacted by the rolling wheel compaction method to produce specimens with target air void contents of 4 and 7 percent. The factorial experiment is summarized below:

Factor	Levels
Asphalt Source	AAA, AAB, AAC, AAD, AAF, AAG, AAK, AAL, AAM, AAV, AAW, AAX, AAZ, ABA, ABC, ABD
Aggregate Source	RD, RH
Air Voids	4 percent, 7 percent (target levels)
Replicates	1/cell
Total No. of Tests	64

Response variables included the normalized rutting rate (mm/MPa/hr—linear regressed rut rate between 2000 and 4000 passes divided by contact stress) and total rut depth (mm—rut depth after 5000 passes).

Binder properties provided by the A-002A contractor were measured from dynamic mechanical analysis (DMA) and included complex shear modulus (G^*), phase angle (δ), storage modulus (G'), loss modulus (G''), and loss tangent (tan δ).

The SHRP binder specification requires the value of $G^*/\sin\delta$ for any original binder to exceed 2.2 kPa when tested at 10 rad/s at the specified temperature after having been aged according to the rolling thin film oven test (RTFOT). The implication is that asphalt binders with $G^*/\sin\delta$ values exceeding this limit should contribute acceptable resistance to permanent deformation in asphalt-aggregate mixes, while binders with lower $G^*/\sin\delta$ values may contribute to rutting.

Asphalt binders and asphalt-aggregate mixes used in this study were subjected to similar aging and testing conditions. Asphalt binders were aged according to the RTFOT to simulate the short-term aging effects of the construction process. Asphalt-aggregate mixes were also subjected to short-term aging; after mixing, they were placed in an oven at 135°C (275°F) for 4 hours. Asphalt binder properties were calculated for and mixes were tested at a temperature of 40°C (104°F). Binder properties were calculated at a loading frequency of 10 rad/S, or 1.6 Hz. Mixes were tested at a loading frequency of 20 rad/s, or 3.2 Hz. Considering that binder properties are logarithmic functions of loading time, the difference in loading rates is not substantial.

Wheel-tracking tests were performed by SWK Pavement Engineering Ltd. at the University of Nottingham. A wheel fitted with a solid rubber tire passes over the top of a 200 mm (8 in.) diameter cylindrical core specimen at a frequency of approximately 3 Hz, or 20 rad/s. These tests were conducted at a temperature of 40°C (104°F), and each test was run for a duration of 5000 load passes (approximately 2 hours). Tests were performed with an applied load of approximately 620 N (140 lb). The contact area of the tire measured 850 mm^2 (1.32 in^2), which gives a corresponding contact stress of approximately 730 kPa (105 lb/in^2).

Two rutting parameters were measured from the wheel-track test data: normalized rut rate and total rut depth. The normalized rut rate is the rate of increase in rut depth (mm/hr) between 2000 and 4000 load passes divided by the contact stress of the wheel. The total rut depth is the average rut depth (mm) at the end of the test, i.e., after 5000 passes. SWK staff considered rut rate a more reliable indicator of permanent deformation performance because it is less likely to be affected by "initial start-up errors" and, perhaps, additional compaction of the specimen during the initial stages of the test.

Since it was hypothesized that asphalt source would significantly affect rutting response, analysis of variance (ANOVA) was performed to determine the influence of the various factors. The ANOVA indicated each of the factors and interactions accounting for the variation of rutting response by the following approximate proportions:

Rutting Response Variable	Factor or Interaction	Proportional Effect (%)
Rut Rate	Asphalt	26
	Aggregate	29
	Air Voids	8
	Asphalt-Aggregate	27
	ANOVA Model Error	5
Rut Depth	Asphalt	31
	Aggregate	19
	Air Voids	8
	Asphalt-Aggregate	28
	ANOVA Model Error	5

Since the aggregate and air void characteristics appeared to influence the rutting response, it was expected that the effect of asphalt properties might be masked somewhat by these other influences. In view of the aggregate and air void effects, as well as the interaction between asphalt source and aggregate source, the relationships between binder properties and mix rutting response were evaluated separately for each aggregate source and air void level. Complete statistical analyses were performed (SHRP, 1994). Typical results are shown in Figure 2.7.

The results indicate that a poor relationship exists between the binder property, $G^*/\sin\delta$, and mix rutting. As engineering logic would suggest, the value of $G^*/\sin\delta$ increases as rut rate and rut depth decrease. Comprehensive statistical analysis indicated that none of the binder properties (G^*, G', or G'') was highly correlated with rut depth or rut rate. In addition, substantial scatter in the data suggests that it would be difficult to predict rutting based solely on the binder properties. As illustrated by Figure 2.7 only 18 to 30 percent of the variation in rutting response is explained by the parameter $G^*/\sin\delta$. Thus, most of the variation in rutting response probably can be attributed to other variables such as aggregate characteristics or the testing process.

Although all the binders used in the wheel tracking experiment exceed the minimum specification value of 2.2 kPa (0.3 lb/in^2) for $G^*/\sin\delta$ (Harrigan et al, 1994), Figure 2.7 indicates that at least one of the asphalts, when combined with aggregate RH, produced a

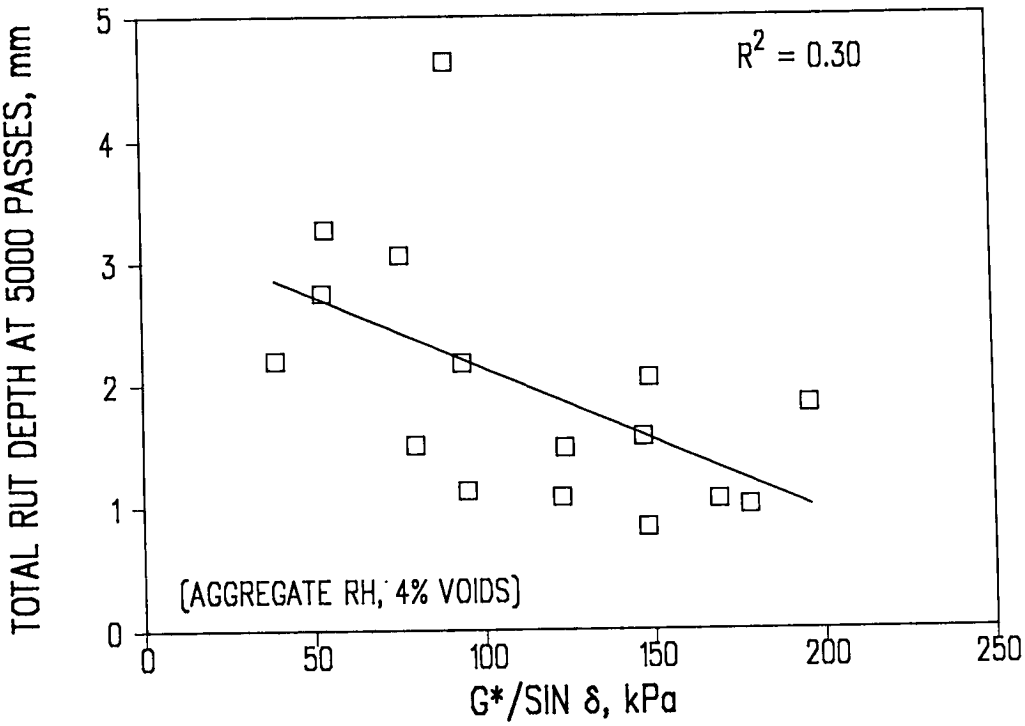

Figure 2.7a. Relationship between $G^*/\sin\delta$ and total rut depth

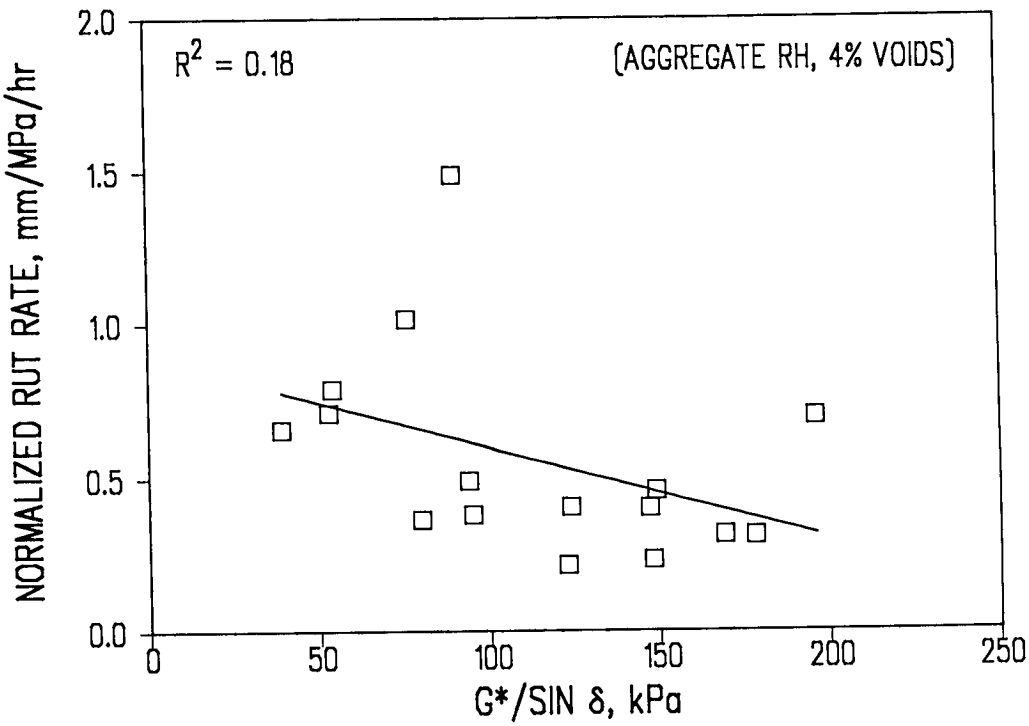

Figure 2.7b. Relationship between $G^*/\sin\delta$ and normalized rut rate

relatively high rut depth. It is uncertain that this level of rut depth measured in the wheel-tracking test would occur in a pavement built with that particular asphalt, nor does it imply that the specification limit is questionable. Rather, it underscores the need for mix evaluation in addition to the binder testing.

The results of this study might suggest that $G^*/\sin \delta$ is not a reliable predictor of potential rutting. Aggregate and air void characteristics appear to have more influence on the rutting response of asphalt-aggregate mixes than does the asphalt binder. However, several considerations temper this conclusion:

1) SWK staff acknowledged that the repeatability of wheel-tracking tests can be poor—i.e., a significant number of replicate tests should be conducted to obtain a reliable estimate of the rutting rate. A similar wheel-tracking study was performed on mixes made from two asphalts and two aggregates. Each cell of the experiment in that study included two replicates, from which test precision was calculated. The testing error in that study was nearly as significant as the asphalt effect was in this study. Thus, the relatively low test precision probably contributed to the low coefficients of determination (R^2) when trying to predict rutting response from $G^*/\sin \delta$.

2) Binder and wheel-tracking tests were conducted at 40°C (104°F). This temperature may not be sufficiently high to allow the viscous characteristics of binders to affect the mixture rutting response. Note that the SHRP binder specification does not provide for a climatic region for which binders would be tested at 40°C (104°F) for permanent deformation evaluation; the lowest test temperature is 45°C (113°F). At higher test temperatures, the binder effect might be more pronounced.

3) The magnitude of total rut depths for the better-performing mixes was relatively small in comparison with the testing error. SWK noted this fact as well, suggesting that an increase in the contact pressure and load applications may reduce the testing error.

4) While the wheel-tracking test equipment at the University of Nottingham is considered useful, it is relatively small. The surface area of the mix specimen is 40,000 mm^2 and the contact area of the rubber wheel is 850 mm^2 (1.32 in^2). Yet the aggregate size was typical of that used in conventional pavement mixes. Thus, the dimensional ratios in the wheel-tracking test were not the same as those that occur in real pavements.

Although not part of the SHRP research effort, other wheel-tracking tests conducted by SWK with modified mixes yielded more encouraging results with respect to the relationship between $G^*/\sin \delta$ and permanent deformation (Bouldin et al, 1994). As shown in Figure 2.8, there was excellent correlation between $G^*/\sin \delta$ and both rut rate and strain accumulation rate.

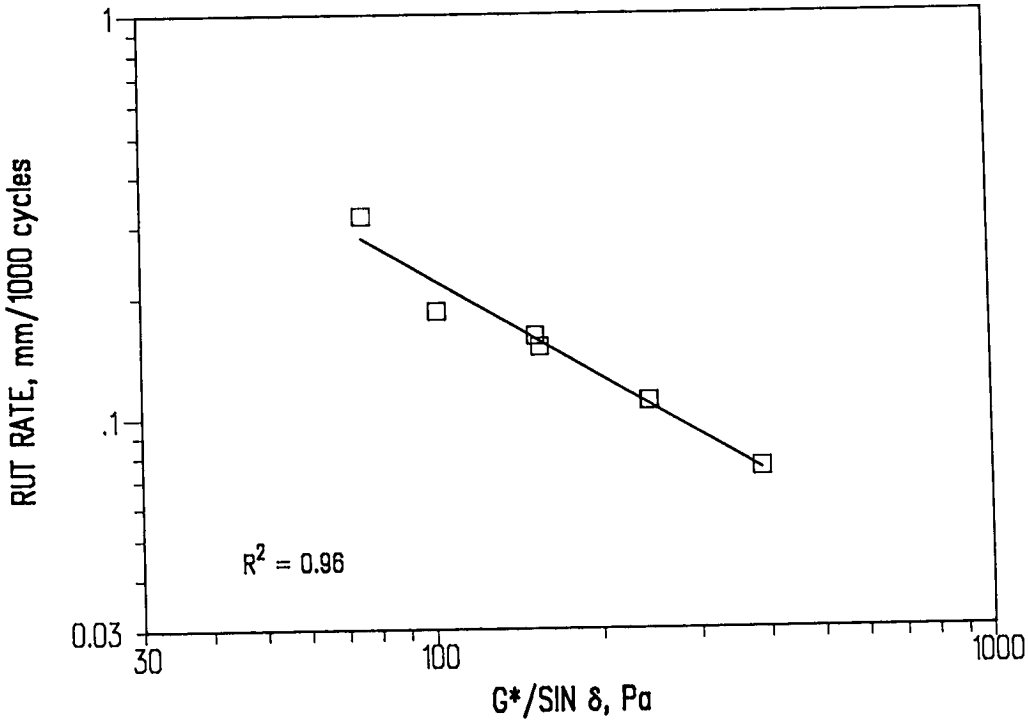

Figure 2.8a. Relationship between $G^*/\sin\delta$ and rut rate (Shell data)

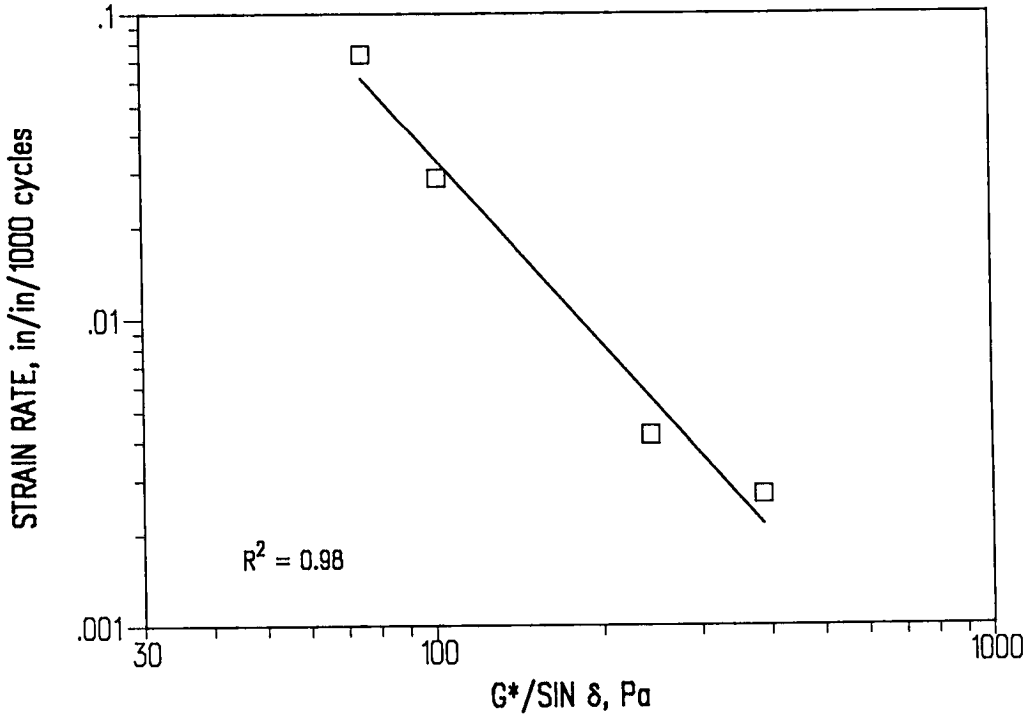

Figure 2.8b. Relationship between $G^*/\sin\delta$ and strain rate (Shell data)

Based on the conflicting data, it is apparent that additional testing with both modified and unmodified mixes is necessary to determine the effect of $G^*/\sin \delta$ on permanent deformation. It is recommended that future permanent deformation studies that employ wheel-tracking devices use higher contact stresses and/or more load repetitions. The precision of wheel-tracking test equipment should be improved to minimize testing error. Fortunately, larger wheel-tracking test equipment is beginning to appear in the United States. These devices will permit testing of larger slabs of asphalt concrete with boundary conditions representative of actual pavement structures.

2.4.2 Shear Tests

Binder properties were compared with the permanent deformation response of asphalt-aggregate mix specimens subjected to repetitive simple shear loading under controlled conditions in the laboratory. The hypotheses related to permanent deformation in asphalt-aggregate mixes are as follows:

1) Permanent deformation (rutting) in an asphalt concrete layer is caused by a combination of densification (volume change) and shear deformation resulting from the repetitive applications of traffic loads.

2) Permanent deformation is caused primarily by large shear stresses in the upper portions of the asphalt concrete layer.

3) Properties of asphalt (elastic and viscous) and aggregate that contribute to permanent deformation in asphalt-aggregate mixtures can be determined by using a simple shear test.

Therefore, the selection of the simple shear test is consistent with both A-002A and A-003A hypotheses regarding permanent deformation. It can measure the elastic (linear and nonlinear) and viscous influences of the binder in the asphalt-aggregate mixture. It also can simulate the shear stress conditions believed to be the primary cause of permanent deformation in asphalt concrete pavements.

Specimen conditioning, compaction, and target void contents were as reported in the wheel-tracking validation effort. All shear testing was conducted on cylindrical specimens 152 mm (6 in.) in diameter by 51 mm (2 in.) in height. A full factorial experiment was designed to evaluate all main effects and two-factor interactions. The factorial matrix consisted of 9 asphalts, 3 aggregates, and 2 air void levels, resulting in a total of 36 cells. Each cell had only one replicate, for a total of 36 tests for each shear test condition. Thus, a total of 72 shear test results were analyzed. Since no replicates were provided, the three-factor interaction of asphalt source, aggregate source, and air voids was used as an estimate of experimental error. The factorial experiment is summarized below:

Factor	Levels
Asphalt Source	AAB, AAC, AAD, AAG, AAK, AAM, AAV, AAZ, ABC
Aggregate Source	RD, RH
Air Voids	4 percent, 7 percent (target levels)
Replicates	1/cell
Test Condition	constant height (CH) or field state of stress (FS)[1]
Total No. of Tests	72

The response variables were as follows: load cycles to 2 percent strain, ($N_{2\%}$—number of shear load cycles at which the asphalt-aggregate mixture specimen exhibits 2 percent cumulative permanent shear strain) and cumulative permanent shear strain, ($\Sigma\gamma_p$—cumulative permanent shear strain after a constant number of load cycles).

Half the specimens in this study were tested under a *constant height* condition (CH), and the other half were tested under a *field state of stress* (FS) condition. The CH shear test is sensitive to elastic and viscous characteristics of the asphalt binder. It also measures the effect of dilatancy. Dilatancy in this case is the tendency of a mix to change in volume as aggregate particles are forced to slide past each other during shear deformation. The FS shear test incorporated loading conditions thought to represent the state of stress occurring in an asphalt concrete layer near the edge of a truck tire. An instrumented specimen is shown schematically in Figure 2.9.

The CH shear test applied a cyclic (haversine) shear stress of 103 kPa (15 lb/in^2) $\pm$ 10% to the specimens. The load pulse duration was 0.1 sec with 0.6 sec between load pulses. In addition, vertical compressive loads were applied as necessary to maintain the original specimen height throughout the test. The magnitude of the vertical compressive load is a function of the specimen's propensity to dilate under shear loading. Shear strain was calculated from the difference between displacements measured by two LVDTs (linearly variable differential transducer) located $\pm$ 1.27 cm (0.5 in.) at mid-height on each side of the specimen. Each test was scheduled to run for 3600 load cycles. But many were stopped before reaching this number of load cycles if the specimen exhibited 4 percent permanent shear strain or if failure occurred.

The FS shear test simultaneously applied a cyclic shear stress of 173 kPa (25 lb/in^2) $\pm$ 10% and a cyclic compressive axial stress of 345 kPa (50 lb/in^2) $\pm$ 10%, both with load pulse durations of 0.1 sec and 0.6 sec between load pulses. In addition, a constant confining pressure of 138 kPa (20 lb/in^2) was applied to the specimen. Each test also was scheduled to run for 3600 load cycles; all but three of the FS tests completed the scheduled 3600 load cycles.

---

[1]Field state of stress (FS) describes the state of stress in which there is a constant ratio between the vertical stress and horizontal shear stress, i.e., σ/τ = constant.

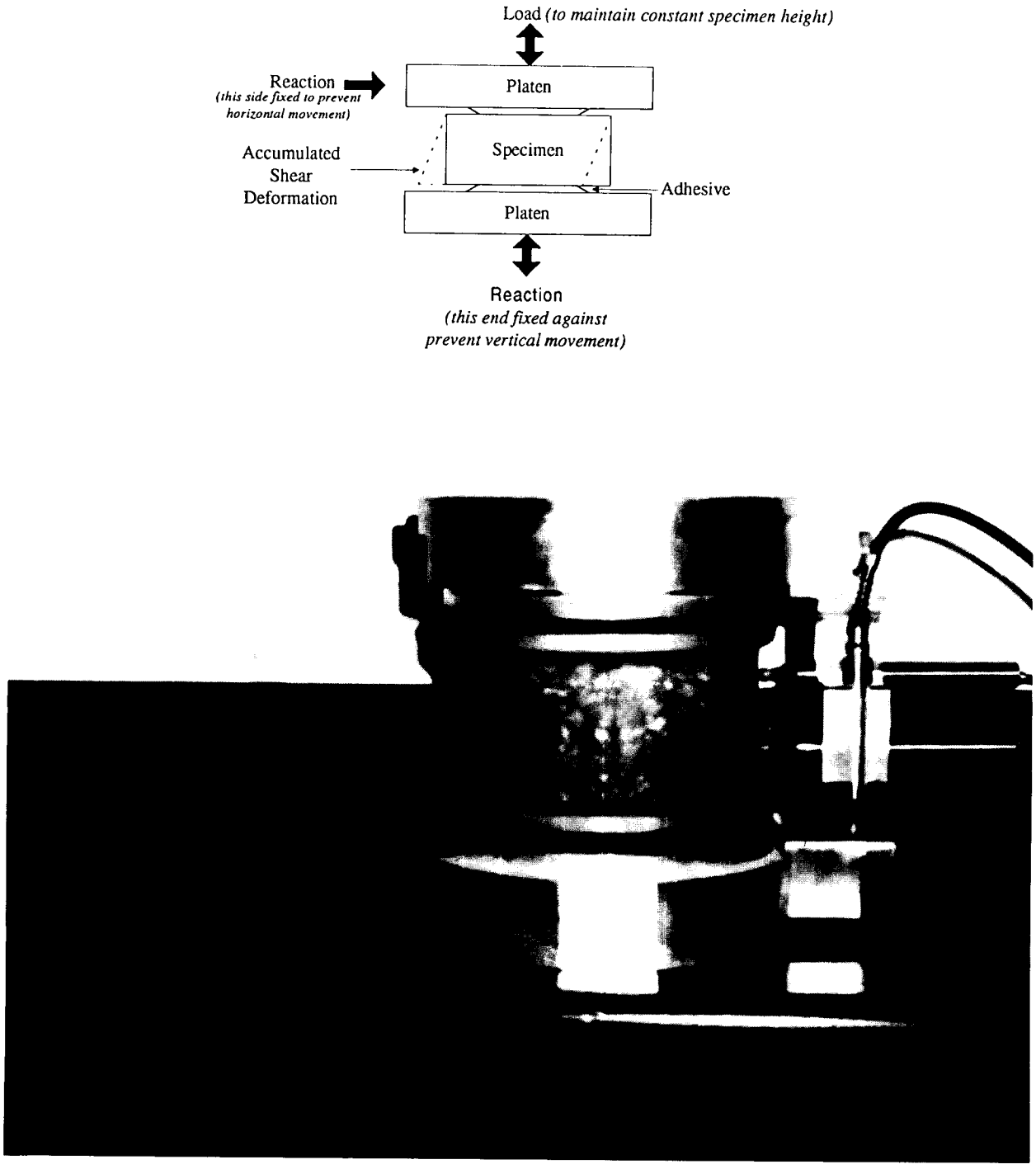

Figure 2.9. Simple shear test load conditions and instrumented specimen

Two shear response parameters were calculated from each of the above shear test conditions for comparison with asphalt binder properties:

1) the number of load cycles at which the specimen exhibited 2 percent cumulative permanent shear strain, or $N_{2\%}$; and

2) the cumulative permanent shear strain after a constant number of load cycles, or $\Sigma\gamma_p$.

For CH tests, $\Sigma\gamma_p$ values at 32 load cycles were used in the following analyses. This was the highest number of load cycles that allowed all specimens to be analyzed. Similarly, for FS tests, $\Sigma\gamma_p$ values at 602 load cycles were used.

Although binders and asphalt-aggregate mixes both were tested at a temperature of 60°C (140°F), they were tested at substantially different loading frequencies: Binders were tested at a loading frequency of 10 rad/s (1.6 Hz); and the mixes at 62.8 rad/s (10 Hz). Because of the faster loading, it is possible that the binders in the asphalt-aggregate mixes exhibited more of their elastic nature and less of their viscous nature than the binders tested alone (i.e., in the asphalt binder tests).

The results of an ANOVA model on the shear test data indicated that asphalt source, aggregate source, and air void level each significantly affect the shear response ($N_{2\%}$ and $\Sigma\gamma_p$) of asphalt-aggregate mixtures. The model indicated each of the factors influencing shear response in the following approximate proportions:

		Factor	Proportional Effect (%)
CH Shear Test:	$N_{2\%}$	Asphalt	28
		Aggregate	20
		Air Voids	18
		Model Error	19
	$\Sigma\gamma_p$	Asphalt	29
		Aggregate	21
		Air Voids	18
		Model Error	18
FS Shear Test:	$N_{2\%}$	Asphalt	24
		Aggregate	52
		Air Voids	5
		Model Error	17
	$\Sigma\gamma_p$	Asphalt	33
		Aggregate	39
		Air Voids	6
		Model Error	22

Note that the influence of asphalt in the CH shear tests was approximately equal to that observed in the FS shear tests. Note the substantial effect of aggregate in the FS shear tests.

Since asphalt source significantly affected rutting response, it was expected that additional analyses would show some relationship between asphalt binder properties and asphalt-aggregate mix shear response, especially for data from CH shear tests. But since aggregate and air void characteristics appeared to influence shear response more, it was expected that the effect of asphalt properties might be obscured somewhat by these other influences, especially for data from FS shear tests. In light of the aggregate and air void effects, the relationships between binder properties and mix shear response were evaluated separately for each aggregate source and air void level (SHRP, 1994). Typical results are shown in Figures 2.10 and 2.11.

While there is significant scatter in the data, there does appear to be some relationship. The strongest relationships and least data scatter are exhibited for mixes containing RH aggregate at 7 percent air voids tested under CH test conditions. In Figures 2.10 and 2.11, for example, the expected relationships between the binder property, $G^*/\sin\delta$ (or G^*, G', and G'') and mix response are observed: As parameter $G^*/\sin\delta$ increases, the number of load cycles before the specimen exhibits 2 percent permanent shear strain increases (i.e., $N_{2\%}$ increases); the amount of permanent shear strain after a given number of load cycles decreases (i.e., $\Sigma\gamma_p$ decreases). Although not shown here, graphical analysis of the data indicates that the strength of the relationship between $G^*/\sin\delta$ (or G^*, G', and G'') and mix shear response weakens considerably as air voids change from 7 to 4 percent and as the aggregate source changes from RH to RD. Furthermore, it was noted that data resulting from CH shear tests generally provide stronger relationships and less data scatter than FS shear test data. The lower correlations from the FS shear test data probably are the result of the overwhelming effect of aggregate characteristics; recall the proportional effect determined by the ANOVA model.

A comparison was made between the SHRP binder specification limit for $G^*/\sin\delta$ related to permanent deformation and $\Sigma\gamma_p$ observed in laboratory simple shear testing. As illustrated in Figure 2.11, MRL binder AAV with a $G^*/\sin\delta$ of 1333 Pa (0.2 lb/in^2) (at 60°C [140°F] and 10 rad/s) does not meet the minimum specification requirement of 2.2 kPa (0.3 lb/in^2); binder AAC ($G^*/\sin\delta$ = 2674 Pa (0.4 lb/in^2)) barely meets the specification. The results shown in Figure 2.11 indicate that a minimum of 2.2 kPa (0.3 lb/in^2) is generally a valid specification requirement. Mixes containing AAV asphalt exhibited the highest values of $\Sigma\gamma_p$ in most cases. For mixes containing RH aggregate and compacted to 4 percent air voids, however, the value of $\Sigma\gamma_p$ for AAC was equal to that of AAV, yet AAC meets the specification (Figure 2.12). For mixes containing RD aggregate and compacted to 4 percent air voids (Figure 2.13), it was observed that AAB and AAG ($G^*/\sin\delta$ = 3251 (0.5 lb/in^2) and 4311 Pa (0.6 lb/in^2), respectively), while meeting the specification limit, produce higher values of $\Sigma\gamma_p$ than do either AAV or AAC. One cannot be certain that the magnitude of $\Sigma\gamma_p$ in Figure 2.13 suggests a potential rutting problem in the pavement. This comparison does demonstrate, however, the possibility of accepting an asphalt according to the specification limit that may result in rutting, or rejecting an asphalt that would provide acceptable performance.

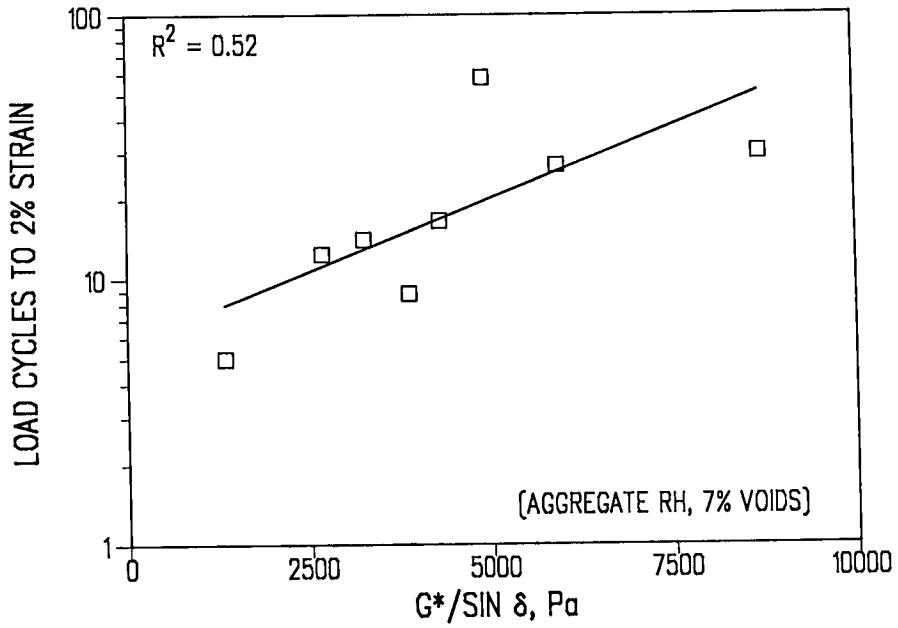

Figure 2.10. Relationship between $G^*/\sin\delta$ and load cycles to 2 percent strain

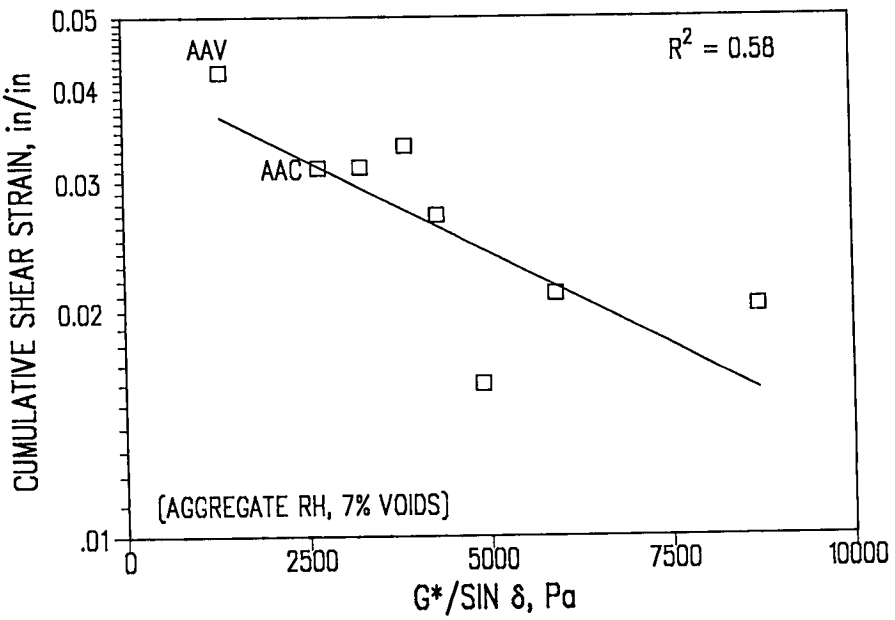

Figure 2.11. Relationship between $G^*/\sin\delta$ and cumulative shear strain

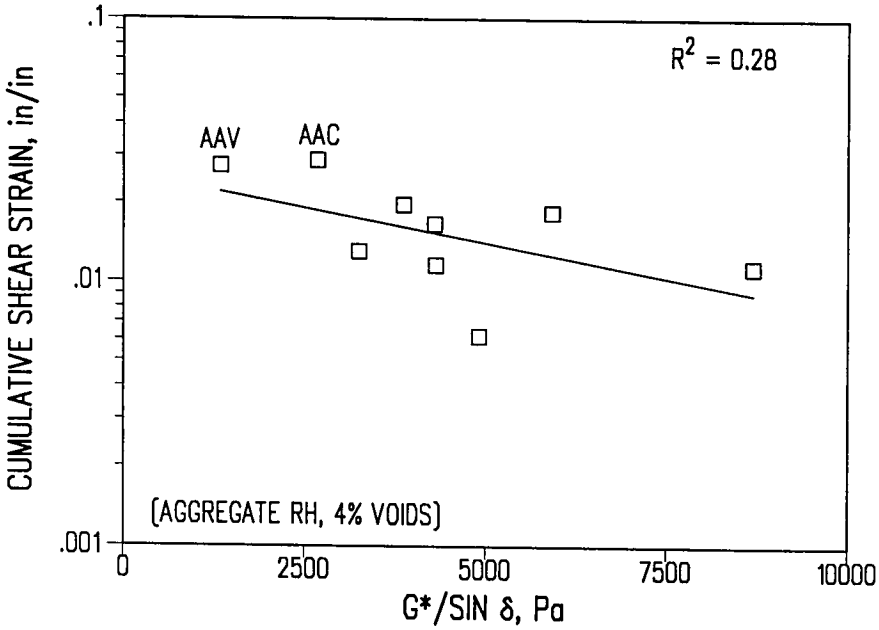

Figure 2.12. Relationship between $G^*/\sin\delta$ and cumulative shear strain (aggregate RH, 4 percent air voids)

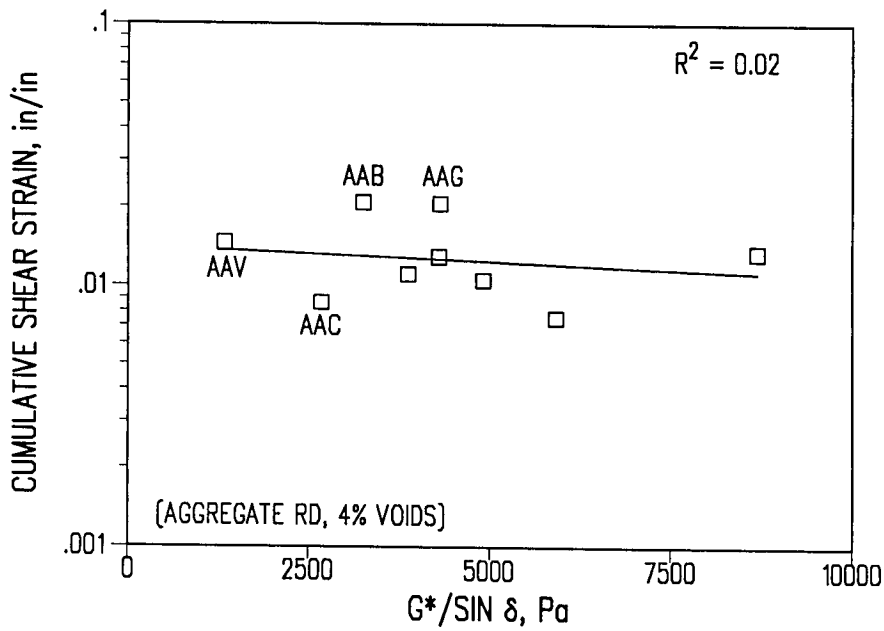

Figure 2.13. Relationship between $G^*/\sin\delta$ and cumulative shear strain (aggregate RD, 4 percent air voids)

Overall, the results of this study indicate that binder properties can affect the shear response of asphalt-aggregate mixes. Aggregate characteristics, however, can be equally or more significant. Specific findings from this study include the following:

1) Stronger relationships between asphalt binder properties and mix shear response ($N_{2\%}$ or $\Sigma\gamma_p$) were observed for mixes tested under CH conditions than for mixes tested under FS conditions. The researchers believe this is the result of the overwhelming influence of aggregate in the FS shear test. The confining pressure in the FS shear test provides stability to the aggregate skeleton of the mix. This minimizes strains in the asphalt binder, reducing the influence of the binder properties. The results of the ANOVA support this hypothesis; the influences of binder properties and air void level are less pronounced in the FS shear test. The CH shear test, however, confines specimen deformation in only one direction (i.e., the height of the specimen remains constant). Aggregate particles are allowed to "slide" past each other during shear loading, causing larger strains in the asphalt, which highlights the influence of the binder.

2) Although the relationships between binder properties and mix shear response generally are weak, it appears that any binder property ($G^*/\sin\delta$, G^*, or G'') can be used to estimate mix shear response with the same degree of reliability (poor). Thus, the significance of the sin δ term in $G^*/\sin\delta$ is questionable, although it may have more of an effect with modified binders.

3) The strongest relationship between asphalt binder properties and mix shear response was observed for mixes containing RH aggregate and 7 percent air voids. This suggests that when mix characteristics are such that they result in low interparticle friction, the influence of asphalt binder properties becomes more significant. Aggregate RD was a quarried product that is 100 percent crushed; RH was a partially crushed river gravel that would be expected to provide less interparticle friction than RD. This underscores the influence of aggregate characteristics on permanent deformation.

2.4.3 Conclusions

The results of A-003A's efforts to validate the effect of A-002A's asphalt binder properties on the permanent deformation response of asphalt-aggregate mixes indicate that the influence of asphalt is highly dependent on the conditions to which the mix is subjected. ANOVA showed the effect of asphalt was significant but that its influence was small compared with that of aggregate, especially when the mix was tested at lower temperatures (e.g., 40°C [104°F]) or was subjected to states of stress that amplified the aggregate influence (e.g., FS shear test).

The correlations between $G^*/\sin\delta$ and the various measures of permanent deformation response were generally poor, with the exception of the wheel-tracking data reported by

Shell. The weak correlations are partly the result of the dominant effect of aggregate characteristics on permanent deformation response. But in cases where interparticle friction is low (e.g., RH aggregate and 7 percent air voids) and the mix is subjected to harsh environmental and loading conditions (e.g., 60°C [140°F] and CH shear test), the influence of the binder becomes more readily apparent. When aggregate characteristics and/or compaction conditions are expected to result in a mix that is susceptible to permanent deformation, selection of an asphalt that can overcome these deficiencies will be important. It appears that the value of $G^*/\sin \delta$ may be used to screen binders that will provide inferior performance in such cases.

The results of these studies underscore the importance of mix testing, in addition to binder testing, for evaluation of permanent deformation in pavements. It is recognized that the mix tests used in these validation efforts are only estimates of the permanent deformation response that would actually occur in a pavement. Nevertheless, the general conclusions presented herein are expected to hold when future studies compare binder properties with permanent deformation response of mixes measured from larger-scale wheel-tracking tests and actual pavement performance.

2.5 Thermal Cracking

The A-002A ranking for resistance to low-temperature cracking is based on the limiting stiffness temperature and the ultimate strain at failure. The limiting stiffness temperature is estimated based on a stiffness value of 200 MPa (29 k/in^2) at a loading time of 2 hours in the bending beam rheometer. The ultimate strain at failure is estimated at -26°C (-15°F) and a loading time of 2 hours in the direct tension test. The experiment design for this task was developed to relate fundamental properties of asphalt cement suggested by the A-002A contractor to the low-temperature cracking characteristics of asphalt concrete mixes, as measured by the thermal stress restrained specimen test (TSRST).

The experiment design included 14 asphalt cements and two aggregates. Two degrees of aging and two levels of air void content are employed. The fully replicated factorial design was developed as follows:

Experiment Design Variable	Levels
Asphalt Type	14
Aggregate Type	2
Degree of Aging	2 (Short, Long)
Air Void Content	2 (4 percent, 8 percent)
Rate of Cooling	1 (10°C/hr [50°F/hr])
Replicates	2
No. of tests	224

The MRL asphalts and aggregates used in the study are listed below.

Asphalts: AAA, AAB, AAC, AAD, AAF, AAG, AAK, AAL, AAM, AAV, AAW, AAX, AAZ, ABC

Aggregates: RC, RH

As noted above, two aging levels were considered. After mixing, the loose mix was subjected to short-term oven aging (STOA) for 4 hours at 135°C (275°F). Following short-term oven aging, the mix was compacted. Some of the specimens also were long-term oven aged (LTOA) for 5 days at 85°C (185°F).

Prismatic specimens 5 cm × 5 cm × 25 cm (2 in. × 2 in. × 10 in.) were prepared using a kneading compactor. The TSRST was used to evaluate all mixes (STOA and LTOA). Placed in a stand to ensure proper alignment, specimens were glued to end platens with an epoxy compound. After the epoxy had cured, the test specimen was cooled to a temperature of 5°C (41°F) for 1 hour to establish thermal equilibrium before testing. The specimen and end platens were then placed in an environmental cabinet and cooled at a rate of 10°C/hr (50°F/hr) until fracture.

Typical TSRST results are shown in Figure 2.14. From the test results, four parameters were identified to relate the fundamental properties of asphalt cement and aggregate to thermal cracking characteristics of asphalt concrete mixes. The TSRST results illustrated in Figure 2.14 include fracture temperature, fracture strength, slope of the thermally induced stress curve, and transition temperature. Only fracture temperature and strength are discussed here. Of the 224 specimens prepared, 201 were used in analysis, 23 were deemed unacceptable because void contents were not within the acceptable range.

Fracture temperature is defined as the temperature at which fracture occurs and corresponds to the temperature at which the thermal stress induced is maximum. A summary of the fracture temperature data is shown in Table 2.2. Mean values and the coefficients of variation of fracture temperature for a specific asphalt type, aggregate type, and degree of aging may be found elsewhere (SHRP, 1994).

The repeatability of TSRST for fracture temperature is quite good, as the coefficients of variation for fracture temperature are typically less than or equal to 10 percent. As expected, fracture temperature varies with asphalt type. For mixes with the RC aggregate, fracture temperature ranged from -32.1°C to -18.6°C (-25.8°F to -1.5°F) and from -27.8°C to -13.6°C (-18.0°F to 7.5°F) for STOA and LTOA specimens, respectively. For specimens with the RH aggregate, fracture temperatures ranged from -32.2°C to -16.3°C (-26.0°F to 2.7°F) and from -29.3°C to -13.6°C (-20.7°F to 7.5°F) for STOA and LTOA specimens, respectively.

Fracture strength is defined in terms of the maximum stress. Mean values and the coefficients of variation of fracture strength for a specific asphalt type, aggregate type, and degree of aging were determined (SHRP, 1994). A summary of the fracture strength data is shown in Table 2.3.

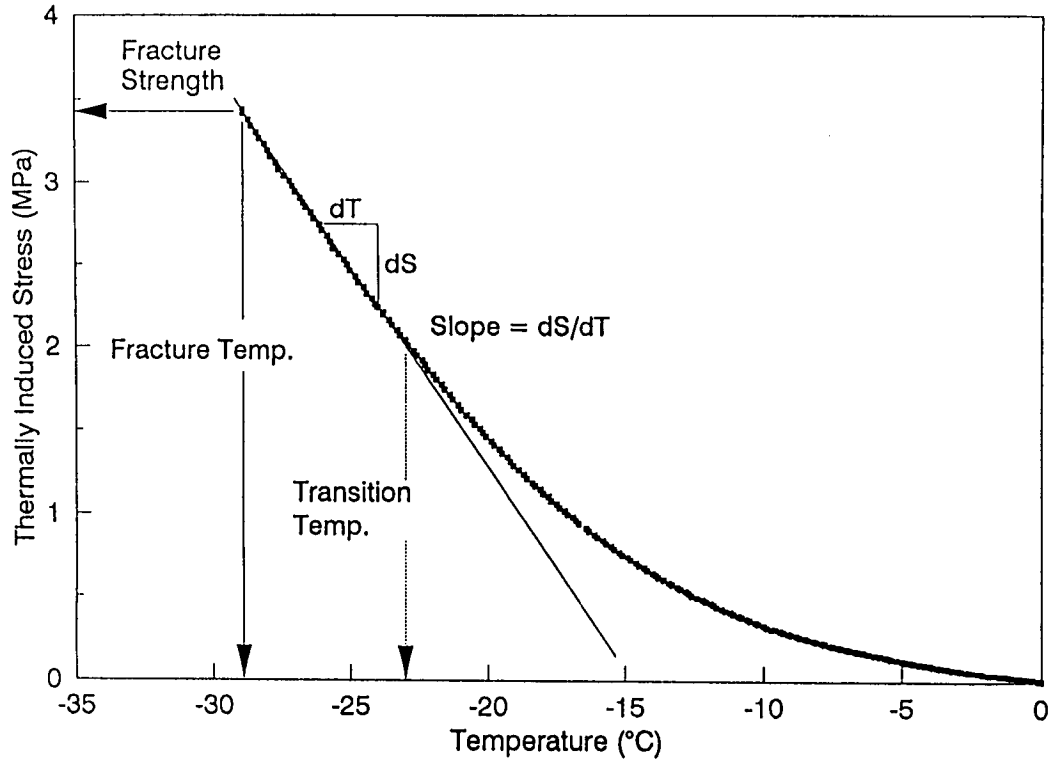

Figure 2.14. Typical TSRST results

Table 2.2. Summary statistics for fracture temperature

Aggregate Type	Degree of Aging	Warmest Fracture Temperature (°C)	Coldest Fracture Temperature (°C)	Range (Warm-Cold)
RC	STOA	-18.6	-32.1	15.4
	LTOA	-13.6	-27.8	12.9
	Difference (STOA-LTOA)	Minimum -0.6	Maximum -6.5	Average -3.8
RH	STOA	-16.3	-32.2	15.7
	LTOA	-13.6	-29.3	14.8
	Difference (STOA-LTOA)	Minimum -0.6	Maximum -5.5	Average -2.9
Difference in STOA (°C) (RC-RH)		Maximum: -3.8 Minimum: 0.9 Average: -1.16		
Difference in LTOA (°C) (RC-RH)		Maximum: -2.0 Minimum: 1.6 Average: -0.42		

Table 2.3. Summary statistics for fracture strength

Aggregate Type	Degree of Aging	Maximum Fracture Strength (MPa)	Minimum Fracture Strength (MPa)	Range (Maximum-Minimum)
RC	STOA	2.922	1.877	1.045
	LTOA	2.903	2.109	0.794
	Difference (STOA-LTOA)	Maximum 0.726	Minimum -0.670	Average 0.20
RH	STOA	3.512	2.584	0.928
	LTOA	3.447	1.983	1.464
	Difference (STOA-LTOA)	Maximum 0.379	Minimum -0.634	Average -0.02
Difference in STOA (MPa) (RC-RH)		Maximum: 1.105 Minimum: -0.296 Average: 0.467		
Difference in LTOA (MPa) (RC-RH)		Maximum: 0.763 Minimum: -0.260 Average: 0.249		

The repeatability of TSRST for fracture strength is considered reasonable, as coefficients of variation are, with few exceptions, less than 20 percent. The fracture strengths exhibit a wide range of values, depending on asphalt type.

Although comprehensive statistical analyses were performed to assess the influence of asphalt type, aggregate type, void content, and degree of aging on the TSRST results, this discussion focuses on a comparison of the binder specification properties and A-003A mix properties.

The A-003A performance ranking of asphalts and aggregates for resistance to low temperature cracking of mixtures was compared with the A-002A ranking (Anderson, et al, 1994). Also, fracture temperature was related to the A-002A low-temperature index test results and asphalt cement properties. Linear regression analyses were performed to correlate fracture temperature to A-002A low-temperature index test results and asphalt cement properties.

Fracture temperature was compared with the A-002A low-temperature index test results—specifically, the temperature at limiting stiffness and *m*-value from the bending beam rheometer test, and the ultimate strain at failure from the direct tension test. Fracture temperature shows an excellent correlation with the A-002A test results. Figures 2.15 and 2.16 show the relationship between fracture temperature and temperature at limiting stiffness (S(t)=200 MPa (29 k/in^2) at 2 hours) and *m*-value, respectively. The relationship between fracture temperature and ultimate strain at failure is shown in Figure 2.17.

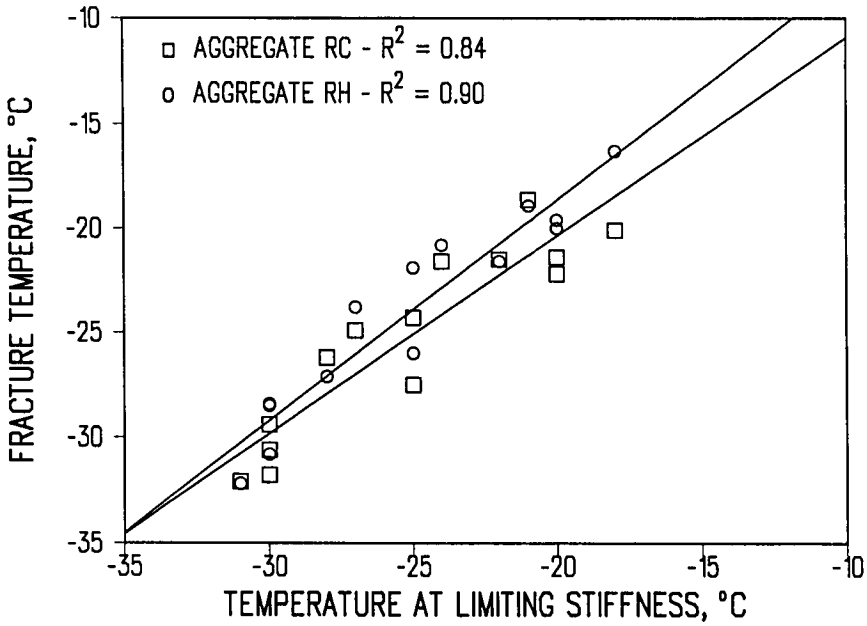

Figure 2.15. Relationship between limiting stiffness and fracture temperature

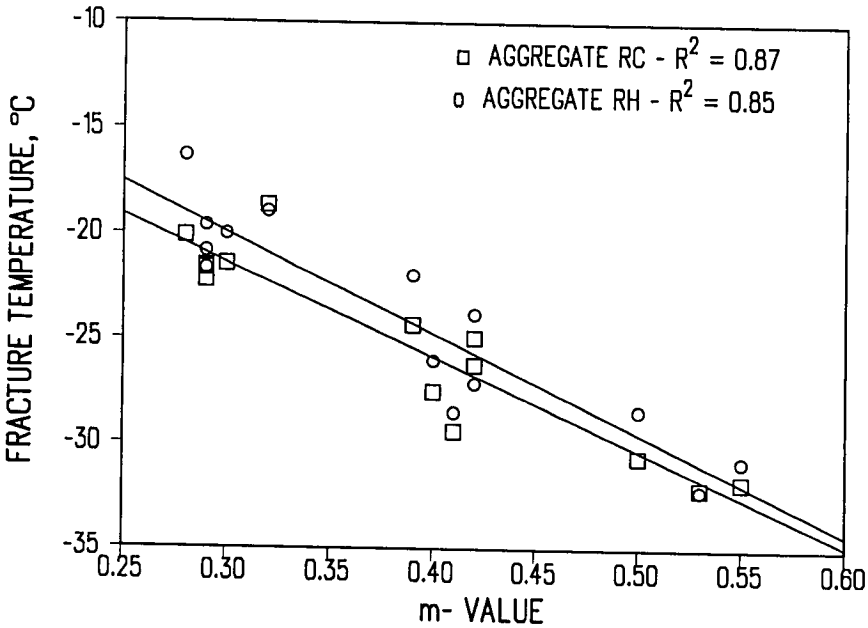

Figure 2.16. Relationship between *m*-value and fracture temperature

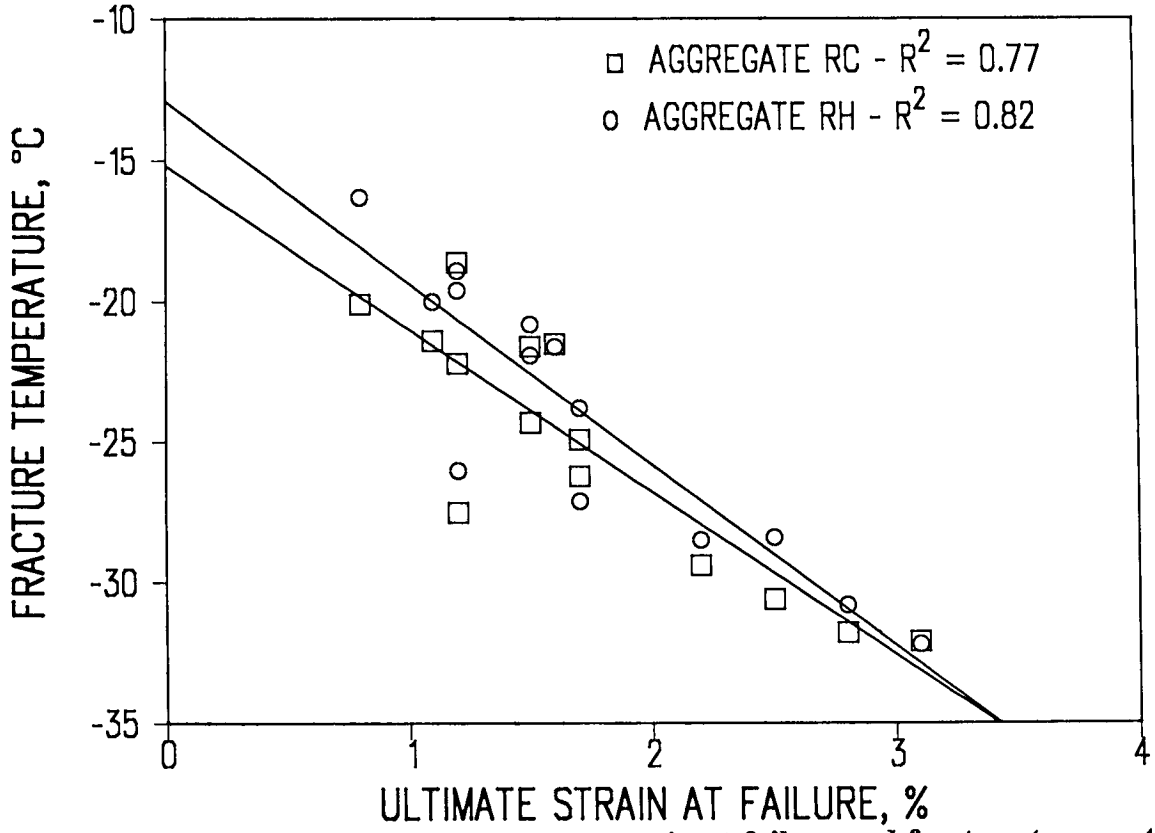

Figure 2.17. Relationship between ultimate strain at failure and fracture temperature

2.5.1 Conclusions

Based on the results presented here, the following conclusions are appropriate:

1) Asphalt type, aggregate type, degree of aging, and air void content all have a substantial effect on the low-temperature cracking characteristics of asphalt concrete mixtures. The effect of interactions between mix properties is considered minor.

2) Asphalt type, degree of aging, air void content, and the interaction between asphalt and degree of aging are significant factors for the fracture temperature. Fracture temperature was warmer for long-term-aged mixes. Fracture temperature is most affected by asphalt type and degree of aging. Air void content and interaction between asphalt type, also affect fracture temperature, though to a much lesser extent.

3) Asphalt type, aggregate type, air void content, and the interaction between aggregate and degree of aging are significant factors for fracture strength. Fracture strength is highly influenced by air void content and aggregate type. Fracture strength was greater for mixes with lower air voids compared with those with higher air voids, and greater for mixtures with RH aggregate than for those with RC aggregate. Asphalt type and the interaction between

aggregate type and degree of aging have a minor influence on fracture strength. The effect of degree of aging on fracture strength is inconclusive.

4) As shown below, fracture temperature measured in the TSRST was highly correlated to A-002A low-temperature index test results—specifically, the temperature at limiting stiffness, the *m*-value, and the ultimate strain at failure.

A-003A Mix Property	A-002A Binder Property	R^2
Fracture Temperature	Limiting Stiffness	0.84 - 0.90
Fracture Temperature	Ultimate Strain at Failure	0.77 - 0.82
Fracture Temperature	*m*-value	0.85 - 0.87

2.6 Conclusions

The A-003A contractor attempted to validate the findings and recommendations of the A-002A contractor relative to the influence of asphalt on the three key distresses incorporated in the SHRP asphalt research program.

The findings are encouraging for fatigue and low-temperature cracking, but less so for permanent deformation. No specific properties have been associated with aging and water sensitivity in the SHRP binder specification. The specifications do stipulate, however, that tests for rheological properties will be made with either tank, short-term- or long-term-aged materials, depending on performance requirements. The results indicate that asphalt properties, as well as aggregate properties, influence the effect of both of these distress-related factors. These effects should be evaluated in the asphalt-aggregate mix to be confident of their effects on pavement performance.

3

Stage 2 Validation

Researchers at the Texas Transportation Institute (TTI) and Pennsylvania State University were charged with the validation of binder and mix tests/properties as they relate to the field performance in terms of fatigue cracking, permanent deformation, and low- temperature cracking. This stage 2 validation is described in Development and Validation of Performance Prediction Models and specifications for Asphalt Binders and Paving Mixes (Lytton et al, 1994).

3.1 Limitations of the Stage 2 Validation

The term "validation" does not mean verification of the specifications by means of incontrovertible evidence. To do so would have required more time and a more thorough study of the SHRP data from the laboratory and field than were available to the A-005 researchers. Rather, to validate the selected properties for the specification is to determine whether the trends in the data are correct and of reasonable proportion. It will remain a task for the future, as in the Long Term Pavement Performance (LTPP) SPS-9 study, to use properly calibrated performance prediction models with long-term field data from controlled experiments to refine the specification limits.

The validation efforts reported here address the following:

1) an empirical study of the strain and stiffness of the asphalt binder in tension;

2) a study of the slopes of the log compliances of the mix and of the binder, and their relationship to binder rheology (these relationships are evaluated for the load-related distress of rutting and fatigue cracking);

3) a study of binder stiffness (S) and slope of the log compliance curve (m) for thermal cracking; and

4) calibration of performance prediction models.

It is important to note that each investigation *independently* found it impossible to set any binder specification limit independent of the properties of the aggregate. The thermal coefficient of contraction of the mix is strongly dependent upon that property of the aggregates. A range of mix performance maybe observed with the same or virtually the same binder because of this property of the aggregate. In permanent deformation, only a fraction of the total rut depth can be attributed to the properties of the asphalt-bound layer because the supporting layers contribute to the rutting as well. A careful analytical study with a calibrated performance prediction model to isolate the effect of the asphalt-bound layer would be necessary to further refine the binder specification. Fatigue cracking occurs more rapidly in pavements with underdesigned structures, as well as with asphalts with little resistance to fracture.

3.2 Experimental Design

As noted above, one of the key objectives of the A-005 contract was to validate the selected binder and mix properties with field performance data. Ideally, this would require a widespread geographic distribution of sites to encompass a range of climatic zones and data from well-documented, in-service pavement sections in which the following are known:

- complete construction, traffic, and environmental histories;
- distress history and deflection test measurements; and
- layer thicknesses and material properties, including base course(s) and subgrade.

Although data from several excellent field studies were available, none had all the characteristics described above. Hence the preponderance of the data were generated from the LTPP's General Pavement Studies (GPS) sites.

The experimental design for the validation effort is shown in Figure 3.1. Two experiments were designed: one for the load-related distresses (rutting and fatigue cracking) and one for the non-load-related distress (low-temperature cracking). Each was designed to have pavement sections located in different climatic zones with the different types and varying distress levels. The total number of pavement sections in the overall experiment was 72, with 48 in the load-related portion and 24 in the non-load-related portion. The validation program required extensive sampling and testing of the field cores and extracted binders, as well as maximum use of nondestructive testing data.

Thirty-six to 46 cores were taken from each site and tested for the following:

- compressive and tensile creep and recovery;
- frequency sweep in compression and tension;

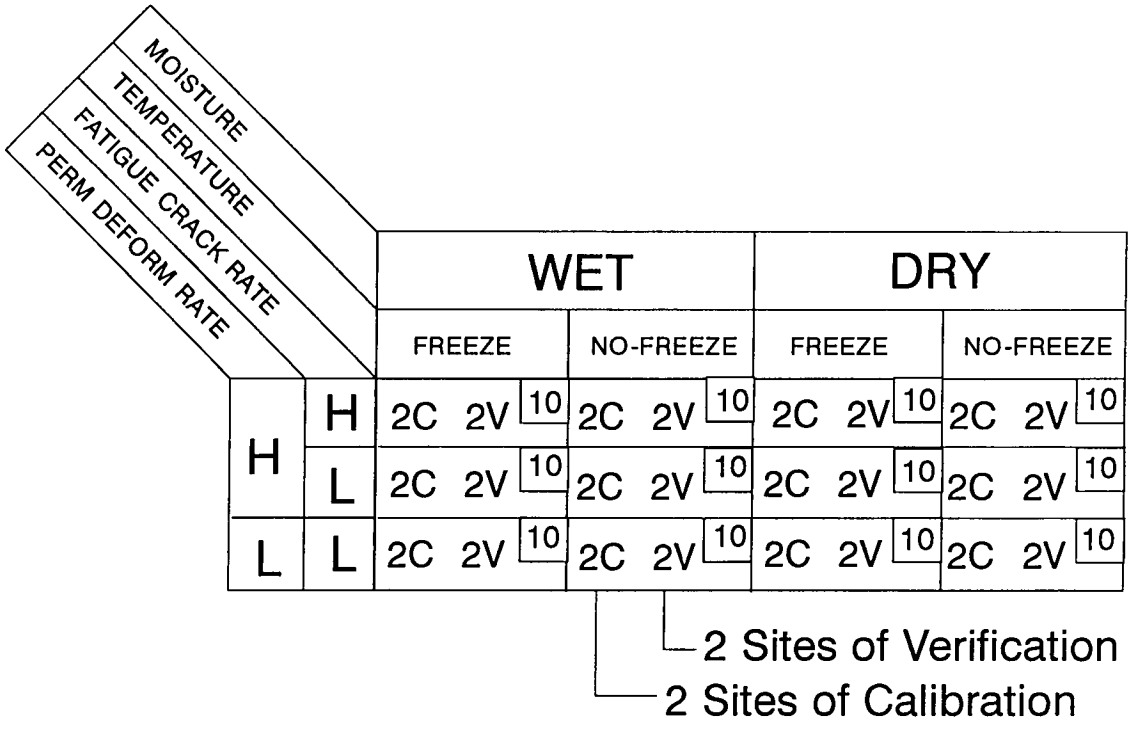

a. **Load-related experiment**

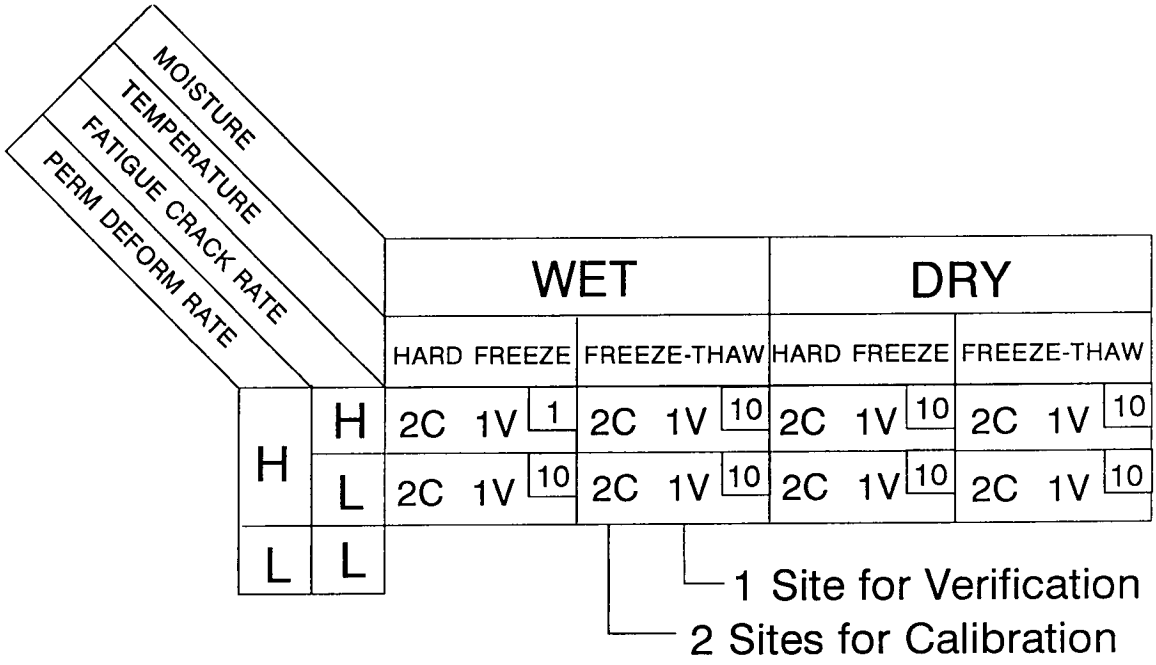

b. **Non-load-related experiment**

Figure 3.1. Experimental design for stage 2 validation

- indirect tensile creep and recovery; and
- indirect tensile strength.

After testing, the binder was extracted and recovered from the cores for evaluation of its physical and rheological properties. Rheological tests were conducted to determine the linear viscoelastic properties, which were then used to develop master stiffness and creep compliance curves.

3.3 Binder and Mix Compliance: Load-Related

Frequency sweep tests were made on core samples from all of the load-related GPS sites. The test results were analyzed with nonlinear regression analysis to produce the creep compliance parameters of the mix. The binder was extracted from cores from each load-related GPS site, and rheological tests were conducted at a variety of frequencies and temperatures. This resulted in a master shear creep compliance curve and a time-temperature shift function for the extracted binder. Figure 3.2 illustrates the relationship between the slope of creep compliance of the binder and the mix.

3.4 Empirical Validation: Load-Related

Figure 3.3a shows a comparison of G^* and sin δ versus rutting. The G^* and sin δ values were calculated at 52°C and 70°C (126°F and 158°F) for pavement sections in freezing and nonfreezing climates, respectively. The 52°C and 70°C (126°F and 158°F) temperatures are the lowest and highest temperatures, respectively, at which the SHRP binder specification tests are conducted. The G^* and sin δ plots for fatigue cracking in Figure 3.3b also show an interspersion of high and low cracking rates over the entire area of the graph. Shown in Figure 3.4a is the relationship between the binder specification property and measured rut depth; Figure 3.4b illustrates the relationship between the binder specification property and observed fatigue cracking. Note in Figure 3.4a that all the field sections but one meet the binder specification requirement for permanent deformation. Note also that in the data set there was not excessive rutting, as the maximum rut depth observed was less than 1.8 cm (0.7 in.). The adequacy of the binder specification with respect to fatigue cracking is more tentative. As seen in Figure 3.4b, there were very few sections in the data set that exhibited fatigue cracking, all of which had a G^*sin δ well below the specification maximum of 5000 kPa (725 lb/in^2).

By normalizing the data to eliminate the pavement geometry, it is clear from Figures 3.3 and 3.4 that there is an equal chance of the pavement having a high rate of either rutting or fatigue cracking, regardless of the binder property. This may reflect the effect of mix design, construction, climate, or any combination of these factors. The lack of clear trends in the data highlights the fact that the binder specification cannot be used in isolation to increase the probability of enhanced pavement performance.

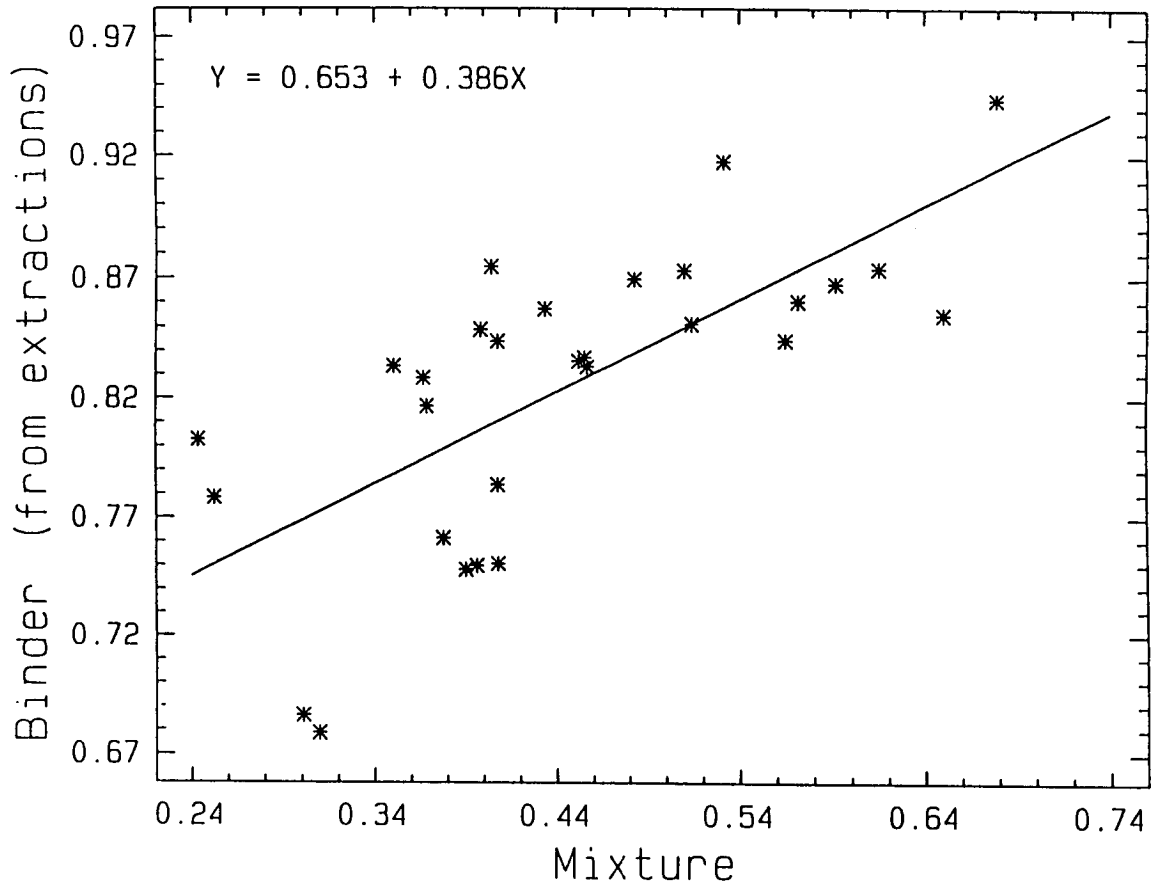

Figure 3.2 Relationship between log of slope of creep compliance of binder and mix

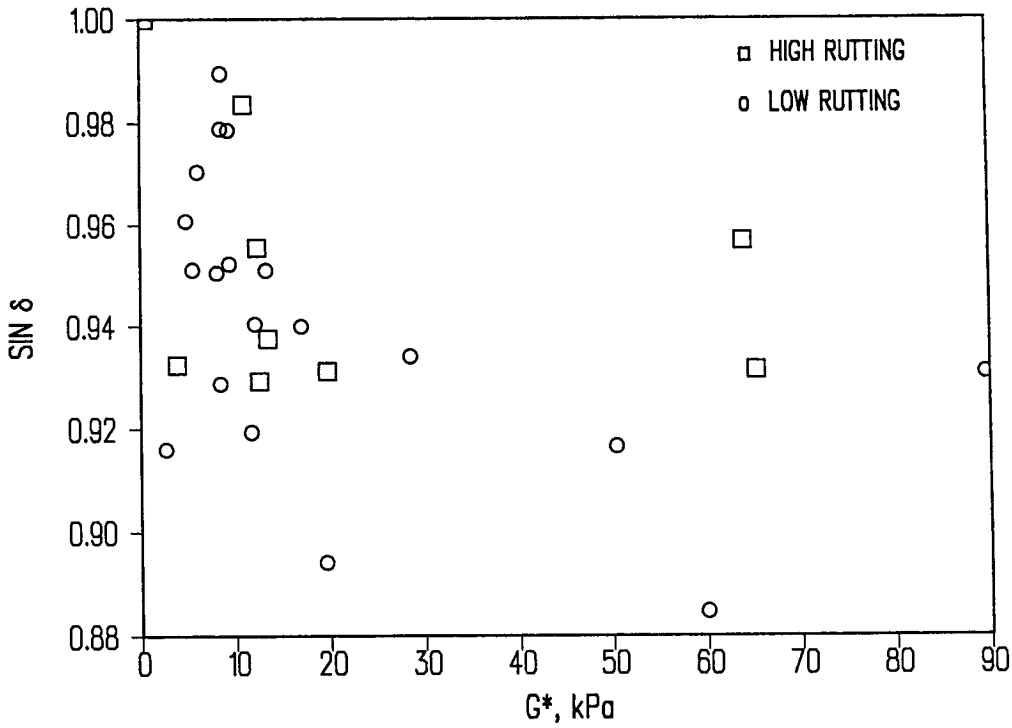

Figure 3.3a. Relationship between G^* and sin δ (rutting)

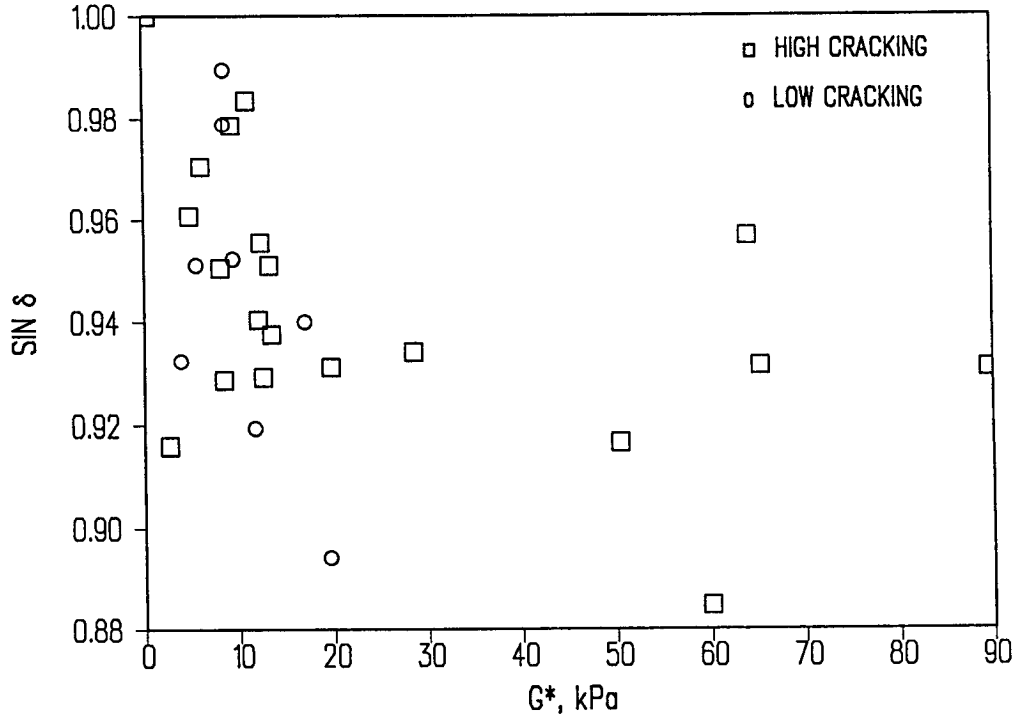

Figure 3.3b. Relationship between G^* and sin δ (fatigue cracking)

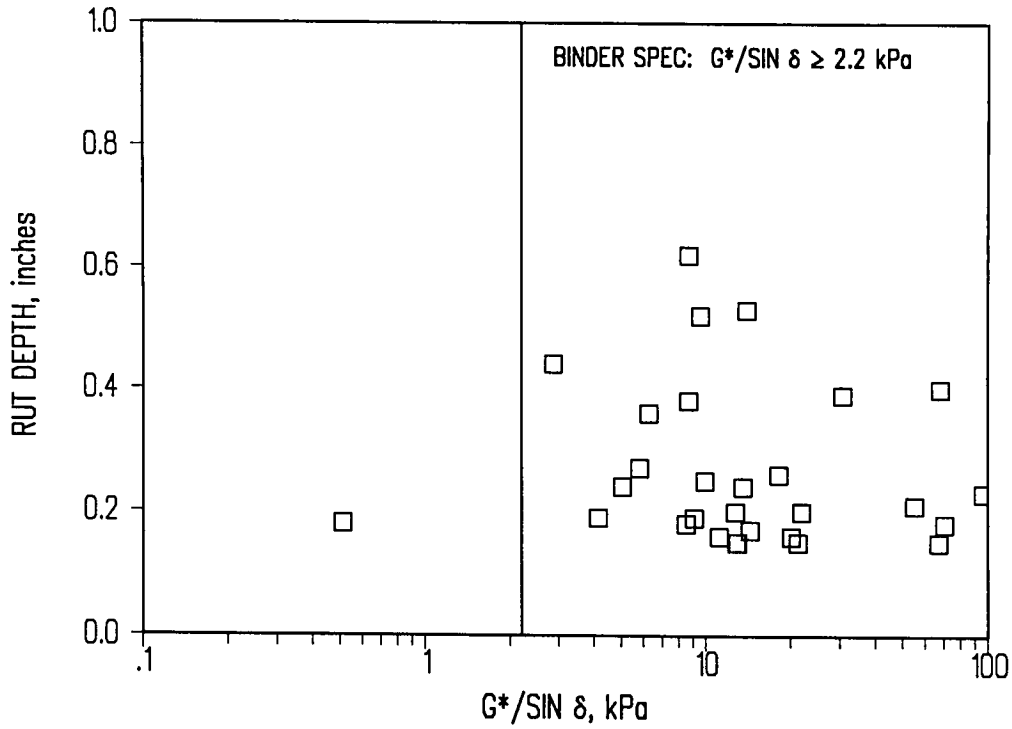

Figure 3.4a. Relationship between binder specification property and observed rutting

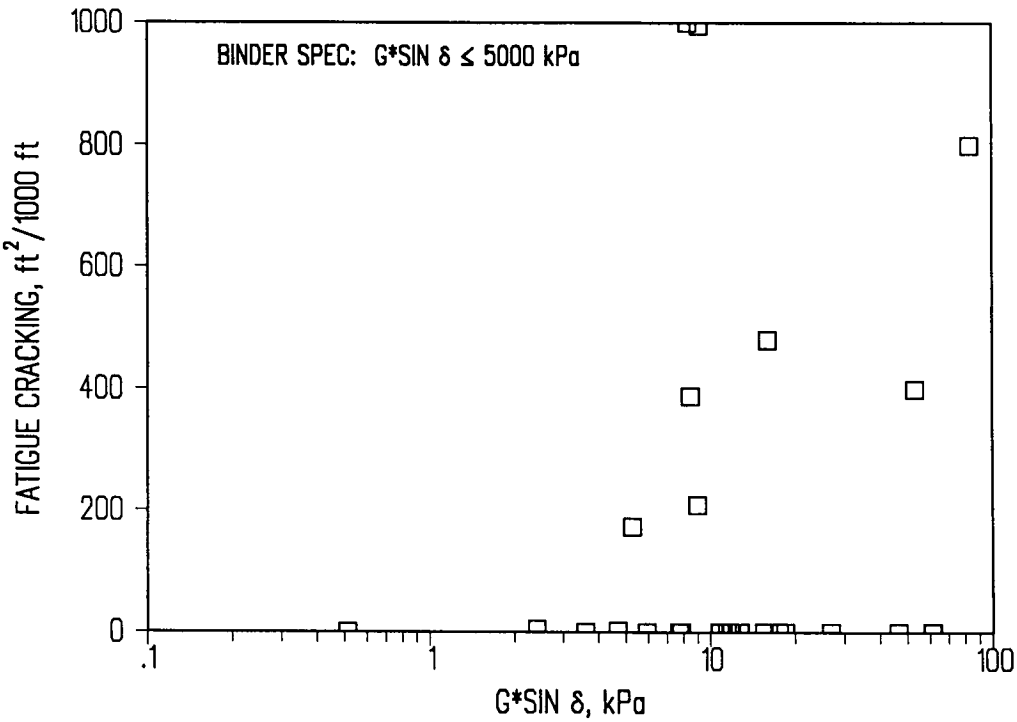

Figure 3.4b. Relationship between binder specification property and observed fatigue cracking

3.5 Limiting Strain and Stiffness of Asphalt Binder

The A-002A contractor found a distinct relationship between tensile strain at failure and secant modulus from the direct tension test of binders (Anderson et al, 1994). This relationship held true for both the unaged and laboratory-aged specimens. Direct tension tests also were performed at different temperatures on binders recovered from each of the non-load-related GPS sites.

Figure 3.5 shows that substantial differences between the two sets of data. Those sections with less severe low-temperature cracking mirrored the tests performed on the SHRP Material Reference Library (MRL) asphalts. Those GPS sections with greater amounts of low temperature cracking exhibited a more significant difference. Figure 3.5 also shows a typical relationship between the tensile strain at failure and the secant modulus from the indirect tensile test (von Quintus et al, 1991). The effect of the aggregate is illustrated as the typical curves for laboratory-aged binders and mixes begin to diverge.

The tensile strain at failure is a parameter that was proposed for use in the binder specification. To establish the relationship between failure strain and total cracking, the failure strain in tension was determined for a constant secant modulus. This was done to normalize differences between binders with varying stiffness. Figure 3.6 shows a comparison between the total amount of cracking and failure strain estimated at a secant modulus of 100 MPa (14.5 k/in^2). As illustrated, there are three distinct sets of data. Those sites in a colder environment where low failure strains were measured generally had much more cracking. Conversely, those sites where the binders exhibited failure strains in excess of 1 percent generally had low amounts of cracking. Although the data set is limited, the 1 percent failure strain in tension appears to be reasonable in separating those mixes that had low amounts of cracking in colder climates. In essence, binders with greater failure strains normalized to a specific secant modulus were found to be more resistant to cracking, which was expected.

3.6 Empirical Validation: Non-Load-Related

The binder parameters that have been identified as those controlling thermal cracking are the creep stiffness (S) and the slope of the binder stiffness curve (m) at 60 sec loading time. The test temperature at which the two parameters are obtained is selected based on the lowest pavement service temperature.

An empirical approach was used to validate the proposed binder specification. Minimum pavement surface temperatures of the pavement sections varied from -11°C to -31°C (12°F to -23.8°F) which represents a broad range of service temperatures. Direct measurement of specification parameters at the appropriate test temperatures was not available; parameters were generated from the binders' master stiffness curves and shift functions using the time-temperature superposition principle. The stiffness and slope parameters were obtained for the 22 GPS sections and then compared with the specification limits proposed for thermal cracking. The "failed" and "passed" sections, as determined by the specification, were then

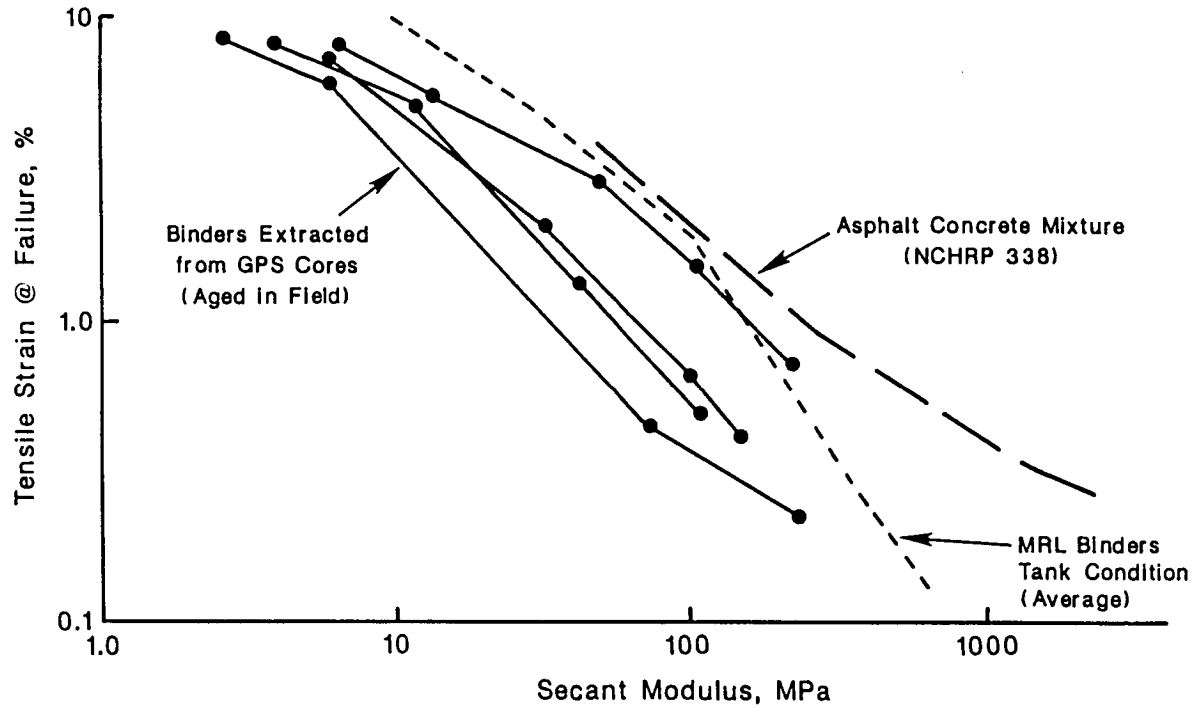

Figure 3.5. Relationship between tensile strain at failure and secant modulus

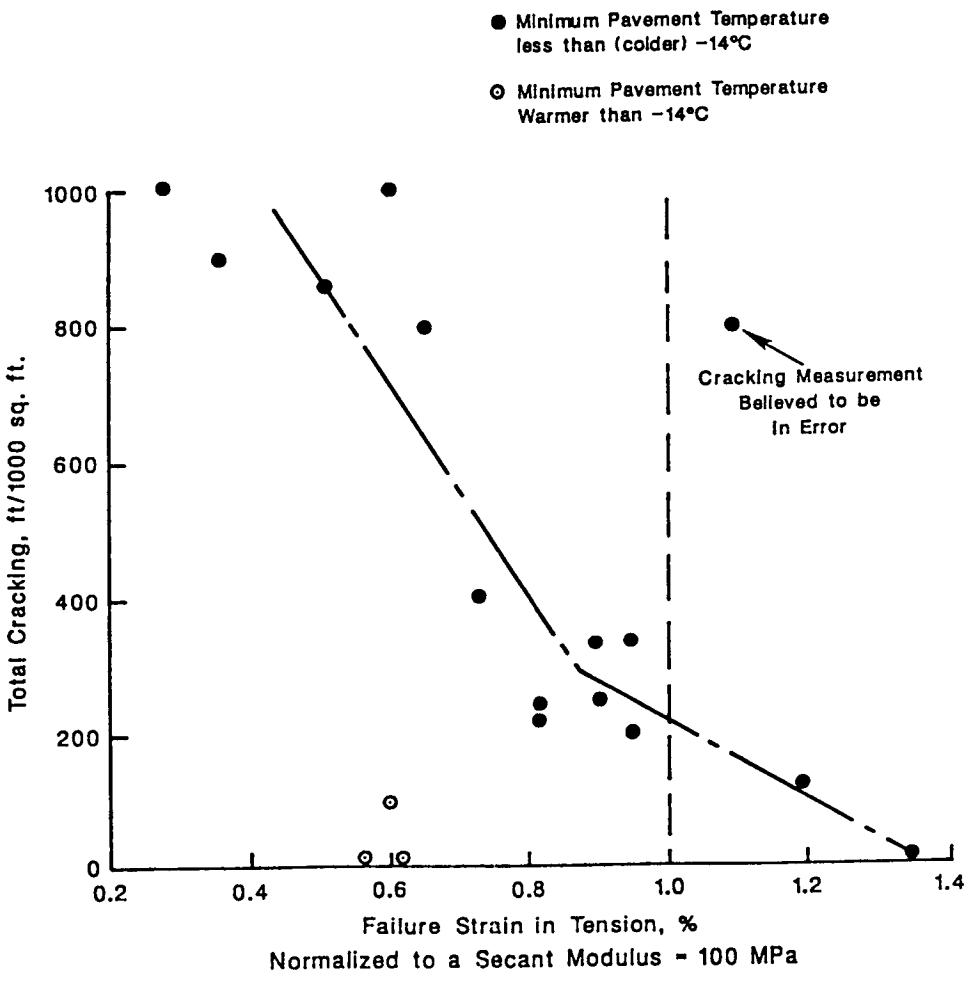

Figure 3.6. Relationship between failure strain in tension for binder secant modulus of 100 MPa (14.5 k/in^2) and observed pavement cracking

compared with actual cracking observed in the field. Only 7 of the 22 binders passed the specification requirements as shown in Figure 3.7. Further examination of these results indicated that the actual cracking observations in the field did not agree with the specification requirements. Some binders used in sections with medium observed cracking passed the specification, while sections with zero and low observed cracking had binder properties that failed the specification. In fact, 5 of the 14 binders that failed the specification were in sections where either zero or low cracking was observed in the field. All sections with observed high cracking did fail the specification. Clearly, these observations warranted further evaluation of the proposed specification.

Additional work was performed to investigate the specification limits and proposed temperature ranges. The sections were categorized into four groups based on the stiffness and slope values as determined by the specification. A check was made for a relationship between failure in either of the specification parameters and cracking potential. Four categories (i.e., quadrants of Figure 3.7) were established based on the magnitudes of stiffness and slope (S and m) at the test temperature, relative to the specification limits for S and m ($S \leq 300$ MPa and $m \geq 3.0$ respectively). Almost all the sections rejected by the specification did not meet the limits for both S and m. On the other hand, only one of the sections was rejected based on the stiffness requirement alone. Figure 3.7 also shows that one section did not pass the specification requirement for slope only. All the binders used in the remaining GPS sections that did not pass the specification also failed to meet both the stiffness and slope limits; neither parameter is solely responsible for rejection of these binders. As illustrated by Figure 3.7, there is no clear correlation between adherence to *either* of the specification limits and observed cracking in the field.

A key observation was made with respect to the test temperatures at which these parameters were obtained. It was noted that all binders with test temperatures of -10°C (14°F) passed the specification. On the other hand, all sections with parameters obtained at test temperatures of -20°C or -30°C (-4°F or -22°F) failed. In its current format, the outcome of the specification is driven primarily by test temperature. It seems that the current specification is not as sensitive to differences between different binder properties as it is to differences between test temperatures.

The temperature ranges used in the specification were examined to determine whether the sensitivity to differences in binder properties could be improved. The stiffness and slope parameters were obtained at the lowest pavement temperature plus 10°C (50°F). This approach resulted in acceptance of most of the binders used in sections with observed low cracking as shown in Figure 3.8. Nine of the 14 test sections with binder properties of $S <$ 300 MPa (43.5 k/in^2) and $m > 0.30$ were zero or low cracking sections in the field. Three had medium cracking, and two had high cracking. All eight field test sections that exceeded the specification limits ($S >$ 300 MPa (43.5 k/in^2) or $m < 0.30$) had either medium or high cracking. Considering mix effects, which may temper the binder's performance, it is concluded that stiffness and slope are reasonable parameters.

Figure 3.9 provides additional evidence regarding the effects of test temperature. Binders from each field site were evaluated at -10°C, -15°C, and -20°C (14°F, 5°F, and -40°F) to

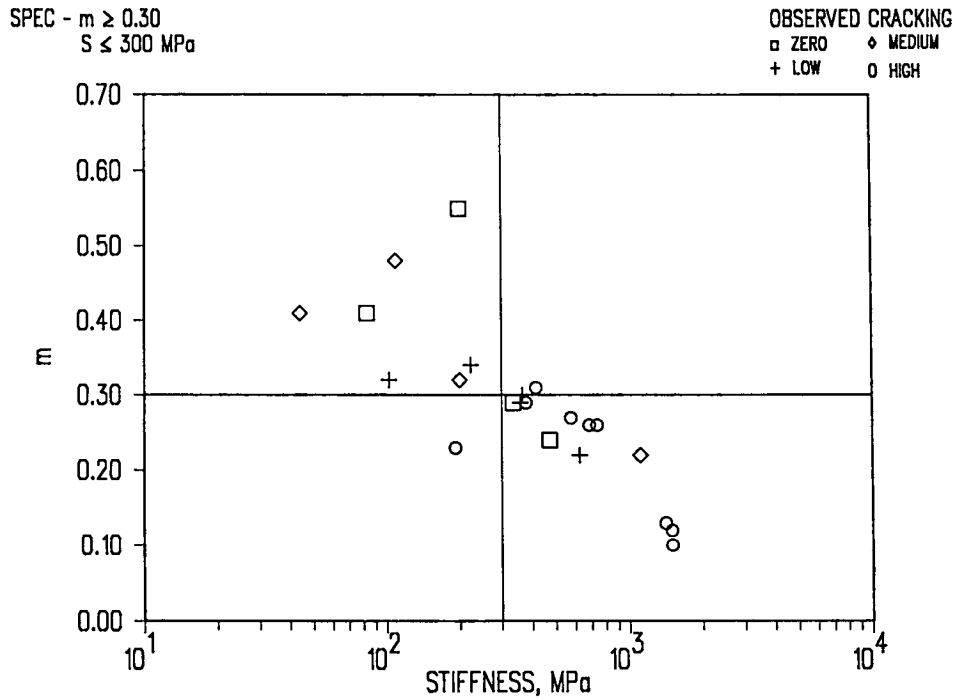

Figure 3.7. Relationship between binder specification properties and observed low-temperature cracking

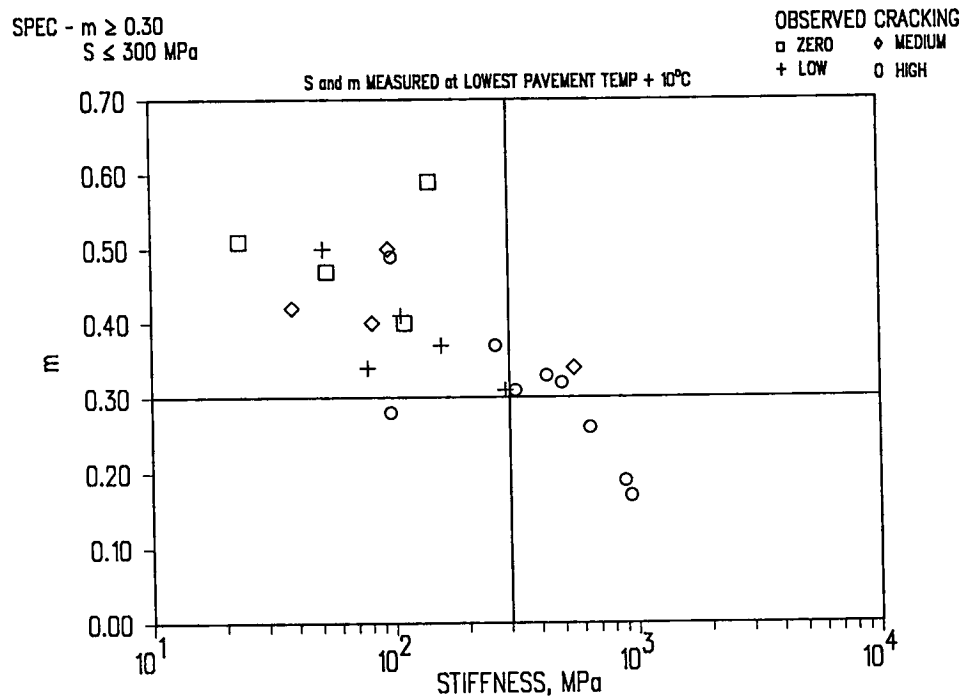

Figure 3.8. Relationship between binder specification properties and observed low-temperature cracking (test temperature at lowest pavement temperature plus 10°C [50°C])

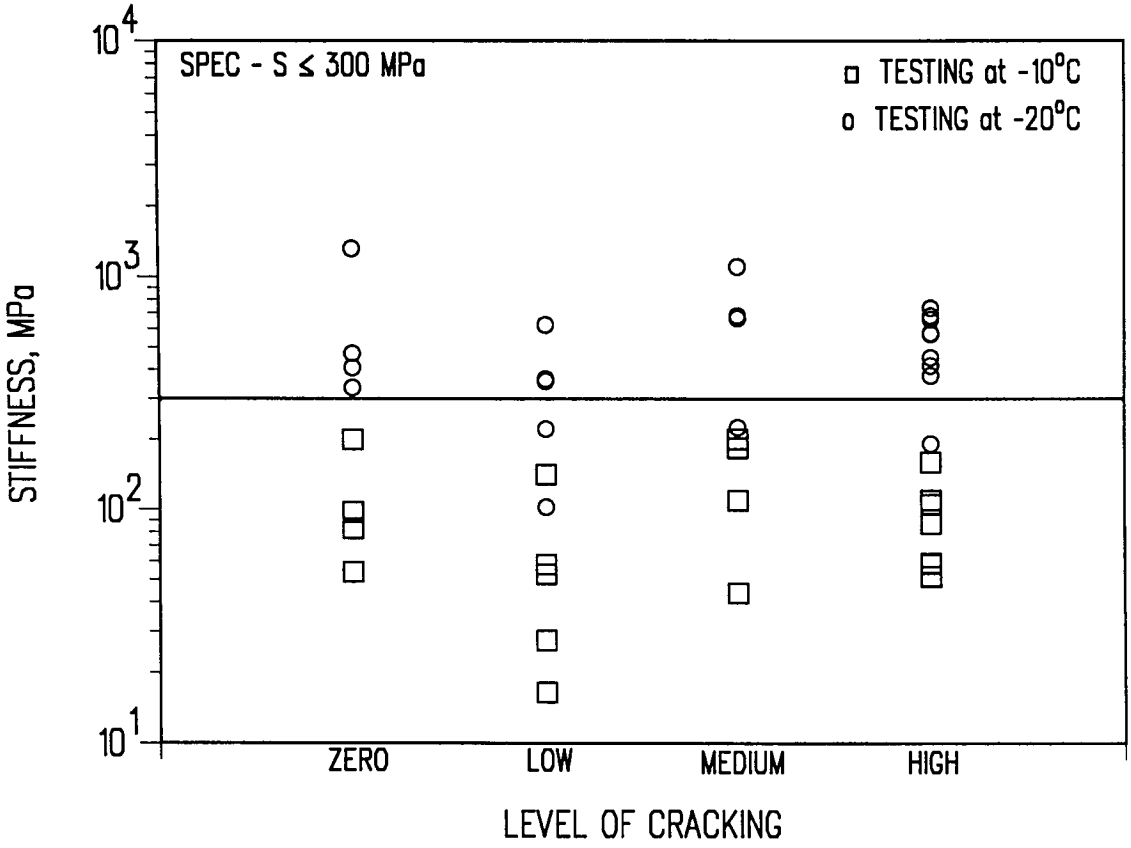

Figure 3.9. Relationship between binder stiffness and low-temperature cracking at various temperatures

determine stiffness and slope. Figure 3.9 shows that all the binders passed at -10°C (14°F), and only four passed at -20°C (-4°F). Furthermore, comparison with the binder specification indicated that none of the asphalts could be used in service temperatures below -20°C (-4°F), whereas available performance date indicate that several of the binders were adequate.

The primary conclusions drawn with respect to the binder specification are as follows:

- Stiffness and slope (S and m) appear to be reasonable parameters for controlling thermal cracking.
- The specification limits (S < 300 MPa (43.5 k/in^2) and m > 0.30) may be refined, but are they quite reasonable.
- The 6°C (43°F) temperature range used to define different binder grades in the binder specification seems to allow for a reasonably accurate evaluation of thermal cracking performance.
- Thermal cracking performance of a particular binder is mix-dependent i.e., mix performance cannot be controlled solely by the binder properties.

- Consideration of additional field data will help to refine the specification testing limits and appropriate test temperature ranges.

3.7 Pavement Performance Models: Predictions and Calibration

One of the primary objectives of the A-005 contract was to develop pavement performance prediction models to support the performance-based specifications and Superpave software (Lytton et al, 1994). The final step in the model-building process was to illustrate that the models could accurately predict the amount of distress observed in the field. To address the shortcomings of the empirical validation approach described in the preceding section, the A-005 contractor proceeded in parallel with a more complex *mechanistic* method of field validation. In this approach, as previously shown in Figure 1.3, material relationships were used in mechanistic models to predict distress. Field cores were taken from distressed pavements and subjected to a series of laboratory binder and mix tests to measure specific properties that were identified by the A-002A and A-003A contractors as related to a particular distress.

The three ways to validate a model are:

- to collect new data to check the model and its predictive ability;
- to compare results with theoretical expectations, empirical data, and simulated results; and
- to use a "hold-out" sample to check the model and its predictive ability.

The best means of model validation is through the collection of new data so that one can determine whether the model developed from the original data still applies to the new data. If the model is applicable to the new data, this permits a reasonable extrapolation of the performance prediction capabilities beyond the limits of the experimental data upon which it was based. Because of time constraints the collection of "new" data was not possible. Future development and refinement of the model should include the expansion of the database upon which the current model is based through the LTPP SPS-9 and other controlled field experiments.

A reasonable alternative to collecting new data is to split the existing data into two sets. The first data set is called the model-building set and is used to *develop* the model. The second data set is called the validation or prediction set and is used to *evaluate the reasonableness* and predictive ability of the selected model. For small data sets where data splitting is impractical, nonlinear regression techniques may be used.

With respect to pavement performance, calibration is the process of systematically adjusting the predicted values of distress so that the predicted and observed values of distress match as closely as possible throughout the pavement's known history.

Several methods of calibration were used toward this end. For example, rutting predictions were calibrated by adjusting the factor by which the predicted rut depth is multiplied to give an accurate estimate of the observed rut depth. Calibration of this kind may be performed one pavement section at a time; for the SHRP validation, however, calibration was done on sets of pavements grouped by the four LTPP climatic zones: wet-freeze, wet-no-freeze, dry-freeze, and dry-no-freeze. As expected, the multiplying factors varied with climatic zone.

3.7.1 Fatigue Cracking

Calibration of the fatigue model required adjustment of material properties: healing properties in the crack initiation phase; and the tensile strength, stiffness, and log slope of the creep compliance in the crack propagation phase. Two sets of calibration coefficients were developed. The first of these used moduli that were backcalculated from the falling weight deflectometer (FWD) tests on cores extracted from the GPS sections. The second set used moduli that were calculated from a series of tests conducted in the SHRP shear test device. Comparisons of the predicted and measured values for both sets of coefficients are shown in Figures 3.10 and 3.11.

3.7.2 Permanent Deformation

Calibration of rut depth predictions was accomplished using a system identification iterative method to converge to a final multiplying factor for each climatic zone. The final values were the same regardless of the moduli used, i.e., backcalculated from FWD data or the A-003A-recommended accelerated laboratory tests. Comparison of the predicted and measured values is shown in Figure 3.12.

3.7.3 Thermal Cracking

Calibration of the thermal cracking model required the use of nonlinear regression analysis to find the best values of a stress intensity factor (k) and two empirical coefficients (β_1 and σ) that describe the amount of surface cracking. In summary, the calibration determined the unknown parameters (β_1 and σ) included in the relationship between the amount of cracking and the logarithm of the ratio of the average crack depth within the surface layer to the thickness of the surface layer. Perhaps the best way to measure the goodness of fit of the model is to compare directly the predicted and observed amount of cracking by categorizing the predicted and observed levels of cracking as follows:

- Zero cracking: 0 to 7.5 m (0 to 25 ft) of cracking per 150 m (500 ft) section;
- Low cracking: 7.5 to 22.5 m (25 to 75 ft) of cracking per 150 m (500 ft) section;

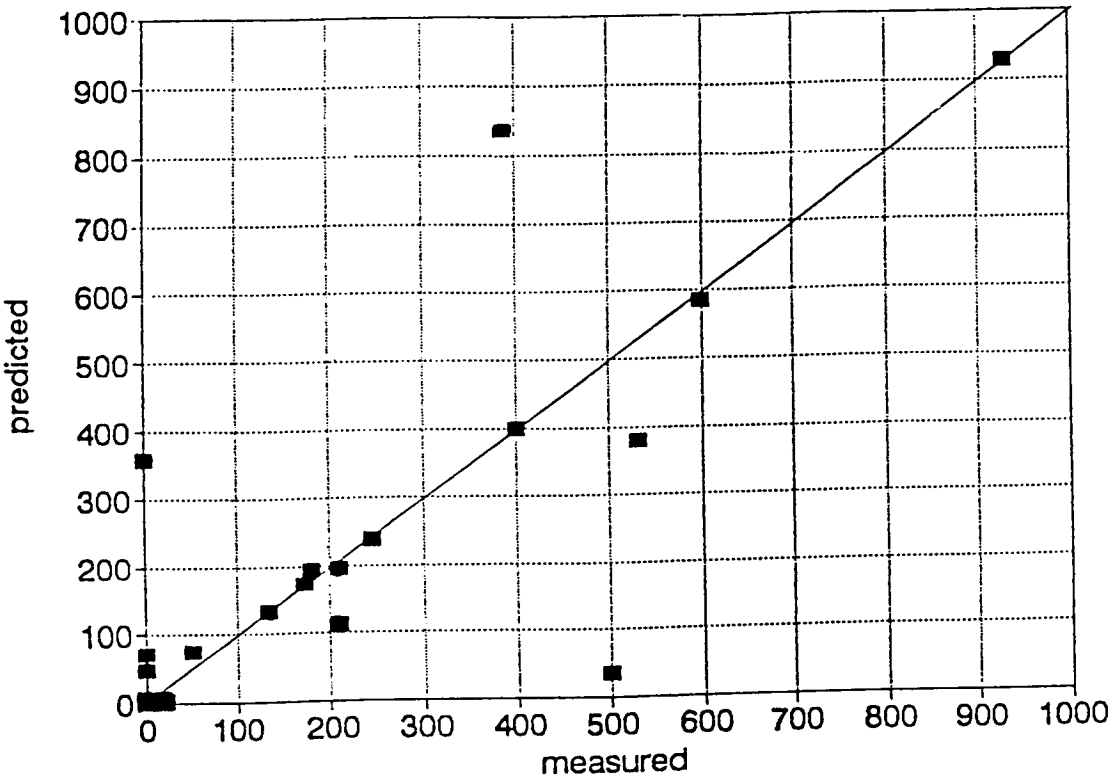

Figure 3.10. Comparison of calibrated predictions with measured fatigue cracking using backcalculated asphalt moduli

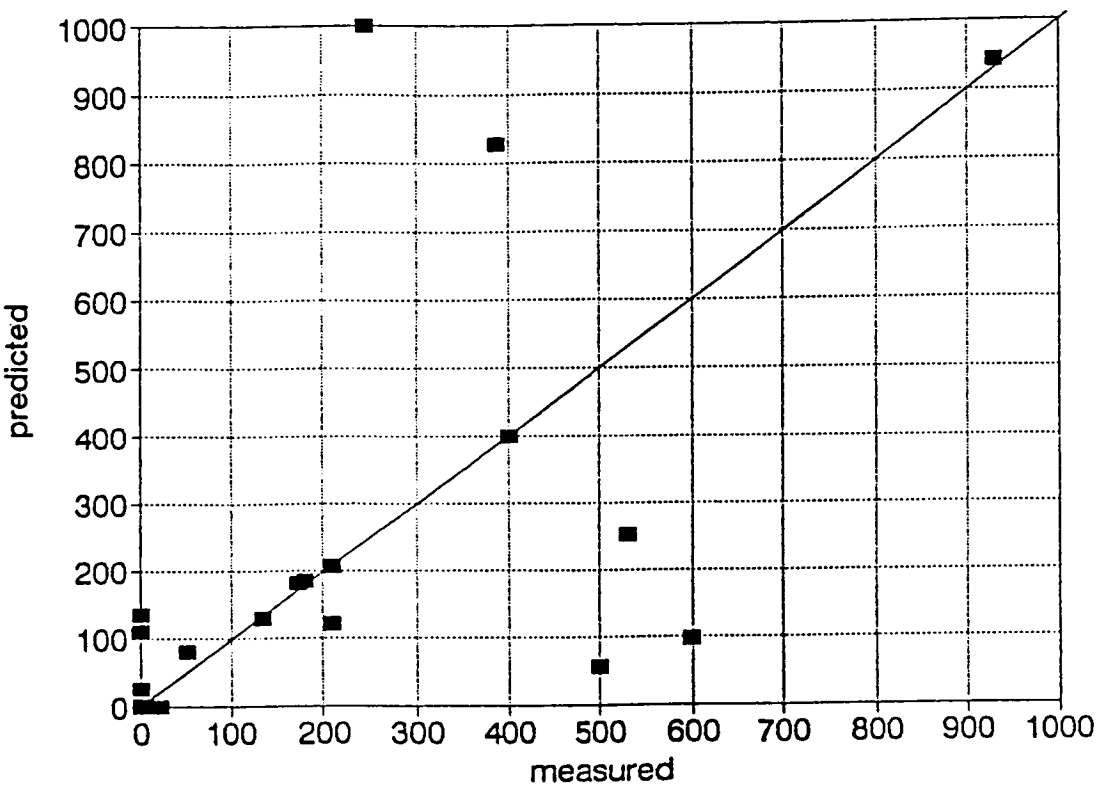

Figure 3.11. Comparison of calibrated predictions with measured fatigue cracking using moduli from accelerated laboratory tests

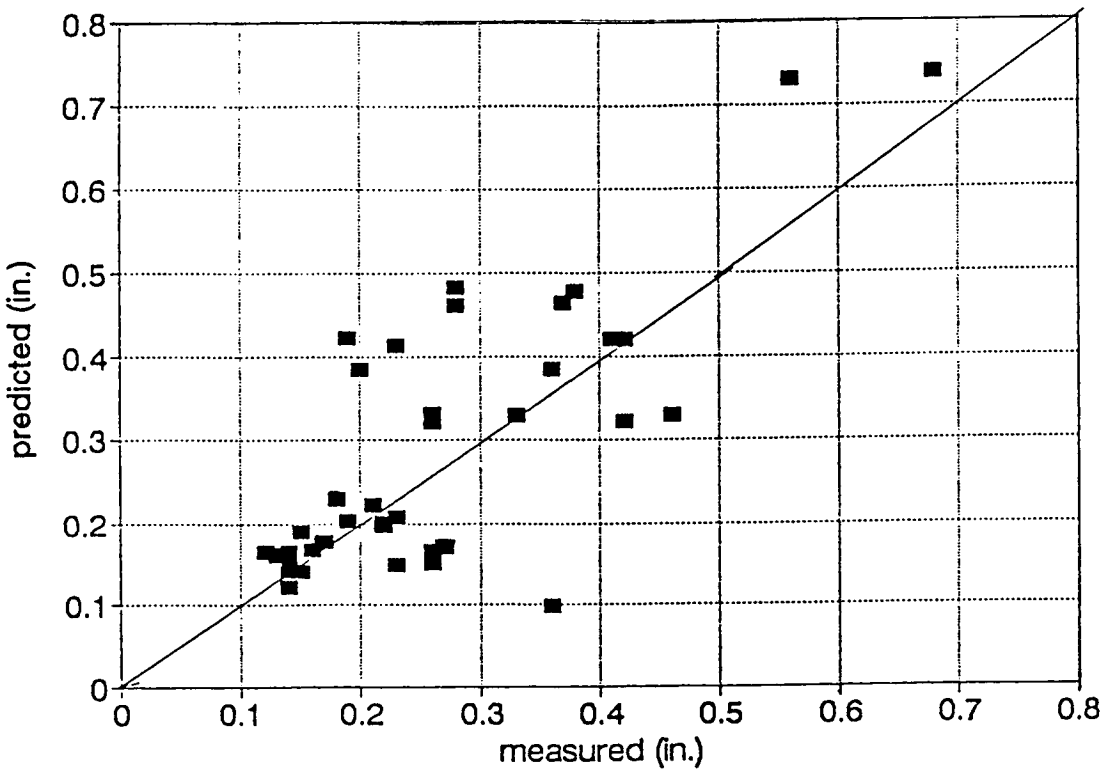

Figure 3.12. Comparison of measured rut depth with calibrated predictions of rut depth

- Medium cracking: 22.5 to 45 m (75 to 150 ft) of cracking per 150 m (500 ft) section; and
- High cracking: greater than 45 m (150 ft) of cracking per 150 m (500 ft) section.

The results of this comparison using predicted cracking determined with the model parameters are shown in Figure 3.13 and are summarized as follows:

- Eight of the high cracking sections were predicted to be high cracking sections. Similar success was observed with the zero cracking sections.
- Of the three low cracking sections, two were predicted to be zero, and one was predicted to be low cracking.
- Only one prediction was off the diagonal by two cells; 16 of 19 predictions were on the diagonal (meaning excellent prediction), and three were just one cell off the diagonal (implying fairly good prediction).

3.8 Conclusions

3.8.1 Load-Related

While it is evident that the properties of the binder are important in extending the service life of asphalt concrete, it also is obvious from the lack of observed patterns of high and low rates of rutting and fatigue cracking that the selection of the binder alone will not ensure good load-related performance. It is clear that the disciplines of pavement analysis and design, mix design, and the effects of construction and weather also play important roles in the appearance and progression of load-related distress.

Performance prediction models were developed and calibrated to observations of rutting and fatigue cracking on a variety of pavements in the United States and Canada. Calibration adjustments were made to the predictions by a mathematical technique known as the systems identification method or by a nonlinear pattern search method. The calibration adjustments were not large, nor did they vary much from one climatic zone to another, indicating that the prediction models developed for both fatigue cracking and rutting are sound.

The calibrated models take into account the traffic, temperature variations in all layers throughout the year, and the seasonal variation in material properties of each layer in computing amounts of rutting and cracking. The calibrated load-related models were shown to be well-suited for use in developing-performance related specification limits and for optimizing mix designs in the Superpave system.

		Observed cracking			
		Zero	Low	Med.	High
Predicted Cracking	Zero	4	2	1	
	Low		1		
	Med.			3	
	High			1	8

Figure 3.13 Final cell groups of predicted versus observed low-temperature cracking

3.8.2 Non-Load-Related

Based on the results of the field validation studies, the following conclusions were drawn regarding the effectiveness of the SHRP specifications:

- The stiffness and slope (S and m-value at 60 sec loading time) determined from bending beam rheometer testing appear suitable for evaluating the thermal cracking performance of binders. Both stiffness and slope correlated reasonably well with observed thermal cracking in the field.

- The limits on stiffness and slope in the binder specification ($S < 300$ MPa (43.5 k/in^2) and $m > 0.30$) seem quite reasonable. Additional field data will help to refine the limits.

- The 6°C (43°F) temperature range used to define different binder grades in the binder specification seems to allow for a reasonably accurate evaluation of thermal cracking performance.

- The binder specification alone does not guarantee adequate thermal cracking performance. Mix characteristics have a significant effect on thermal cracking performance of a particular binder.

- It appears that long-term aging (Harrigan et al) is needed to properly evaluate the thermal cracking resistance of the mix.

- Based on limited data, it appears that aging levels comparable to those observed in the field, as reflected by changes in the low-temperature properties of the binder, can be attained through thin film oven testing (TFOT) followed by pressure aging vessel (PAV) aging as proposed in the SHRP binder specification.

- The thermal cracking model adequately represents and accounts for the most significant factors in the thermal cracking of pavements in the field and has good predictive capability.

4

Validation Testing with Modified Materials

It is readily acknowledged that asphalt cements with optimum properties may not be obtained from all petroleums by conventional refining processes or blending practices because of inherent variability in the characteristics of crude oils. As noted elsewhere (Kennedy et al, 1994) asphalt modification may prove to be the most efficient, cost-effective means for minimizing asphalt deficiencies and producing binders with acceptable performance properties from a wide variety of petroleum sources.

4.1 Scope of Work

It was originally intended on asphalt cement modification would encompass:

- refining operations;
- addition of a chemical modifier; or
- mechanical reinforcement.

The emphasis on this research was to be placed on, but not limited to, modifiers such as mineral fillers, extenders, polymers, rubbers, oxidants, antioxidants, and hydrocarbons. The research was "...to develop test methods to evaluate the effectiveness of modification procedures in enhancing the performance of asphalt binders and mixes." (TRB, 1986). Additional aspects of the research were to include health and environmental effects, recycling potential, and field studies of modified materials. In concert with the evolutionary nature of the SHRP asphalt program, the contract objective was modified somewhat in 1990, as noted in the following (SHRP, 1990):

> **Contract A-004**: Adapt as necessary performance-related test methods for binders and mixes to permit their use with the full range of modified systems. Explore innovative refinery processes to enhance the performance of modified asphalt binders. Develop a modifier evaluation protocol to permit evaluation

and selection of modified binder systems that remedy specific pavement performance gaps.

The scope and complexity of the modification research later were revised because of time and budget constraints, such that the A-004 contract responsibilities were limited to testing modified binders in accordance with the A-002A-recommended test equipment and protocols. Furthermore, responsibility for evaluation of modified mixes was shifted to the A-003A contractor and limited to that associated with permanent deformation and fatigue cracking. Validation testing of *modified binders* is addressed in Section 4.3. Validation testing with *modified mixes* is addressed in Section 4.4.

Because of the lack of field performance data on modified materials, an expert task group (ETG) was formed in February 1990 to assist SHRP and contract staff in selecting modifiers for inclusion in the experimental design. Members of the ETG included refinery personnel, material producers, and state highway administration (SHA) personnel. The final selection of modified materials was based on a survey of SHA materials engineers (conducted by the A-004 contractor) and the ETG's recommendations. Modifiers were selected for each pavement distress based on their *expected* performance. For example, the modifiers selected for evaluation with respect to permanent deformation were expected to span the full range of performance: good, poor, or "no effect." This selection methodology clearly allowed for overlapping use of modifiers. Modifiers that were expected to enhance permanent deformation performance would be expected to detract from fatigue cracking performance.

The modified materials were selected based on the collective knowledge and opinions of the ETG, SHRP, and A-001 staff. The performance data were drawn mostly from *laboratory test data*, not field performance data. Furthermore, the reader is reminded that the conclusions drawn are based on a limited data set. Any inferences made with respect to field performance are preliminary at best.

4.2 Modified Materials

Materials used in the validation testing were drawn from the following general categories of modifiers: polymers such as styrene butadience styrene (SBS), styrene butadience rubber (SBR), ethylene vinyl acetate (EVA); reclaimed rubber, extenders, oxidants, antioxidants, mineral fillers, and antistripping agents.

4.3 Modified Binder Testing

Various combinations of 11 modifiers and five asphalts were evaluated using the dynamic shear and bending beam rheometers, as well as the direct tension device. The binders and modifiers are listed by distress in Table 4.1, and the results are presented similarly, i.e., by distress.

Table 4.1. Materials used in modified binder evaluation

Distress	Modifier	Binder
Aging	SBR oxidant antioxidant mineral fiber	AAG, AAK, AAM
Fatigue	SBR EVA oxidant	AAF, AAG, AAK
Permanent Deformation	SBS mineral filler	ADD, AAG, AAK
Thermal Cracking	SBS extender reclaimed rubber	AAD, AAG, AAK

4.3.1 Aging

Three levels of *age conditioning* were considered: unaged (tank), thin film oven test (TFOT)- aged, and TFOT residue with the pressure aging vessel (PAV). Three binders were used in combination with four modifiers. The three binders considered—AAM, AAG, and AAK—were expected to demonstrate "good," "intermediate," and "poor" performance, respectively.

Age conditioning of the *unmodified binders*, as measured by $G^*/\sin\delta$ from dynamic shear data (Figure 4.1), suggests that TFOT aging would produce the *expected* performance, whereas after PAV aging, AAM and AAG would perform identically, but very differently from AAK. Direct tension results, as measured by tensile strength (Figure 4.2), generally yield the expected results in terms of performance; however, age conditioning does not markedly affect the individual binder's tensile strength. Although not shown, failure strain data indicate that tank and TFOT- aged binders generally yield similar results regardless of binder type. Also, PAV conditioning resulted in lower failure strains for the AAG and AAK binders. Figure 4.3 shows the *m*-value calculated from bending beam rheometer data. The aging trends for the individual binders are as expected, although both AAM and AAG performed nearly identically, but again, differently from AAK. Bending beam stiffness data (Figure 4.4) indicate that the various aging techniques do not markedly affect the behavior of the individual binder. Furthermore, the stiffness data indicate that binders AAM and AAK behave similarly, and that AAG is much stiffer, regardless of conditioning.

Age conditioning of the *modified binders* was evaluated for tensile strength and $G^*/\sin\delta$ as shown in Figures 4.5 and 4.6, respectively. Observations with respect to the test results may be considered from two perspectives: the effect of age conditioning across materials, and the effect of the modifier on the control binder.

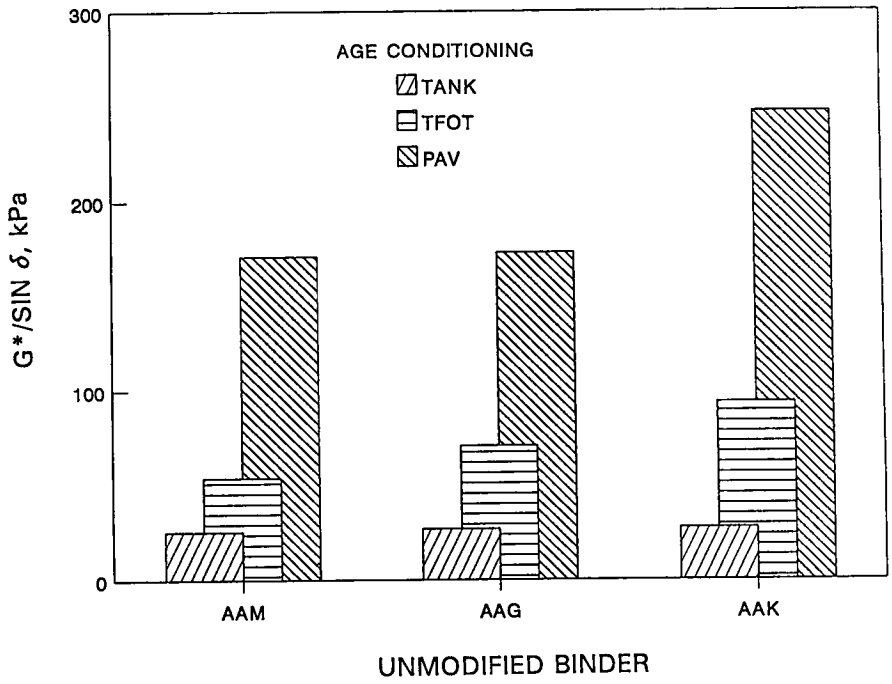

Figure 4.1. Effect of age conditioning on $G^*/\sin\delta$

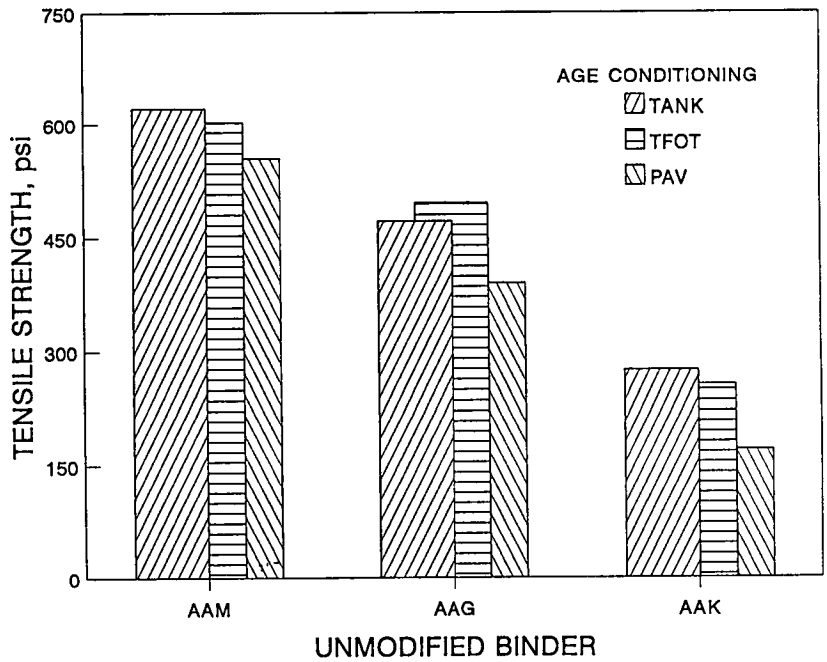

Figure 4.2. Effect of age conditioning on tensile strength

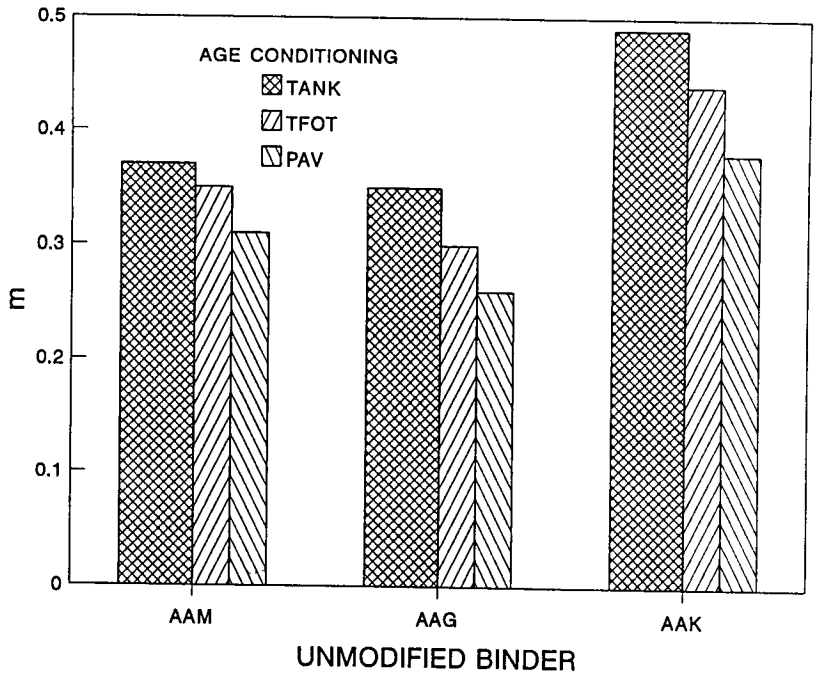

Figure 4.3. Effect of age conditioning on *m*-value

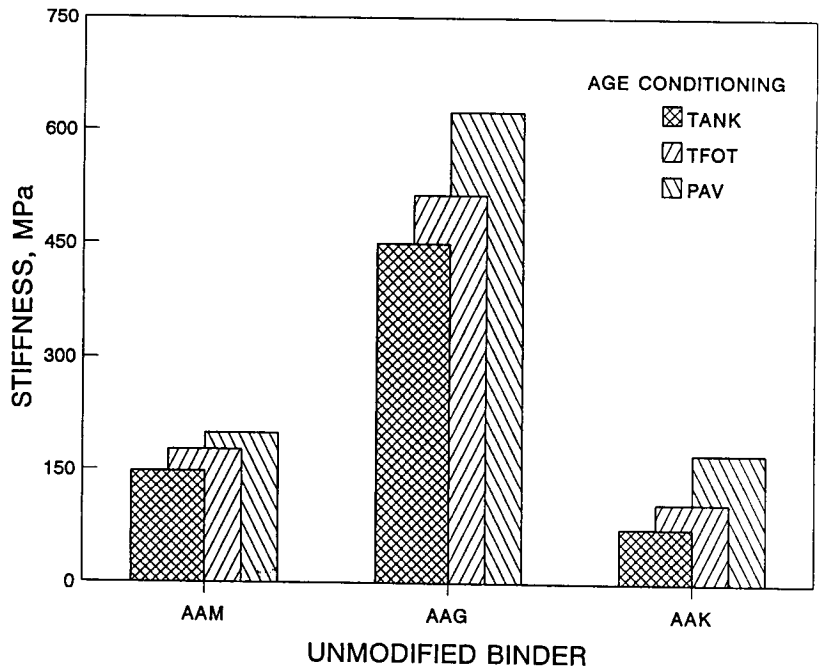

Figure 4.4. Effect of age conditioning on stiffness

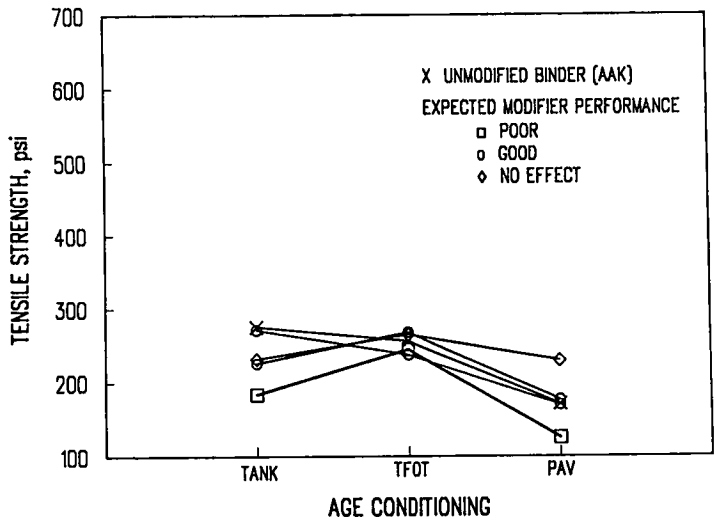

Figure 4.5a. Effect of age conditioning on tensile strength (modified binder AAK)

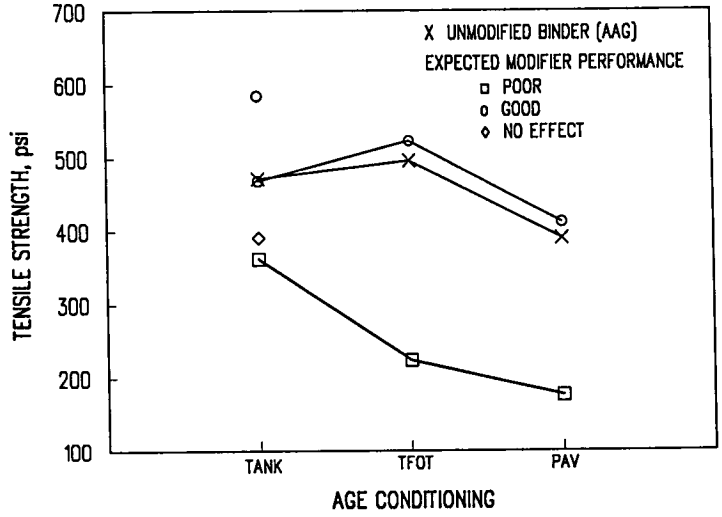

Figure 4.5b. Effect of age conditioning on tensile strength (modified binder AAG)

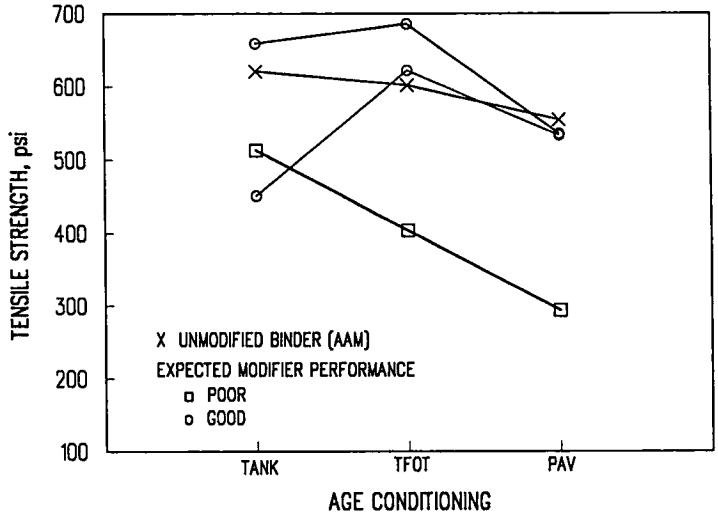

Figure 4.5c. Effect of age conditioning on tensile strength (modified binder AAM)

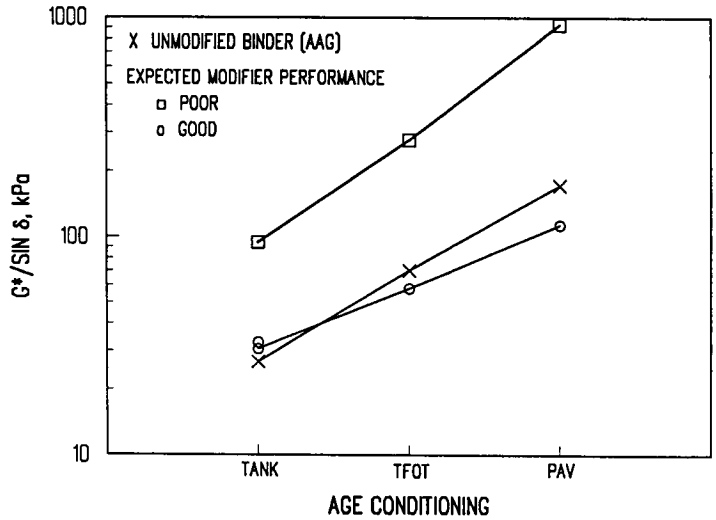

Figure 4.6a. Effect of age conditioning on $G^*/\sin\delta$ (modified binder AAG)

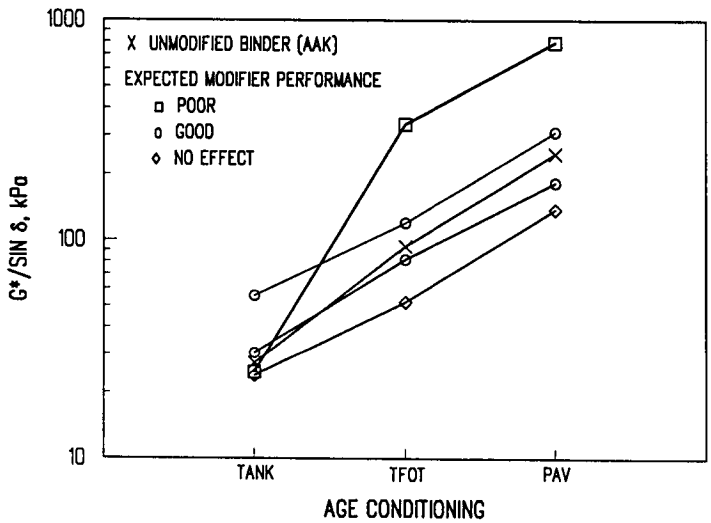

Figure 4.6b. Effect of age conditioning on $G^*/\sin\delta$ (modified binder AAK)

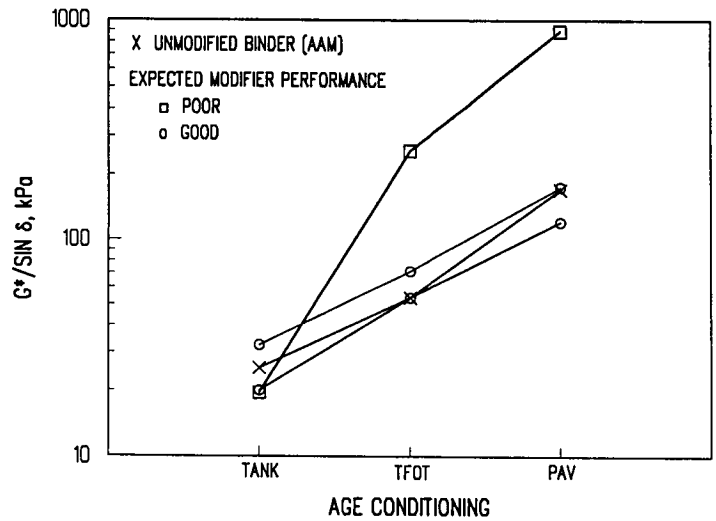

Figure 4.6c. Effect of age conditioning on $G^*/\sin\delta$ (modified binder AAM)

With respect to *tensile strength*, the performance of binder AAK was fairly consistent regardless of age conditioning or modifier, as shown in Figure 4.5a. For binder AAG (Figure 4.5b), the largest difference was observed between TFOT and PAV conditioning for all materials. Also, the difference between the "good" and "poor" modifiers was evident at all conditioning levels, the largest difference between the tank and TFOT procedures. With binder AAM (Figure 4.5c), the "good" modifier showed slightly different behavior between the TFOT and PAV conditioning. With the "poor" modifier, however, the material response deteriorated with each succeeding aging procedure.

Shear rheometer data ($G^*/\sin\delta$) was significantly more sensitive to conditioning procedures, as it increased for all materials with degree of aging. As shown in Figure 4.6, $G^*/\sin\delta$ discriminated among the control, "good," and "poor" modifiers fairly consistently after both TFOT and PAV conditioning. Only with binder AAG (Figure 4.6a) was there a difference in behavior measured in the unaged/tank condition among the control binder, "good," and "poor" modifiers.

Shown in Figures 4.7 to 4.10 are comparisons between various properties of the unmodified and modified binders. The data points are paired in terms of age conditioning, i.e., unmodified tank tensile strength with modified tank tensile strength, unmodified TFOT aged tensile strength with modified TFOT-aged tensile strength, unmodified PAV-aged tensile strength with modified PAV-aged tensile strength, and so on. As illustrated in Figure 4.7, agreement between the unmodified and modified tensile strength regardless of age conditioning is quite good, except for the modifiers that are expected to result in poor performance with respect to aging. Those modifiers that were expected to perform poorly as they were aged consistently yielded lower tensile strengths, suggesting that the age conditioning did affect the modified binder and that the direct tension test is useful to measure this effect. The results for $G^*/\sin\delta$ shown in Figure 4.8 are nearly identical to those shown in Figure 4.7, except that the poorly performing modifiers are virtually a mirror image of those shown for tensile strength, as expected. Bending beam stiffness data in Figure 4.9 may not discriminate as much among unmodified and modified binders as suggested by the nearly linear relationship. Not surprisingly, the *m*-values derived from bending beam data (Figure 4.10) show a similar trend.

In summary, the limited age conditioning of modified binders suggests the following:

- A *poor* modifier tends to have measurable effect on the rheological properties of a *good* binder (Figure 4.5c), but a *good* modifier tends to have a less perceptible effect on a *poor* asphalt (Figure 4.5a).

- Differences among age conditioning procedures are seen more clearly with data derived from dynamic shear rheometer testing ($G^*/\sin\delta$) than with bending beam rheometer data (Figures 4.5 and 4.6).

- Tensile strength and $G^*/\sin\delta$ seem more sensitive to modifier influence than do stiffness and *m*-value measurements derived from bending beam rheometer data (Figures 4.7 and 4.8 versus Figures 4.9 and 4.10).

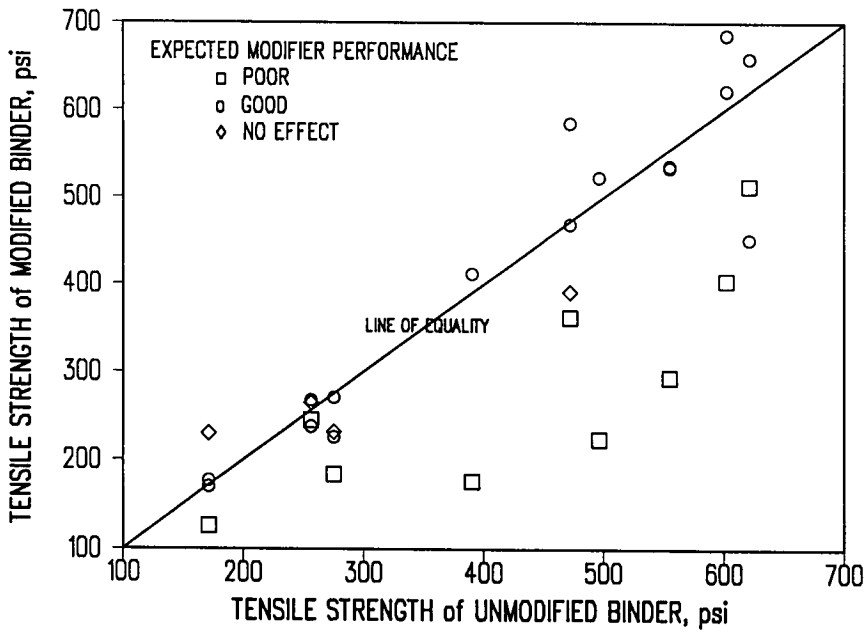

Figure 4.7. Modified binder performance in terms of tensile strength

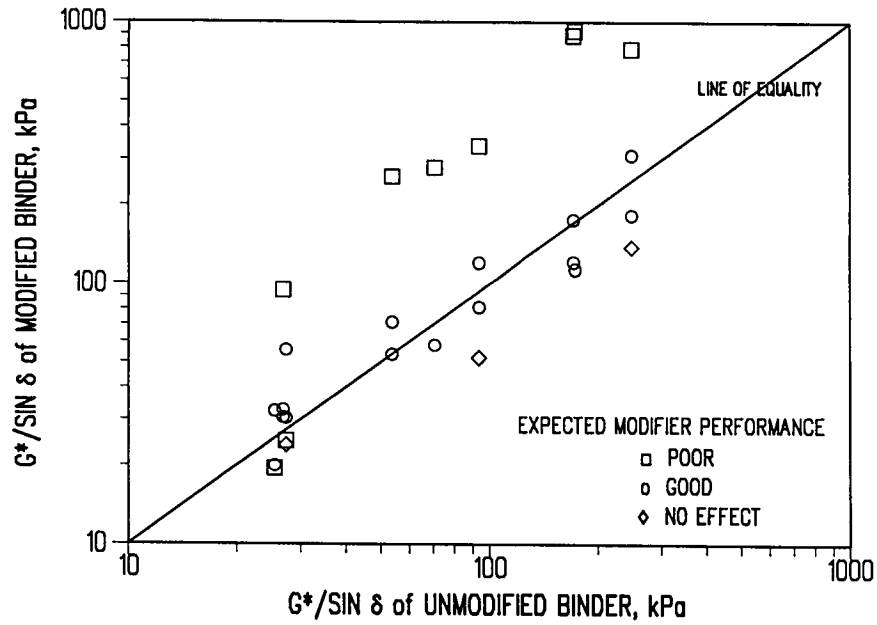

Figure 4.8. Modified binder performance in terms of $G^*/\sin\delta$

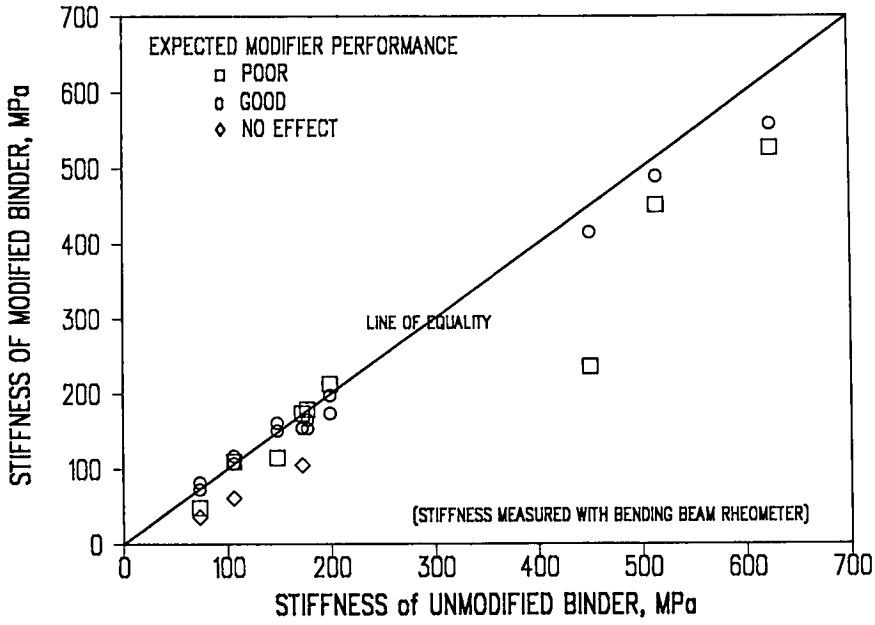

Figure 4.9. Modified binder performance in terms of stiffness

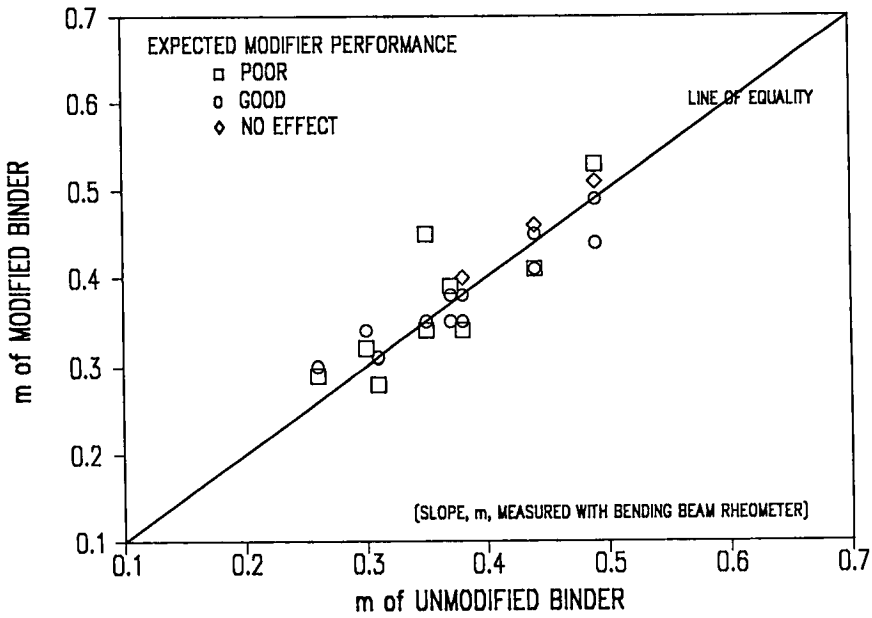

Figure 4.10. Modified binder performance in terms of *m*-value

Additional evaluation of modified binders was conducted by A-002A researchers at the Pennsylvania State University. Four asphalts were used in combination with 10 modifiers. As shown by the bending beam stiffness data in Figure 4.11, the material response was quite diverse. In terms of binder performance, AAD and AAK generally performed consistently, regardless of modifier, with only one exception for each. In the case of binder AAD, the modifier detracted from its performance; with AAK, the addition of a modifier improved its performance. For binder AAG, six of the nine modifiers reduced the stiffness; two left it essentially unchanged, and one increased it only marginally. Binder AAF was evaluated with four modifiers: Two reduced stiffness, one increased it, and one left it identical to the control stiffness. Clearly, these additional data are much more encouraging in terms of the use of the bending beam for evaluating modified binder response.

4.3.2 Permanent Deformation

In the early stages of the modifier evaluation, it was decided that only unaged binders would be considered in the permanent deformation, fatigue, and low-temperature cracking evaluations. This decision, as evidenced by the conditioning procedures included in the binder specification, was later revised. Unfortunately, the data included here are limited to those for unaged binders.

In the permanent deformation evaluation, three binders and three modifiers were combined. From an evaluation of all the rheological data, only the dynamic shear rheometer data provided some relationship to expected performance. As illustrated in Figure 4.12, the $G^*/\sin\delta$ clearly discriminated among the *poor*, *intermediate*, and *good* modifiers that were combined with binder AAK. Similar trends are seen with binder AAG, although the effect of the *good* modifier was not as dramatic as that observed with AAK. The effect of the *good* modifier resulted in a more than doubling of the $G^*/\sin\delta$ term for binder AAD. Admittedly, this data set is relatively small, but it is clear that the dynamic shear rheometer can be used to discriminate among modifier performance.

Data drawn from a number of sources and spanning a wide range of modifiers[2] provides additional corroborating evidence that the dynamic shear rheometer is an effective tool for evaluating the permanent deformation behavior of modified binders (SHRP, 1994). The data shown in Figure 4.13 include both aged and unaged materials tested at various temperatures and clearly demonstrate the effects of modifiers on the high-temperature behavior in terms of $G^*/\sin\delta$.

4.3.3 Fatigue Cracking

As was the case for permanent deformation, all binders evaluated in the fatigue cracking experiment were unaged. Three binders and three modifiers were tested in the A-004

[2]Modifiers in this data set included cellulose fibers, EVA, organic and inorganic fillers, polyethylene, polyfunctional polyolefin, reclaimed rubber, SBR, and SBS.

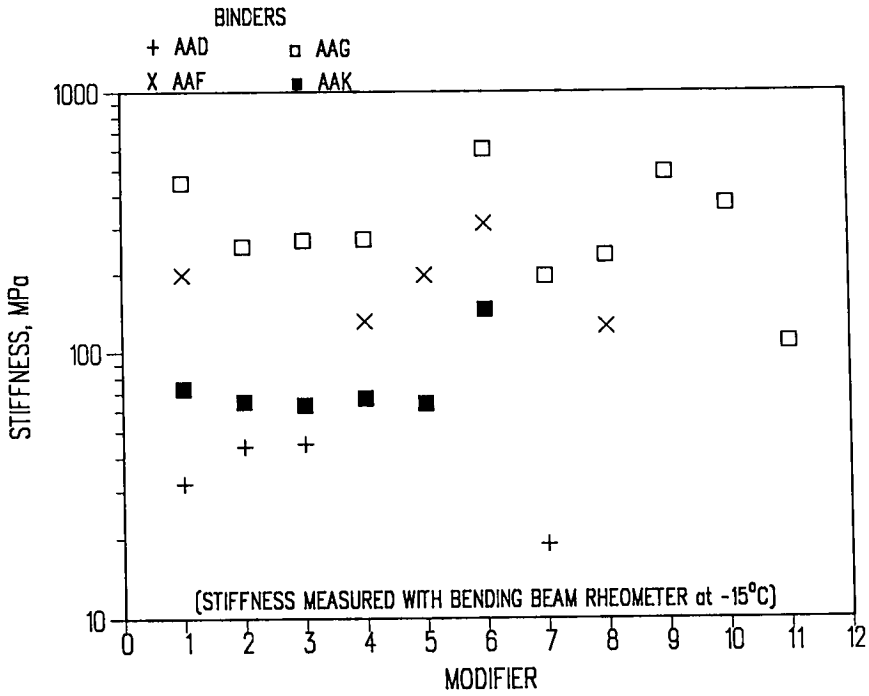

Figure 4.11. Modified binder data

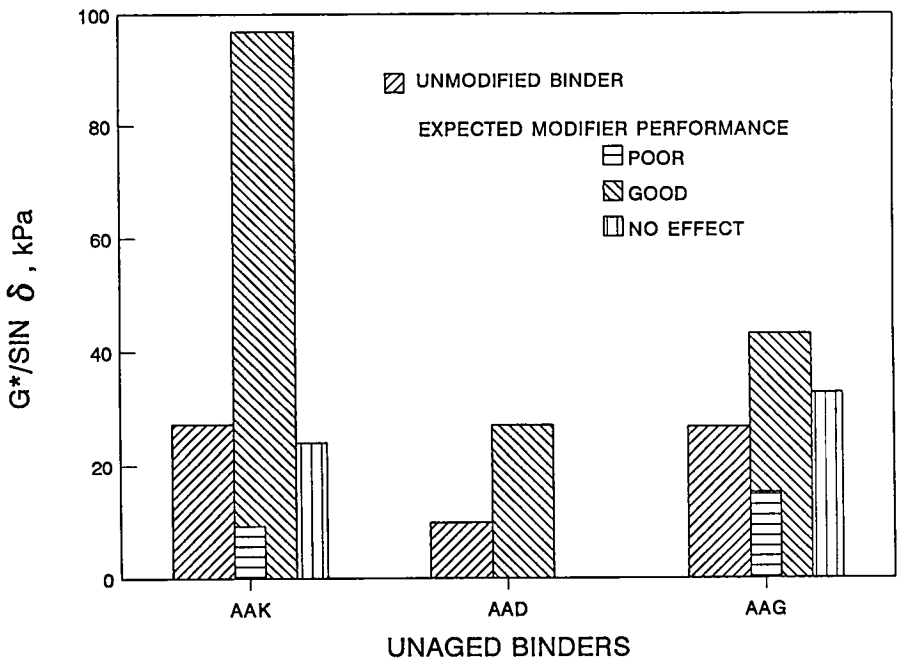

Figure 4.12. Effect of binder modification on $G^*/\sin\delta$

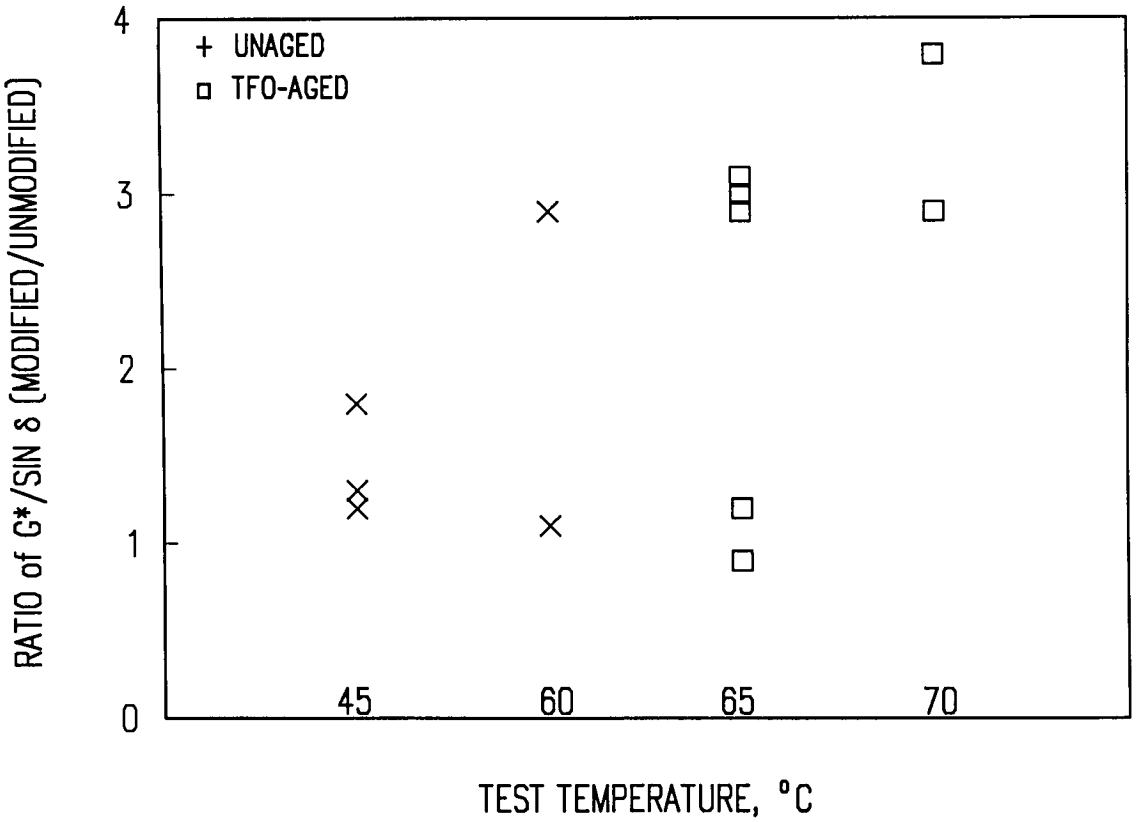

Figure 4.13. Effect of binder modification on high-temperature properties

experiment. The results, unfortunately, are inconclusive. As illustrated in Figures 4.14 and 4.15 the poor modifiers produced a lower tensile strength than the control binders AAK and AAG, but nearly identical to the control for binder AAF. The good modifiers did increase the tensile strength of binders AAG and AAF. However, the modifier that was supposed to have no effect increased the tensile strength when added to binders AAK and AAF. Likely reasons for the lack of correspondence between the material properties and expected performance are that the hypothesized performance of the binders and modifiers may not have been entirely correct. For example, binder AAK was suggested as good for fatigue, but poor for aging. Normally, asphalts which stiffen with aging are also susceptible to fatigue cracking. Also, the use of unaged binders may have been inappropriate for evaluating the fatigue response.

Additional data included both PAV-conditioned material and binders extracted from field cores.[3] As seen in Figure 4.16, shear rheometer data ($G^*\sin\delta$) clearly discriminates among the various types of modifiers, suggesting that rheological properties at intermediate temperatures can be used effectively to predict the fatigue performance of modified binders.

[3]Modifiers used were EVA, polyethylene, and SBR.

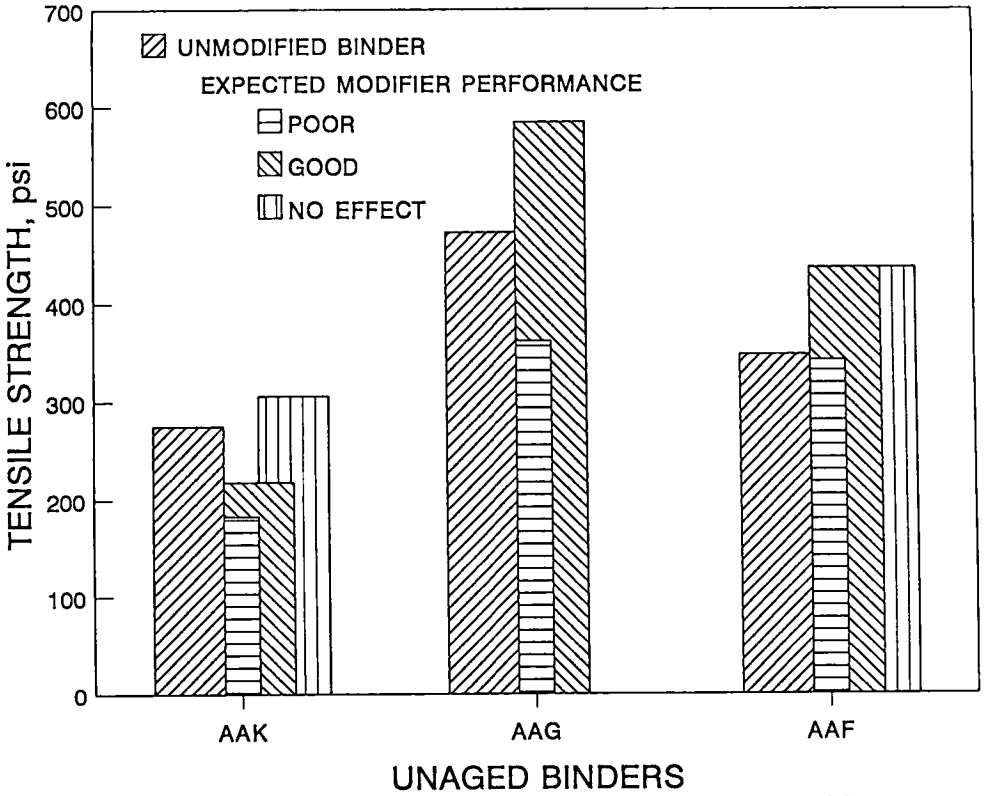

Figure 4.14. Effect of modifiers on unaged binders (tensile strength)

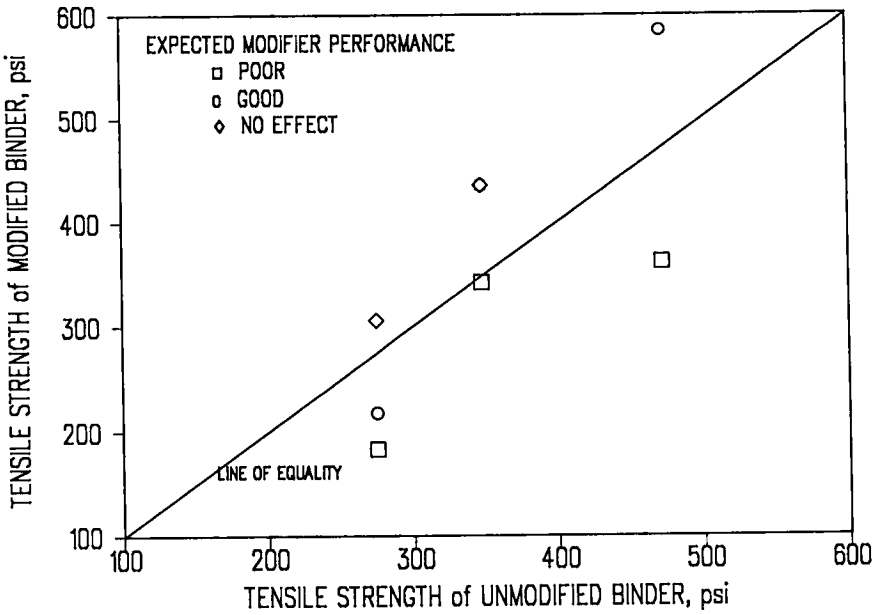

Figure 4.15. Comparison of tensile strength for unmodified and modified binders

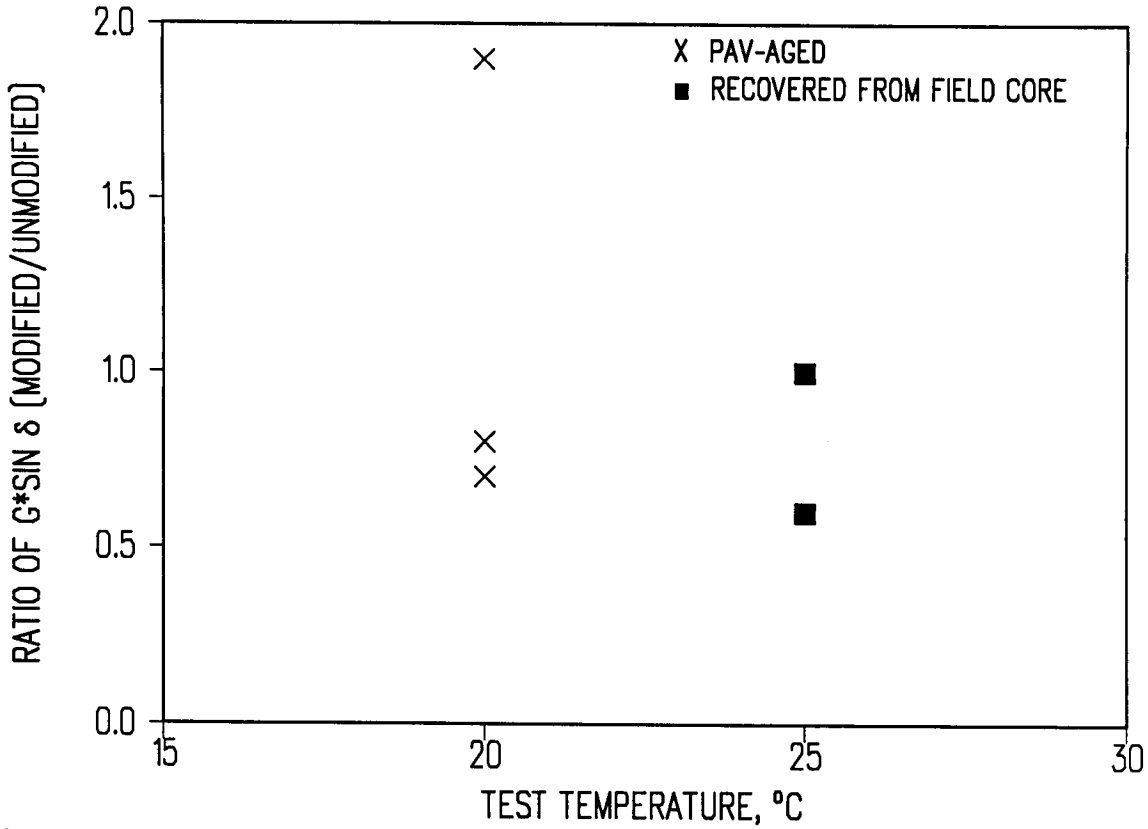

Figure 4.16. Comparison of laboratory- and field-aged modifiers

4.3.4 Thermal Cracking

Three binders and four modifiers were considered in the A-004 thermal cracking experimental design. As noted previously, the materials were tested without age conditioning. In general, none of the properties measured with the direct tension device corresponded to the expected performance, as illustrated in Figures 4.17 and 4.18. The poor modifiers did reduce the tensile strain, as expected. Unfortunately, all the modifiers, even those that were predicted to enhance the thermal cracking response, resulted in lower tensile strains as well. Stiffness, as derived from bending beam rheometer data (Figures 4.19 and 4.20) was somewhat less erratic. The reasons cited for the discrepancies between material properties and expected performance with regard to fatigue cracking are applicable to thermal cracking.

Other researchers have published test data that are substantially less variable and far more encouraging. Data reported by ELF researchers included four penetration graded asphalts, each of which was modified with varying percentages of a styrene-butadiene block copolymer (King et al, 1993). In addition to the conventional binder tests, bending beam rheometer and direction tension tests were used to characterize the control and modified binders. A standard aggregate blend was used for all mixes. Figure 4.21 illustrates the excellent agreement between the binder temperature at bending beam rheometer stiffness of 200 MPa (29 k/in^2) and theoretical mix cracking temperature. Figure 4.22 compares the bending beam stiffness and stress at fracture as measured by the thermal stress retrained specimen test (TSRST). There was good agreement between the binder and mix parameters, especially for

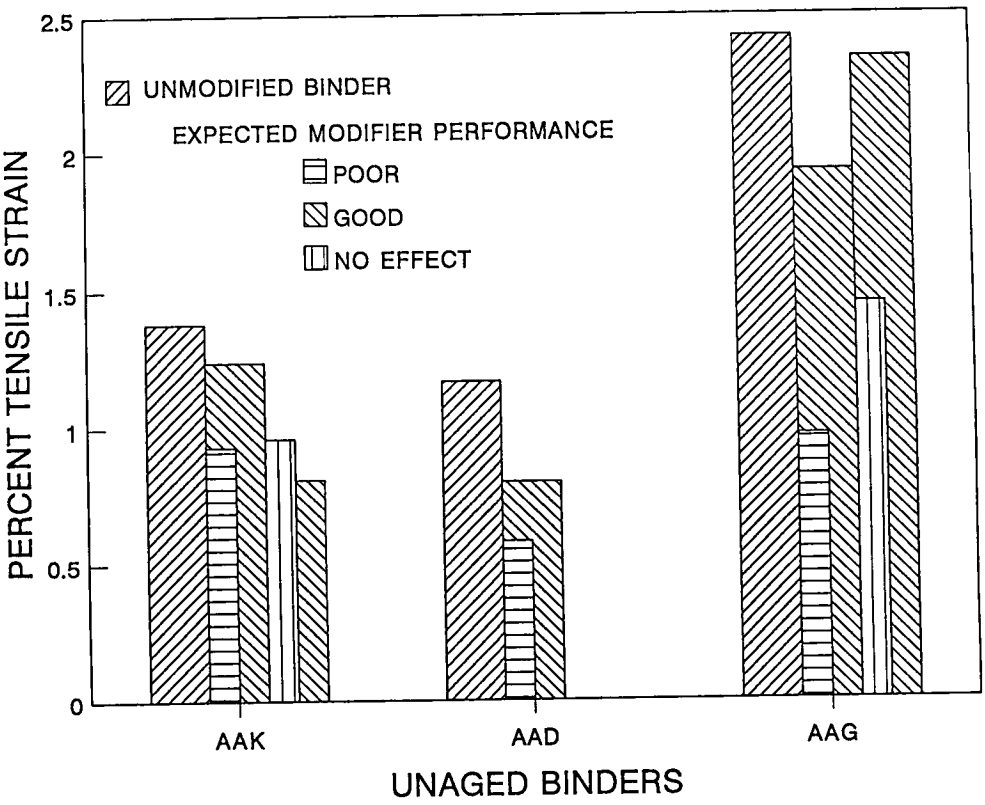

Figure 4.17. Effect of modifiers on unaged binders (tensile strain)

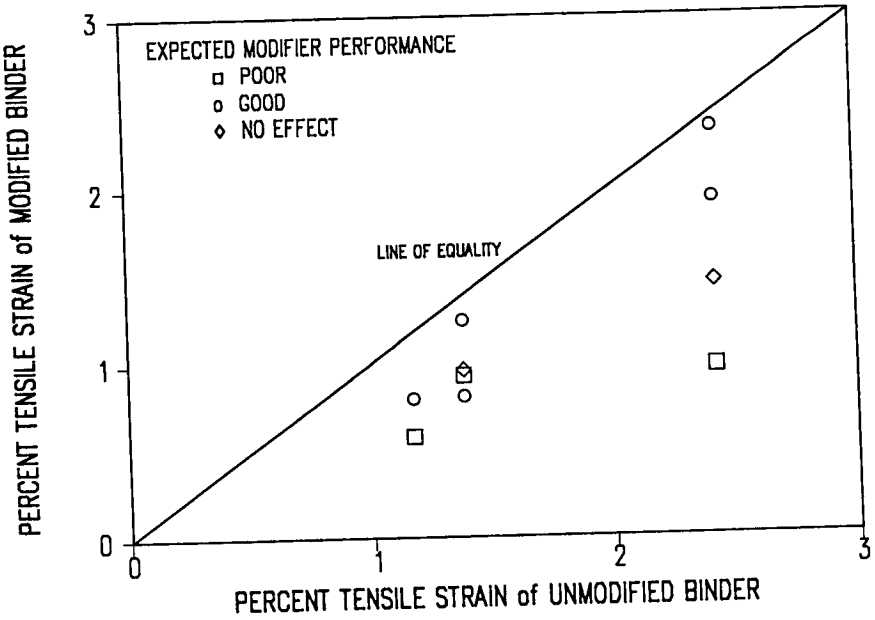

Figure 4.18. Comparison of tensile strain for unmodified and modified binders

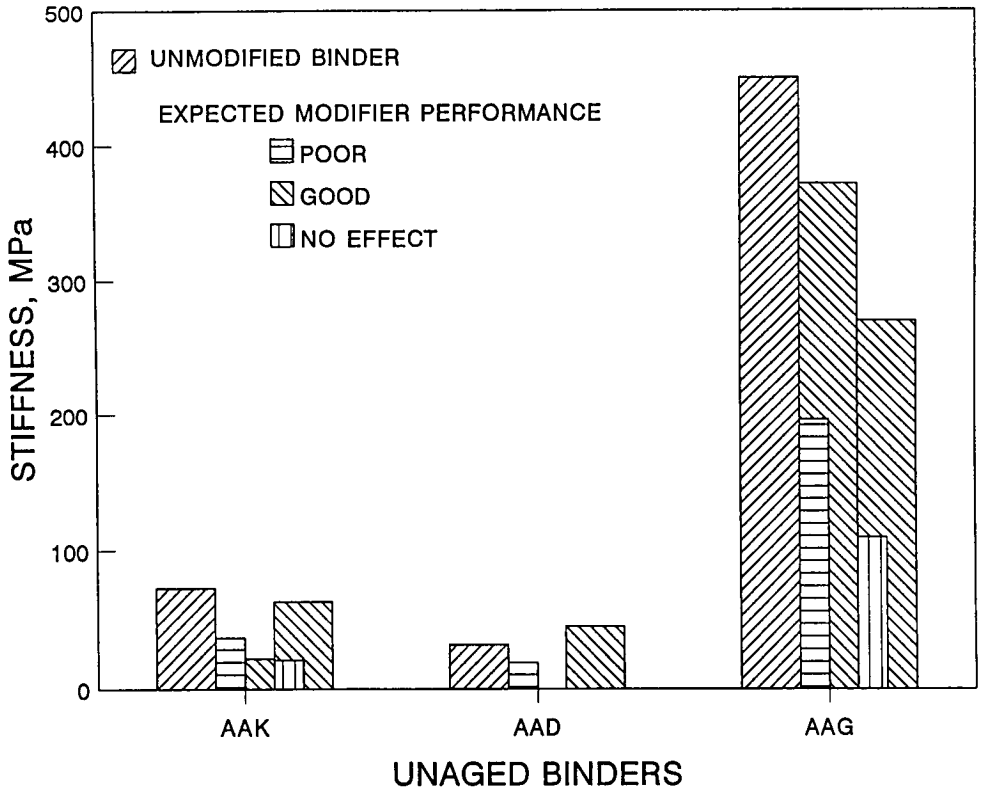

Figure 4.19. Effect of modifiers on unaged binders (stiffness)

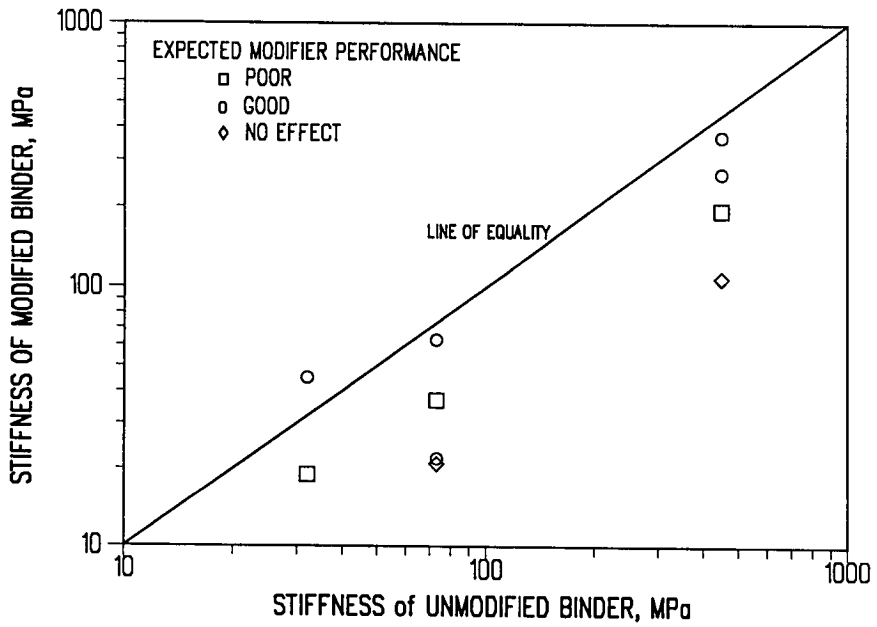

Figure 4.20. Comparison of stiffness for unmodified and modified binders

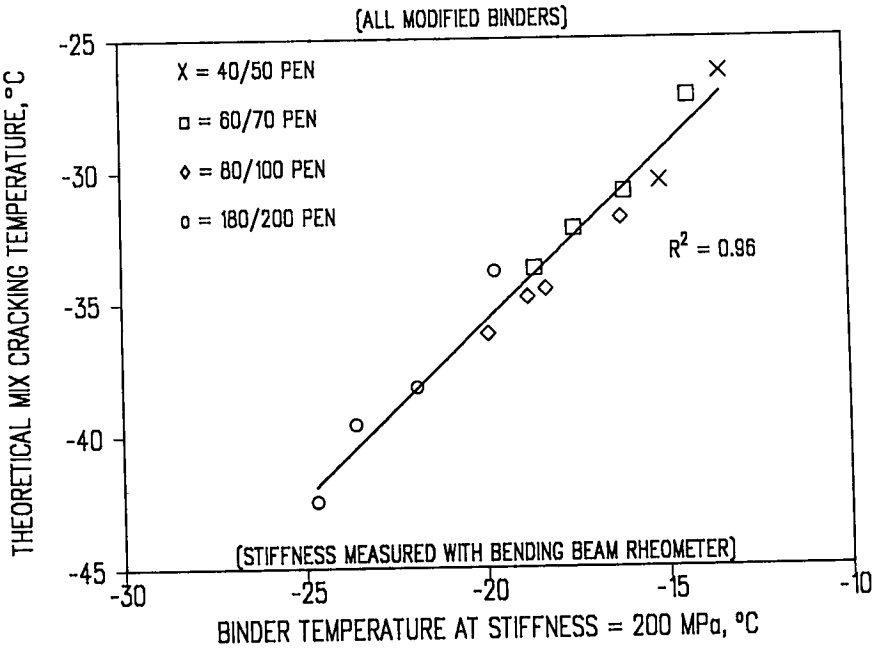

Figure 4.21. Relationship between bending beam rheometer stiffness and theoretical mix cracking temperature

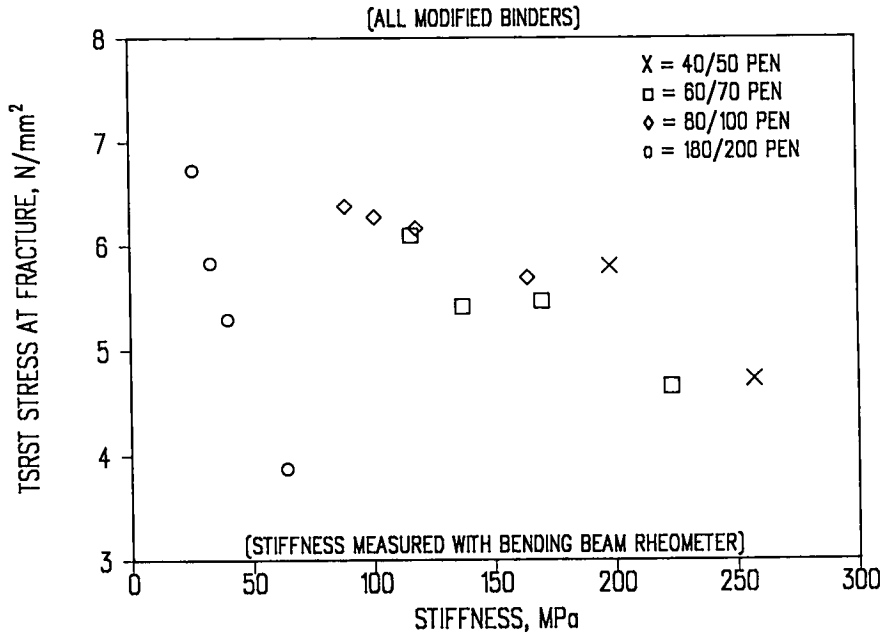

Figure 4.22. Relationship between bending beam rheometer stiffness and TSRST fracture strength

the harder grades of asphalt cement. The softest binder (180/200 penetration) appeared much more sensitive to changes in the modifier content as evidenced by the rapid change in stiffness. Although this data set also is limited, the results do show conclusively that the bending beam rheometer is an effective tool for evaluating modified binder response.

4.3.5 Conclusions

It was originally intended that research conducted under the A-004 contract, *Asphalt Modification*, would encompass modification or adjustment of asphalt cement properties as defined by refining operations, addition of a chemical modifier, and/or mechanical reinforcement. The scope and complexity of the modification research were revised because of time and budget constraints. The A-004 contract was then limited to testing modified binders in accordance with the A-002A recommended test equipment and protocols. Modified materials included in the experiment design were selected based on the collective knowledge and opinions of the ETG, SHRP, and A-001 staff. The expected performance of these materials was based largely on laboratory test data, as field performance data were nonexistent or not readily available.

As noted previously, the A-004 experiment design included 11 modifiers and 5 asphalts that were a subset of the materials used in other asphalt research contracts. This may have limited the full expected range of material response. It therefore, is not surprising that there is no clear correspondence between the material properties of the modified binders and performance as measured by the dynamic shear and bending beam rheometers and the direct tension device. Moreover, the decision to use unaged binders to evaluate the permanent deformation, fatigue, and low-temperature cracking behavior was unfortunate. This decision was made in the early stages of the research and undoubtedly affected the validity of the results. The requirement for age conditioning in the final SHRP binder specification clearly establishes the perils of research conducted in parallel rather than series. Aside from these limitations and constraints, the following general comments are noteworthy.

- Although the binder specification includes tensile strain at failure, this value was observed to be highly variable for modified binders. In some cases, coefficient of variation exceeded 30 percent. Coefficients of variation (CV) for tensile strength data averaged approximately 20 percent, but were consistently less than or equal to 10 percent for bending beam stiffness, *m*-value, and shear rheometer stiffness. Tensile strength rather than tensile strain may be an appropriate specification property for modified binders because of its smaller variability and correspondence to expected performance.

- All the binder tests could accommodate the range of modified binders evaluated. There were no reported difficulties regarding specimen preparation or testing. Test conditions (temperature, load, rate of loading, etc.), however, may need to be adjusted to accommodate the diversity of materials for use as modifiers.

- In general, the results of the A-004 experiment were inconclusive. Again, this may have been the result of the modifier selection process, the use of unaged materials, or some combination thereof. Fortunately, supplemental data provided by other researchers (Shell, Elf, Pennsylvania State University) provided a far more encouraging picture of the efficacy of the SHRP binder tests for performance prediction.

- A comprehensive laboratory investigation with complementary *controlled* field studies would extend and enhance the data generated by SHRP

4.4 Modified Mix Testing

As noted in Section 4.1, the scope of the research was narrowed and many responsibilities were shifted to the A-003A contractor. Validation testing with modified mixes was limited to that associated with permanent deformation and fatigue cracking.

4.4.1 Permanent Deformation

The purpose of this phase of the research was to assess the influence of modifiers on the permanent deformation characteristics of asphalt concrete mixes as measured by the constant height repeated load simple shear test.

Three asphalts (AAD, AAG, and AAK), two aggregates (RB and RL), and four modifiers (coded M401, M412, M415, and M416) were used in the initial experimental design. To establish a baseline performance level, a control (i.e., unmodified) mix was prepared for each combination of binder and aggregate. Performance comparisons were made among the various modified mixes as well as with the control mix.

Specimens for this study were fabricated by the A-004 contractor, Southwestern Laboratories (SWL). The Texas-modified gyratory compactor, was used to compact specimens that were 15 cm (6 in.) in diameter and 15 cm (6 in.) in height. The specimens were then shipped to the University of California at Berkeley (UCB).

Void content measurements were made on the full-sized compacted specimens and on samples sawn into 5 cm (2 in.)-high specimens. Two procedures were used to determine void content: one with Parafilm and one without Parafilm. Table 4.2 contains a summary of void content determinations made by both the A-004 and A-003A staff. UCB void measurements made without Parafilm are similar to those made by SWL while those made with Parafilm are significantly higher. This difference is most likely because at high void content and without Parafilm, water flows freely in and out of the specimen, and air void content typically is underestimated. Similar results are observed for the 5 cm (2 in.) high specimens sawed from the 15 cm (6 in.) cylinders, as seen in Table 4.3.

Table 4.2. Air void content of 15 cm × 15 cm (6 in. × 6 in.) specimens

Specimen Number	Percent Air Voids		
	A-004	A-003A*	A-003A**
1	6.1	6.7	11.7
2	6.7	7.2	11.7
3	6.8	6.5	10.6
4	6.7	6.2	9.4
5	6.8	5.7	12.1
6	6.9	7.3	12.8
7	7.9	7.8	15.0
8	7.4	7.3	12.8
9	6.8	6.0	10.5
10	7.6	8.2	14.2
11	6.9	6.7	11.0
12	6.6	6.2	11.7
13	6.0	6.1	11.8
14	7.5	7.1	11.0
15	7.6	6.4	13.0
16	6.8	6.9	8.8
17	6.0	6.5	11.7
18	6.1	6.0	12.0
19	6.4	4.5	10.9
20	6.4	4.9	9.9
21	6.9	8.7	15.2
22	6.9	6.0	11.5
23	6.8	7.0	14.0
24	6.9	4.9	10.0
25	6.9	7.2	14.8
26	6.1	7.9	13.7
27	6.1	8.4	14.2
Mean	6.8	6.7	12.1
Standard Deviation	0.5	1.0	1.7
Coefficient of Variation (%)	7.5	14.5	14.2

*No Parafilm
**With Parafilm

Table 4.3. Air void content of 5 cm × 15 cm (2 in. × 6 in.) specimens

Specimen Number	Percent Air Voids		
	A-004	A-003A*	A-003A**
1	6.3	7.1	10.2
2	6.8	7.9	10.6
3	6.1	7.3	8.5
4	6.1	7.9	10.7
5	6.2	6.1	7.3
6	7.2	9.0	11.6
7	7.1	8.9	10.7
8	7.1	7.6	9.4
9	7.1	7.0	10.8
10	7.2	8.3	10.1
11	7.1	8.7	10.2
12	7.1	12.5	15.6
13	7.1	11.8	15.8
14	6.2	13.3	17.7
15	6.2	6.1	10.6
16	6.2	7.2	9.3
17	6.7	6.8	9.4
18	7.0	7.9	10.0
19	6.9	6.8	10.9
20	6.8	12.6	14.5
21	6.1	11.9	14.9
22	6.1	13.6	17.2
23	6.4	6.7	9.9
24	6.4	7.8	10.7
25	6.4	7.9	10.8
26	6.4	13.4	15.3
27	6.4	12.1	15.4
28	6.4	8.4	11.2
29	6.3	7.5	9.3
30	6.3	7.2	10.1
31	6.4	7.1	10.7
32	6.0	8.5	12.6
33	6.0	8.5	12.2
34	6.0	8.1	10.2
35	6.0	8.6	10.8
36	6.4	6.9	11.6
37	6.2	7.2	11.7
38	6.2	7.4	10.2
39	6.1	7.4	10.6
40	6.6	6.8	10.2
41	6.8	9.2	11.3
42	6.1	6.9	10.6
43	7.9	8.5	11.6
44	6.2	7.6	8.9
45	7.2	8.1	10.0
46	7.1	8.1	10.3
Mean	6.5	8.5	11.4
Standard Deviation	0.5	2.0	2.3
Coefficient of Variation (%)	6.9	23.9	20.0

*No Parafilm
**With Parafilm

Before testing, aluminum heads that lock into the mechanism on the simple shear device were bonded to the top and bottom of each specimen with an epoxy cement. After capping, the specimens were held in an oven at 40°C (104°F) for approximately 3.5 hours to ensure temperature equilibrium. Constant height repeated load simple shear tests were performed at 40°C (104°F). Each specimen was conditioned with 100 repetitions of haversine shear stress of 6.9 kPa (1 lb/in^2) (0.1 sec haversine pulse with a 0.6 sec rest period between pulses). After conditioning, the specimen was subjected to a repetitive shear stress of 70 kPa (10 lb/in^2). The test was terminated at 5000 load cycles or a maximum shear strain of 5 percent, whichever came first.

In order to test mixes with similar air void content, all specimens containing the RL aggregate were deleted from the experimental design. The testing program was reduced to an evaluation of the five modifiers, one aggregate (RB), and two asphalts (AAG and AAK).

Test results are shown graphically in Figures 4.23 to 4.27. Table 4.4 shows estimated load cycles to 4 percent strain. Significant variations in air void content occurred making comparisons among the mixes questionable. Based on these data an estimate of the relative performance of the mixes over a range of void contents is shown in Figure 4.28. The average load cycles to 4 percent strain (Figure 4.29) suggest the following: Mixes containing binder AAG appeared to be more sensitive to modifiers than did mixes containing AAK. The performance ranking of the modifiers, from good to poor, for mixes containing AAG was 401, 412, 416, 415. All the modifiers except 415 performed better than did the unmodified/control mix. Mixes containing binder AAK were less sensitive to the influence of the modifiers. None of the modifiers improved performance. The performance ranking of the modifiers, from good to poor, for mixes containing AAK is 415, 412, 401, 416. When the measured permanent strain is taken directly from Figures 4.23 to 4.27 (at both 100 and 1,000 load cycles), the performance rankings of the modifiers are somewhat different (Figure 4.30). For binders AAG and AAK the performance ranking (from good to poor) is 401, 412, 415, 416. This performance ranking of the modifiers, despite the difference in void content is nearly identical to that hypothesized by the ETG, whose members were instrumental in the selection of the modifiers to be used in the validation testing.

4.4.2 Fatigue

The purpose of the research was to assess the influence of modifiers on the fatigue characteristics of asphalt concrete mixes as measured by the new flexural fatigue equipment.

Three asphalts (AAF, AAG, and AAK), one aggregate (RB), and three modifiers (coded M405, M415, and M416) were included in the experimental design, as shown in Table 4.5. To establish a baseline performance level, a control (i.e., unmodified) mix was prepared for each combination of binder and aggregate. Performance comparisons were made among the various modified mixes as well as with the control mix.

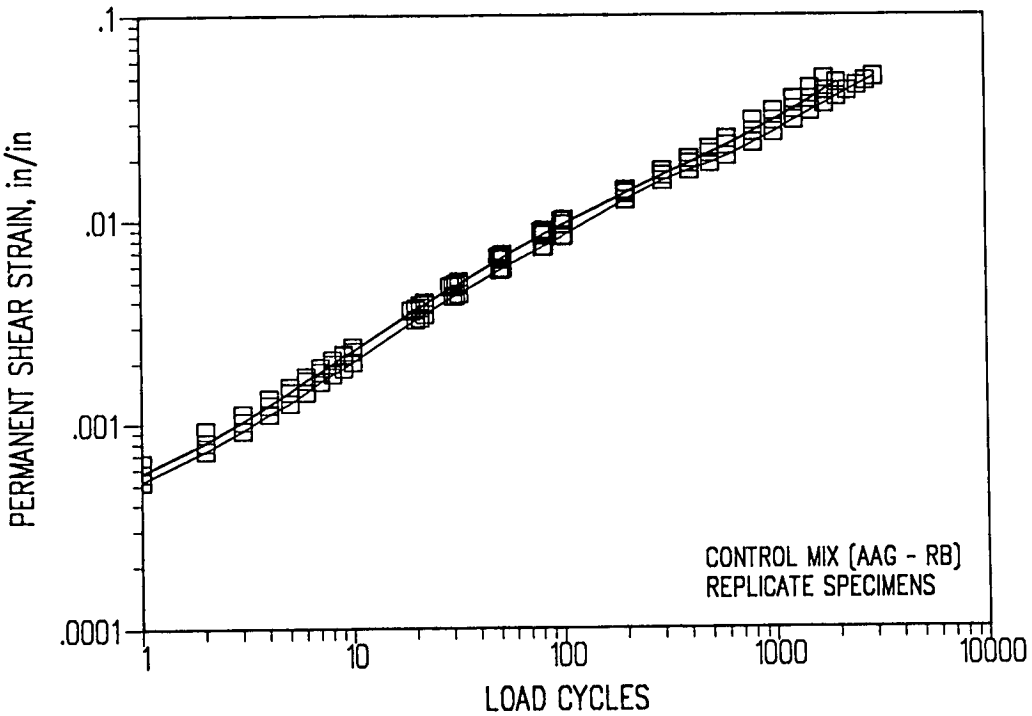

Figure 4.23a. Relationship between load cycles and permanent shear strain (control mix with binder AAG)

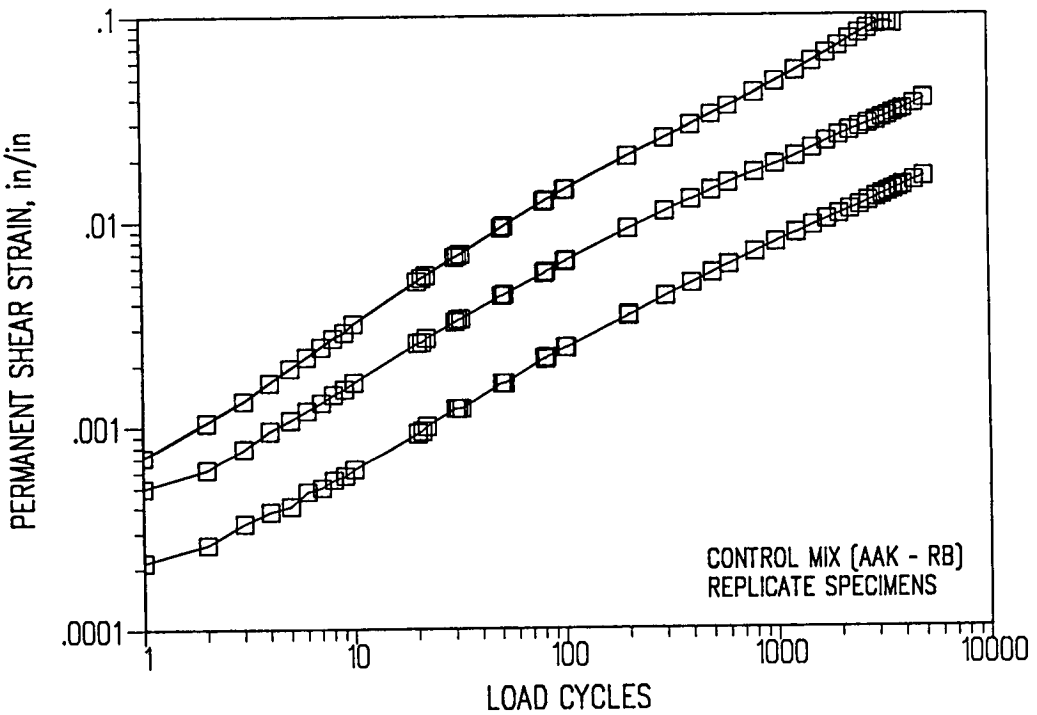

Figure 4.23b. Relationship between load cycles and permanent shear strain (control mix with binder AAK)

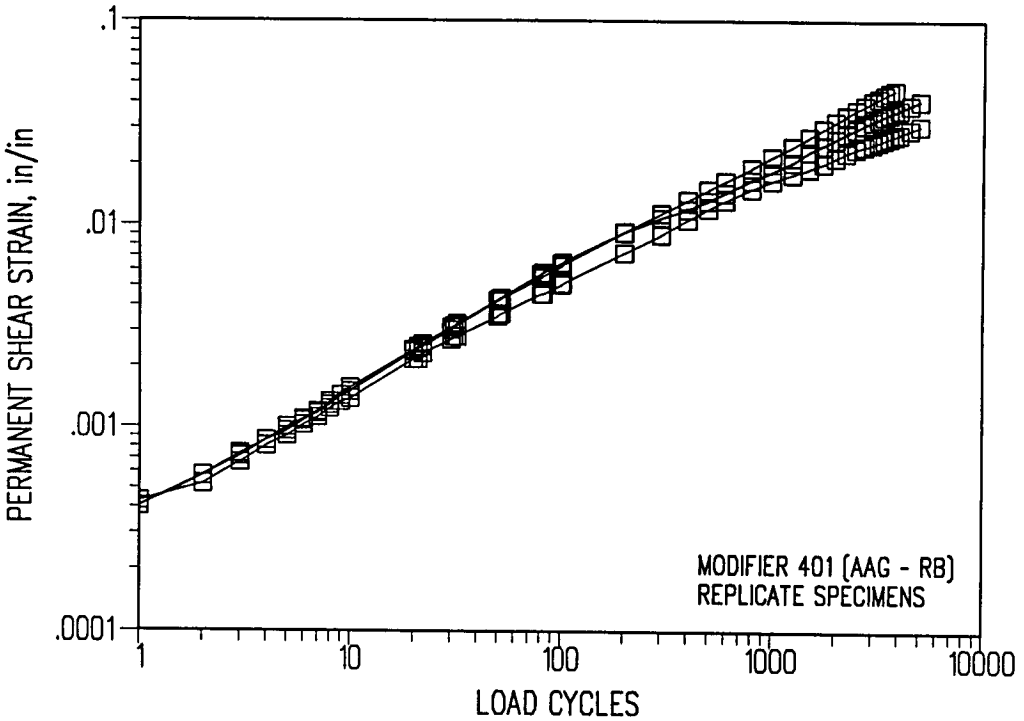

Figure 4.24a. Relationship between load cycles and permanent shear strain (binder AAG with M401)

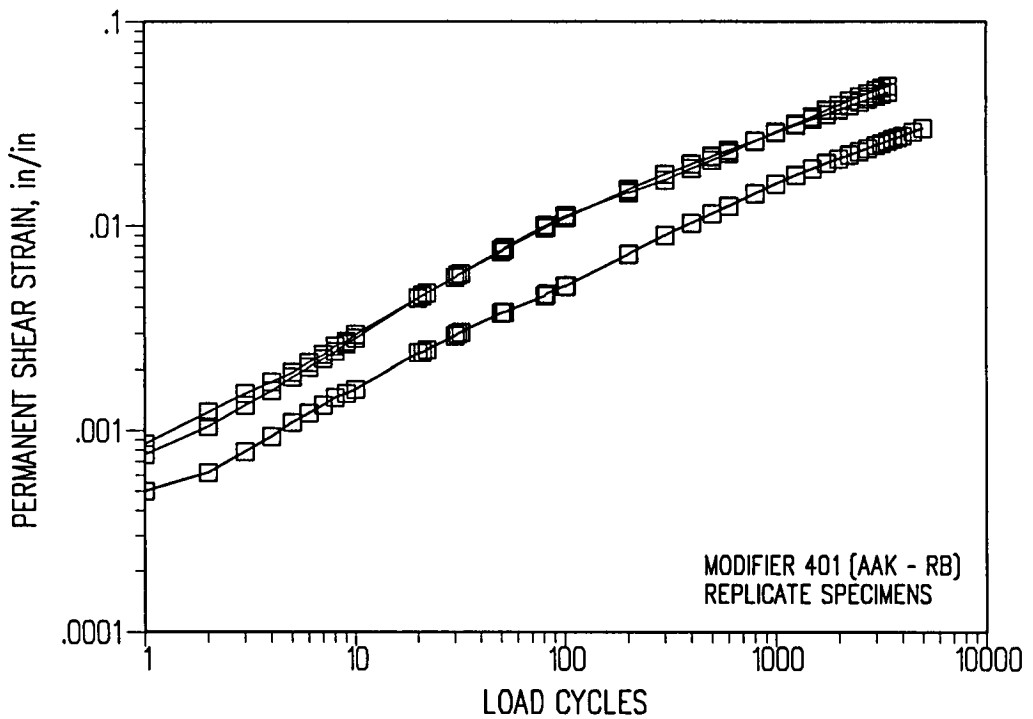

Figure 4.24b. Relationship between load cycles and permanent shear strain (binder AAK with M401)

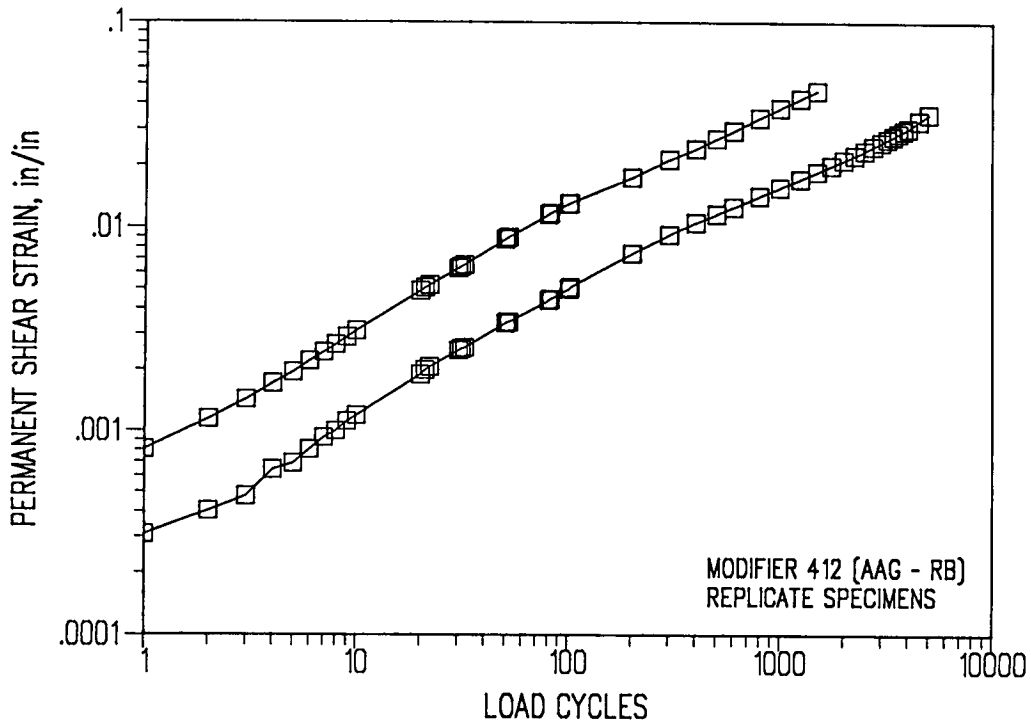

Figure 4.25a. Relationship between load cycles and permanent shear strain (binder AAG with M412)

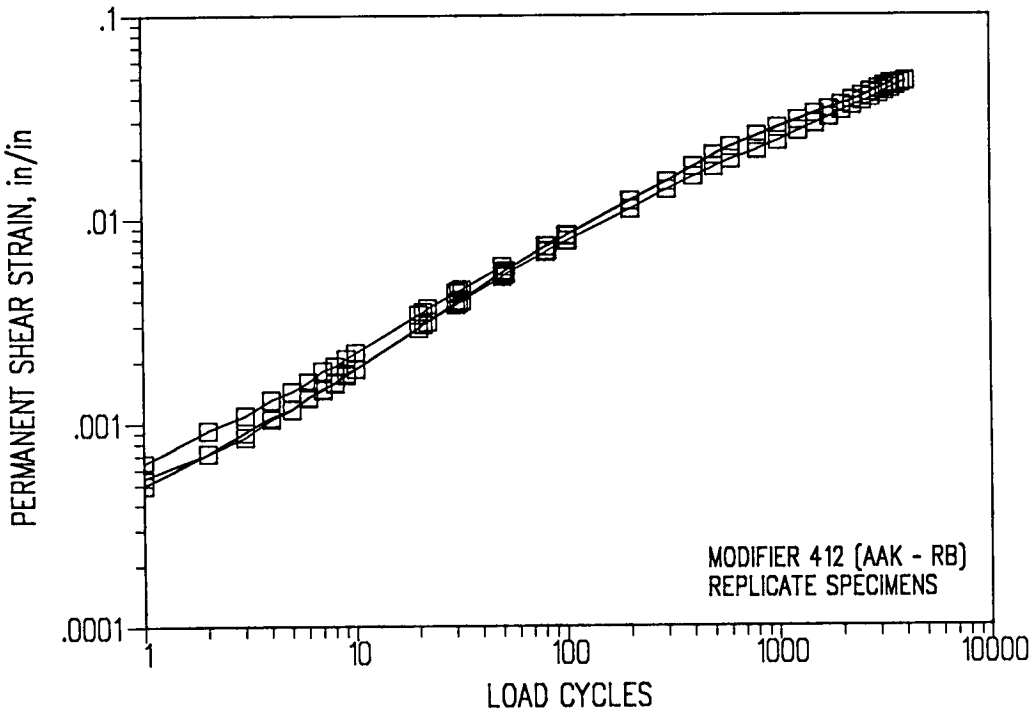

Figure 4.25b. Relationship between load cycles and permanent shear strain (binder AAK with M412)

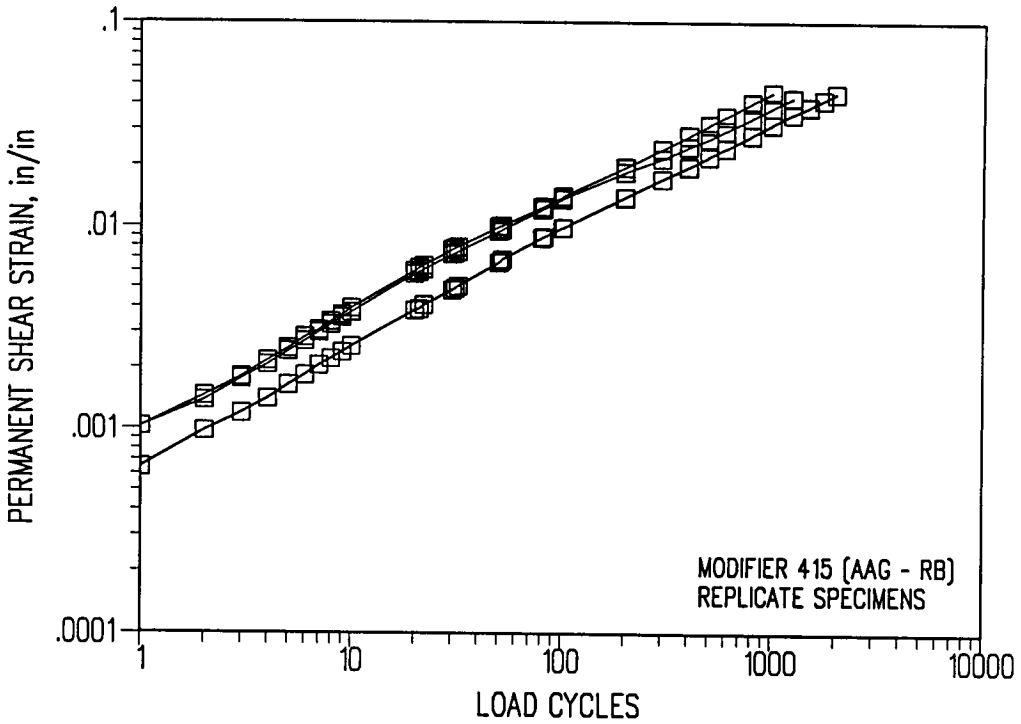

Figure 4.26a. Relationship between load cycles and permanent shear strain (binder AAG with M415)

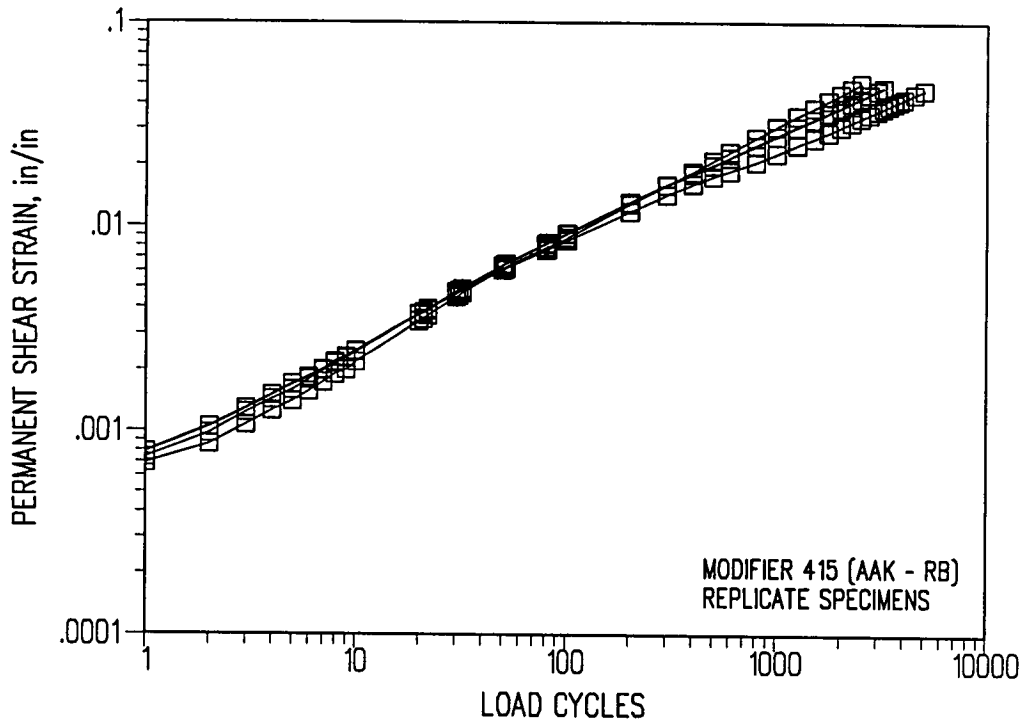

Figure 4.26b. Relationship between load cycles and permanent shear strain (binder AAK with M415)

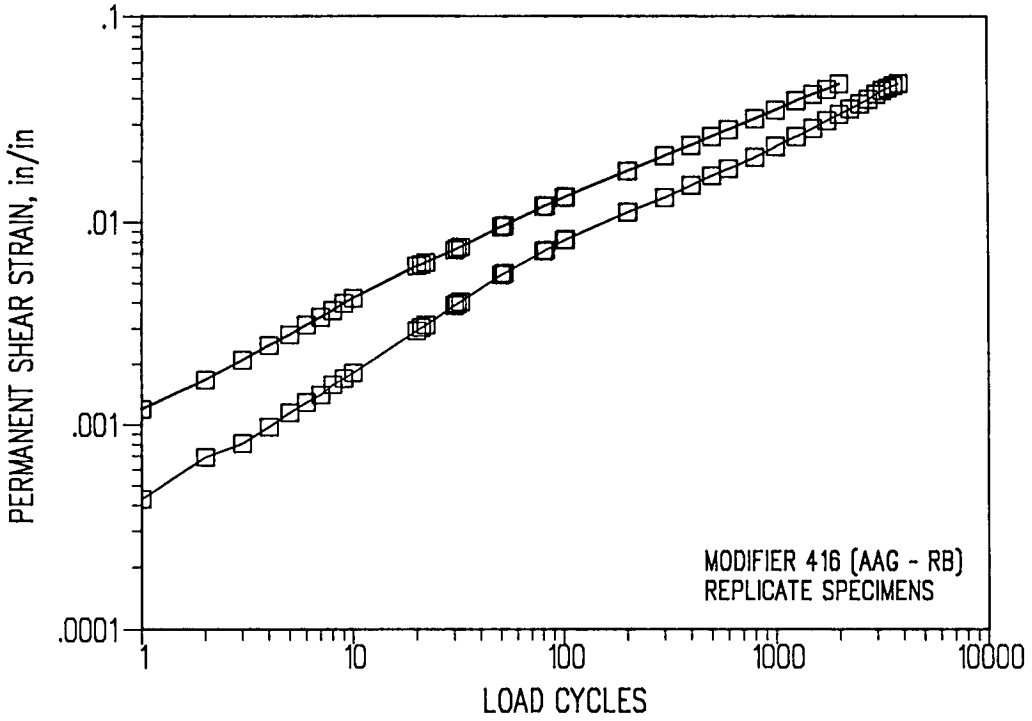

Figure 4.27a. Relationship between load cycles and permanent shear strain (binder AAG with M416)

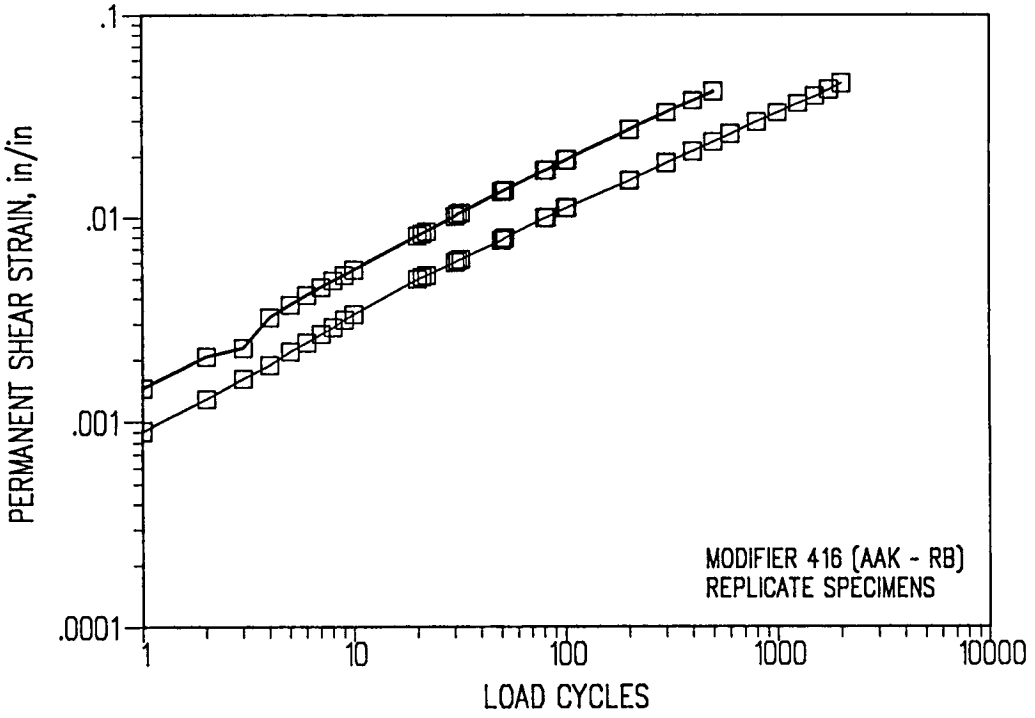

Figure 4.27b. Relationship between load cycles and permanent shear strain (binder AAK with M416)

Table 4.4. Simple shear load cycles to 4 percent strain

Mix Type	Binder Type	
	AAG	AAK
Control	1500	2900
M401	4000	2100
M412	3300	2200
M415	1167	2333
M416	2150	975

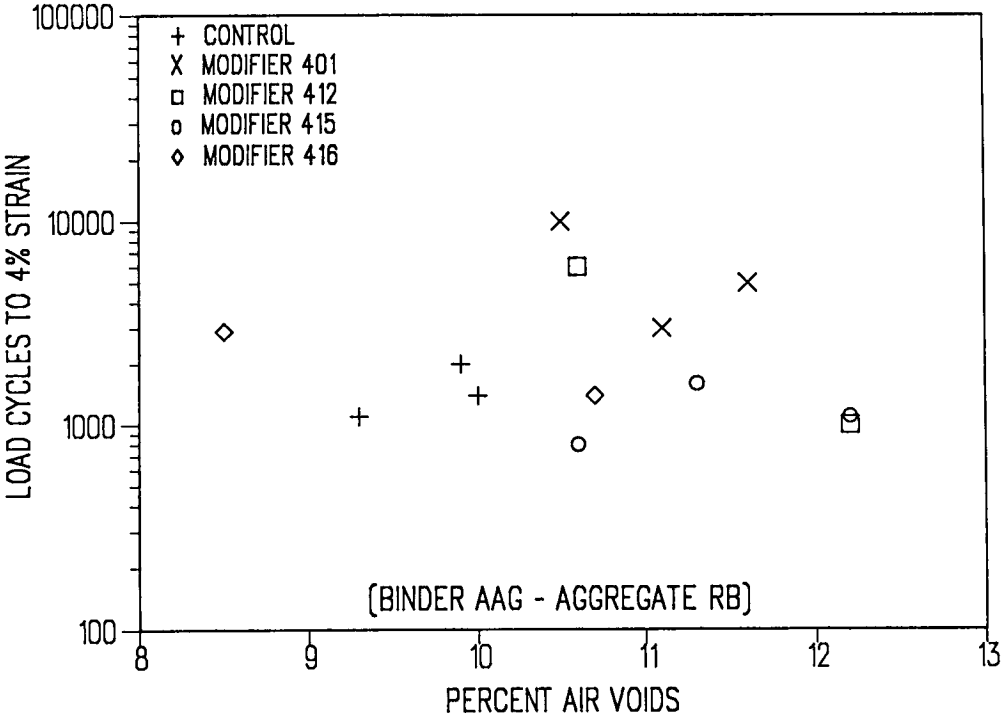

Figure 4.28a. Performance of modified mixes over a range of air void contents (modified binder AAG)

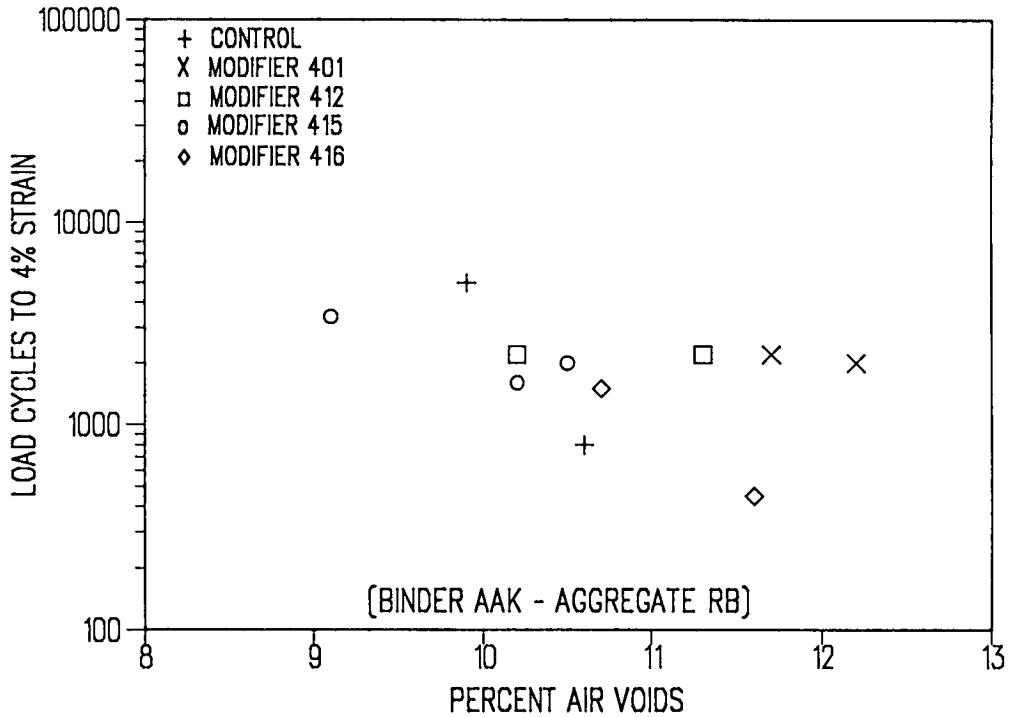

Figure 4.28b. Performance of modified mixes over a range of air void contents (modified binder AAK)

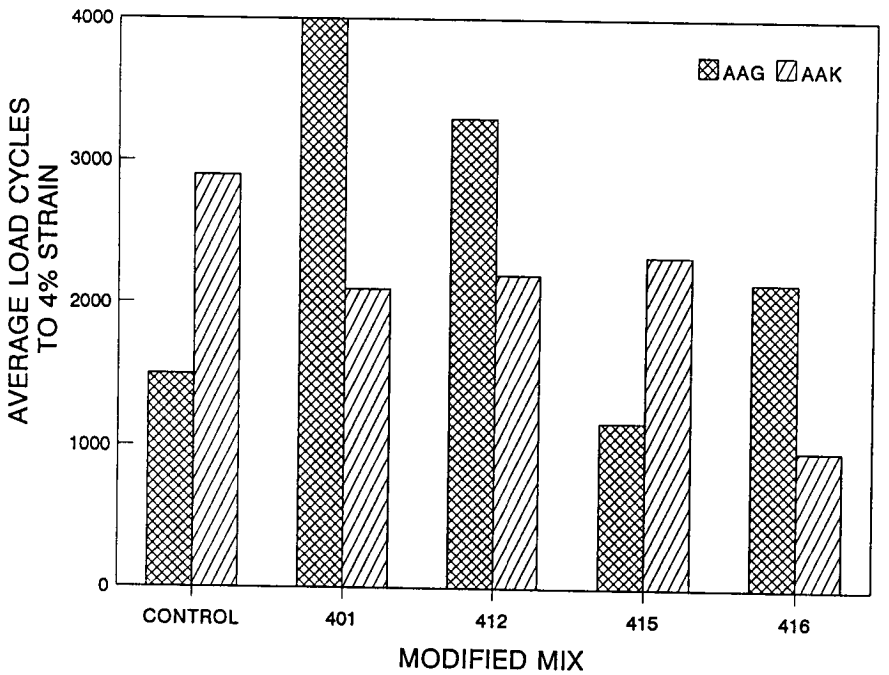

Figure 4.29. Performance of modified mixes in terms of load cycles to 4 percent strain

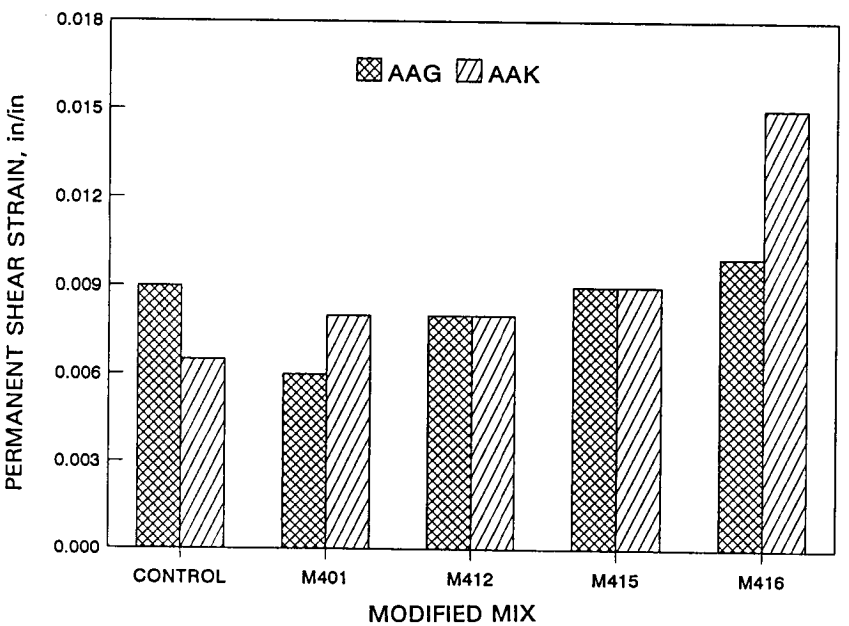

Figure 4.30. Performance of modified mixes in terms of permanent shear strain

Table 4.5. Features of modified asphalt mix experiment

Number of asphalts	3 - MRL core asphalt AAF-1, AAG-1, and AAK-1
Number of aggregates	1 - MRL aggregate RB
Asphalt content	1 - 5.0 percent and 5.2 percent for unmodified and modified mixes, by weight of aggregates
Number of modifiers	3 - Modifiers identified as M405, M415, and M416
Air void levels	1 - 7 ± 1 percent
Strain levels	2 - 400 and 700 μ in./in.
Replicates at each strain level	2
Temperature	1 - 20°C (68°F)
Frequency	1 - 10 Hz (sinusoidal)
Specimen size	6 cm (2 in.) height, 6.25 cm (2.5 in.) width, 37.5 cm (15 in.) length
Method of compaction	Kneading compaction
Total number of mixes tested	10
Total number of specimens tested	39

Specimens for this study were fabricated by the A-004 contractor, SWL, using a kneading compactor. The compacted specimens were then shipped to UCB, where they were sawed to the required dimensions (6.4 cm × 5 cm × 40.7 cm [2.6 in. × 2 in. × 16.3 in.]) and tested. All tests were performed at 20°C (68°F) in the controlled-strain mode with a sinusoidal load at a frequency of 10 Hz. The response variables included initial flexural stiffness measured at the 50th load cycle; fatigue life, as defined by the number of cycles to a 50 percent reduction in stiffness; initial dissipated energy per cycle measured at the 50th load cycle; and cumulative or total dissipated energy associated with fatigue life.

Table 4.6 is a summary of the data for the control and modified mixes. The control mixes, in order of decreasing stiffness, are AAG, AAF, and AAK. Figures 4.31 and 4.32 illustrate the effect of modifier type on the average stiffness and fatigue life of the various mixes. The fatigue life of mixes containing AAK was observed to be the longest, followed by mixes containing binders AAF and AAG. The conventional notion that stiffer mixes under controlled-strain testing performed poorer than their less stiff counterparts was confirmed for the unmodified mixes. The modified mixes, however, did not follow this pattern. Modifier M405 had a detrimental effect on all mixes, regardless of binder type. Addition of this modifier to binder AAF and AAK increased stiffness but decreased fatigue life. Modifiers M415 and M416 produced changes in performance similar to those of modifier M405 on mixes containing AAG. Addition of both modifiers reduced fatigue life, although mix stiffness decreased. For mixes containing AAK, the addition of modifiers M415 and M416 increased fatigue life substantially. In both cases, mix stiffness decreased. The modifier effects on cumulative dissipated energy were similar to those observed for fatigue life.

Though limited in extent, the results of this study indicate that both binder type and modifier type substantially affect stiffness, fatigue life, and cumulative dissipated energy. For thick sections, the ETG ranking of the modifiers in order of decreasing fatigue life was M405, M415, and M416. Results from the controlled strain testing ranked the modifiers in exactly the opposite order.

Table 4.6. Average values for stiffness, fatigue life (at 500 μ in./in.), and cumulative dissipated energy from modified asphalt mix experiment

Mix Type	Stiffness (psi)	Fatigue Life (N_f) (at 500 μ in./in.)	Cumulative Dissipated Energy to N_f (psi)	Voids (%)	Voids filled with Bitumen (%)
AAF-1	581,500	9600	360	7.0	62
AAF-M405	681,600	5200	130	6.6	64
AAG-1	785,100	4300	230	6.4	64
AAG-M405	635,700	1700	50	6.6	64
AAG-M415	606,600	1400	60	6.4	65
AAG-M416	710,900	2400	130	6.6	64
AAK-1	416,200	13,700	440	6.8	63
AAK-M405	473,300	5800	130	7.1	63
AAK-M415	263,700	40,800	930	7.3	62
AAK-M416	254,150	69,200	1530	7.0	63

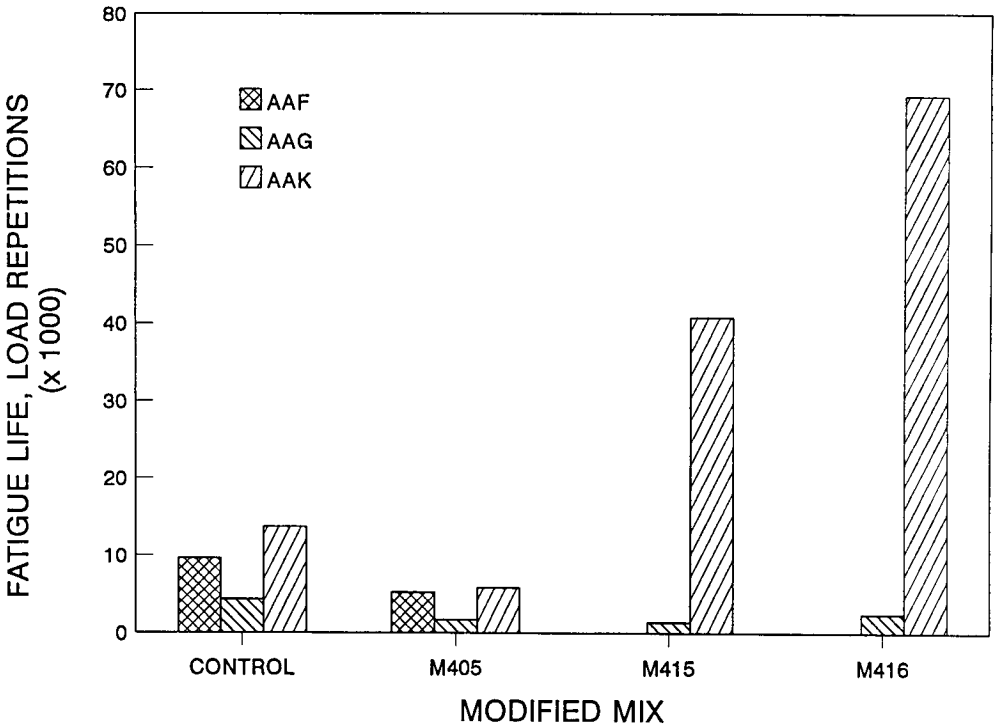

Figure 4.31a. Performance of modified mixes in terms of stiffness (in binder)

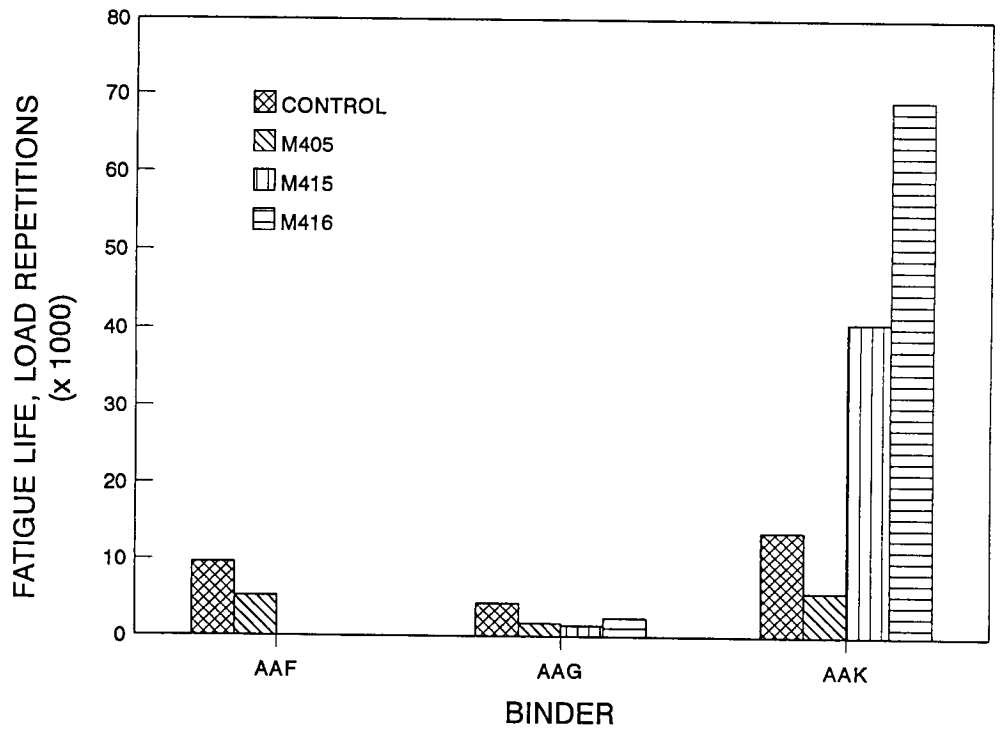

Figure 4.31b. Performance of modified mixes in terms of stiffness (by modifier)

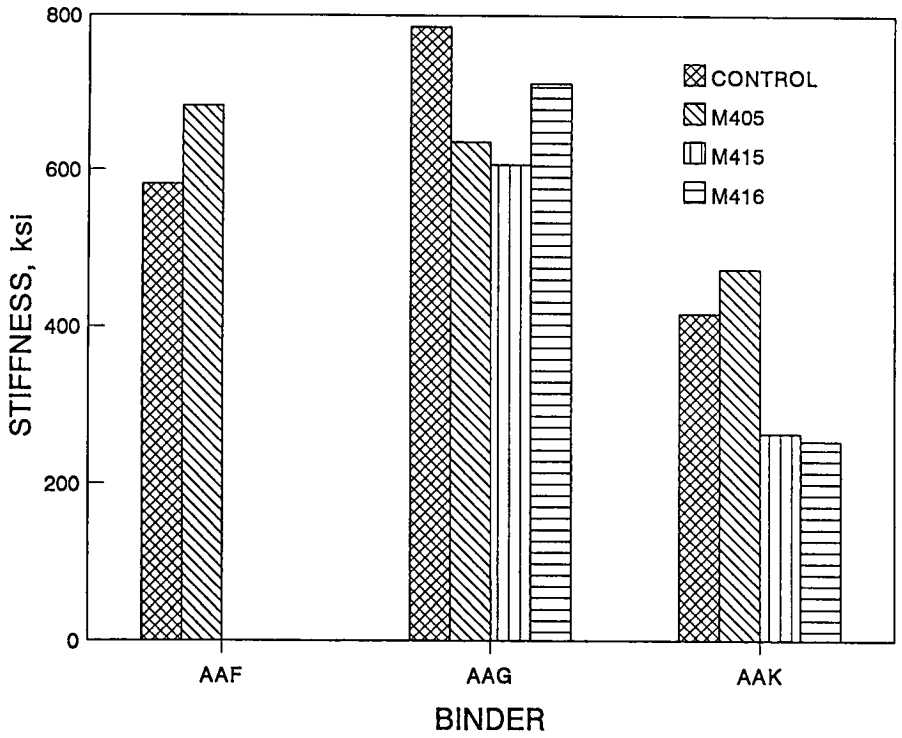

Figure 4.32a. Performance of modified mixes in terms of fatigue life (by binder)

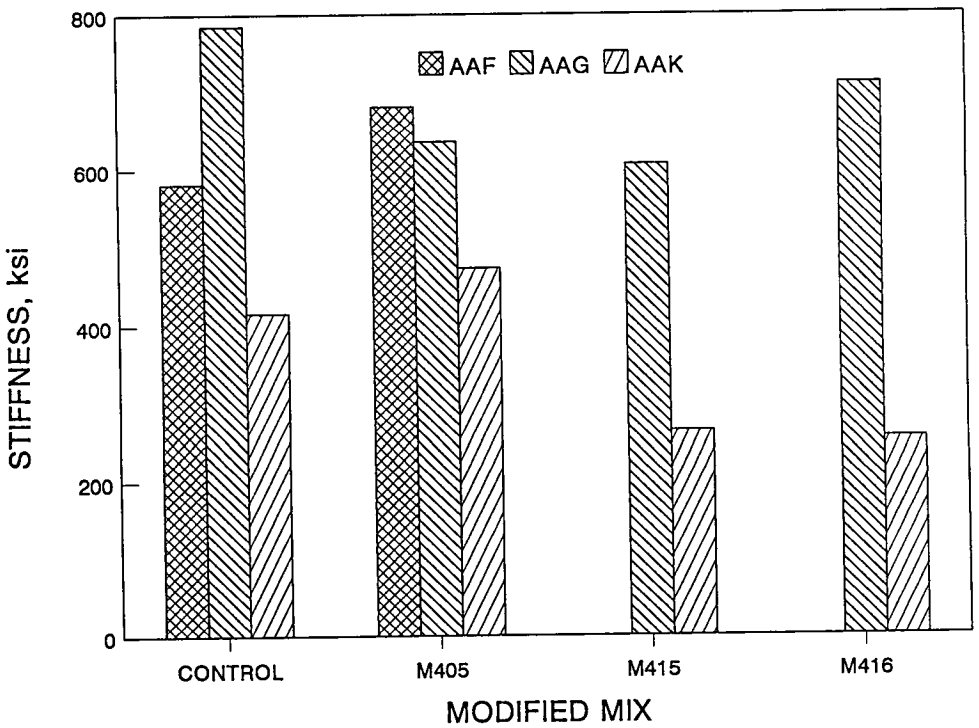

Figure 4.32b. Performance of modified mixes in terms of fatigue life (by modifier

References

Anderson, D., R. Christianson, H. Bahia, R. Dongre, M. Sharma, C. Antle, and J. Button. *Binder Characterization and Evaluation, Volume 3: Physical Characterization.* Report no. SHRP-A-396. Strategic Highway Research Program, National Research Council, Washington, DC. 1994.

Bouldin, M., G. Row, J. Souse, and J. Shamrock (1994). Mix Rheology - a tool for predicting the high performance of hot mix asphalt. Proceedings, Association of Asphalt Paving Technologies, Vol. 63, pp. 1-32.

Harrigan, E., R. Leahy, and J. Youtcheff. *The Superpave Mix Design System Manual of Specifications, Test Methods and Practices.* Report no. SHRP-A-379. Strategic Highway Research Program, National Council, Washington DC. 1994.

Kennedy, T., G. Huber, E. Harrigan, R. Cominsky, H. Von Quintus, C. Hughes, and J. Moulthrop. *Superpave: The Product of the SHRP Asphalt Research Program.* Report no. SHRP-A-410. Strategic Highway Research Program, National Research Council, Washington, DC. 1994.

King, S., H. King, O. Hardens, W. Arand, and Planche (1993). *Influence of Asphalt Grade and Polymer Concentration on the Low Temperature Performance of Polymer Modified Asphalt.* Proceedings, Association of Asphalt Paving Technologists, Volume 62, pp. 1-22.

Lytton, R.L., J. Uzan, E.G. Fernando, R. Roque, D. Hiltunen, and S.M. Stoffels. *Development and Validation of Performance Prediction Models and Specifications for Asphalt Binders and Paving Mixes.* Report no. SHRP-A-357. Strategic Highway Research Program, National Research Council, Washington, DC. 1993.

SHRP 1990. *Asphalt: A Stragetic Plan.* Report no. SHRP-A-301. Strategic Highway Research Program, National Research Council, Washington, DC. 1993.

SHRP 1994. Research Performed by the University of California at Berkeley; Oregon State University, and Austin Research Engineers. *Stage 1 Validation of the Relationship Between Asphalt Properties and Asphalt-Aggregate Mix Performance.* Report no. SHRP-A-398. Strategic Highway Research Program, National Research Council, Washington, DC. 1994.

Transportation Research Board 1986. *Strategic Highway Research Program Research Plans.* NCHRP Project 20-20. Transportation Research Board, National Research Council, Washington D.C.

Von Quintus, H. L., J.A. Scherocman, C.S., and T.W. Kennedy. *Asphalt-Aggregate Mixture Analysis System.* NCHRP Report 338. Transportation Research Board, National Research Council, Washington, DC. 1991.